EUCLID SPACE MISSION

(a few whys and hows)

R. Scaramella (on behalf of Euclid Science Team and Euclid Consortium)

(Euclid Consortium, old timer,
Mission Survey Scientist,
member of the EC Board and EST)

Lots of figures and material courtesy of: EC&ESA (SciRD, CalWG, ECSURV, ESSWG, VIS, NISP, SWGs, OUs ...)

Red Book released in July 2011 (ESA web pages)

kosmobob@inaf.it

6.3.4. Mission Survey Scientist

The Mission Survey Scientist leads the high-level Euclid mission activities that needs a global views and understandings of the survey planed with Euclid, of the VIS and NISP science drivers and of the performances of the telescope and the instrument.

This pivot position aims at strengthening the day-to-day communication between the Science Working Groups and the instrument and ground segment scientists, as well as the coordination of transverse scientific activities (mission definition, mission performances, calibrations, end-to-end simulations).

- He/She is responsible of the definition, modeling and optimization of the Euclid survey in order to maximize the scientific return of the mission;
- He/She is in charge of proposing to the ECL and ECCG mission scenarios and mission trade-offs that are in lines with the core and the legacy programs, and the best scientific return to the Euclid Consortium;
- He/She is the lead of the Mission Survey Group;
- He/She has a co-leading role in the end-to-end simulations activities;
- He/She is has a leading role in the Calibration working group activities;
- He/She is responsible for finding and implementing the funding/manpower resources needed to operate the Mission Survey Group;

EUCLID CONSORTIUM SURVEY GROUP

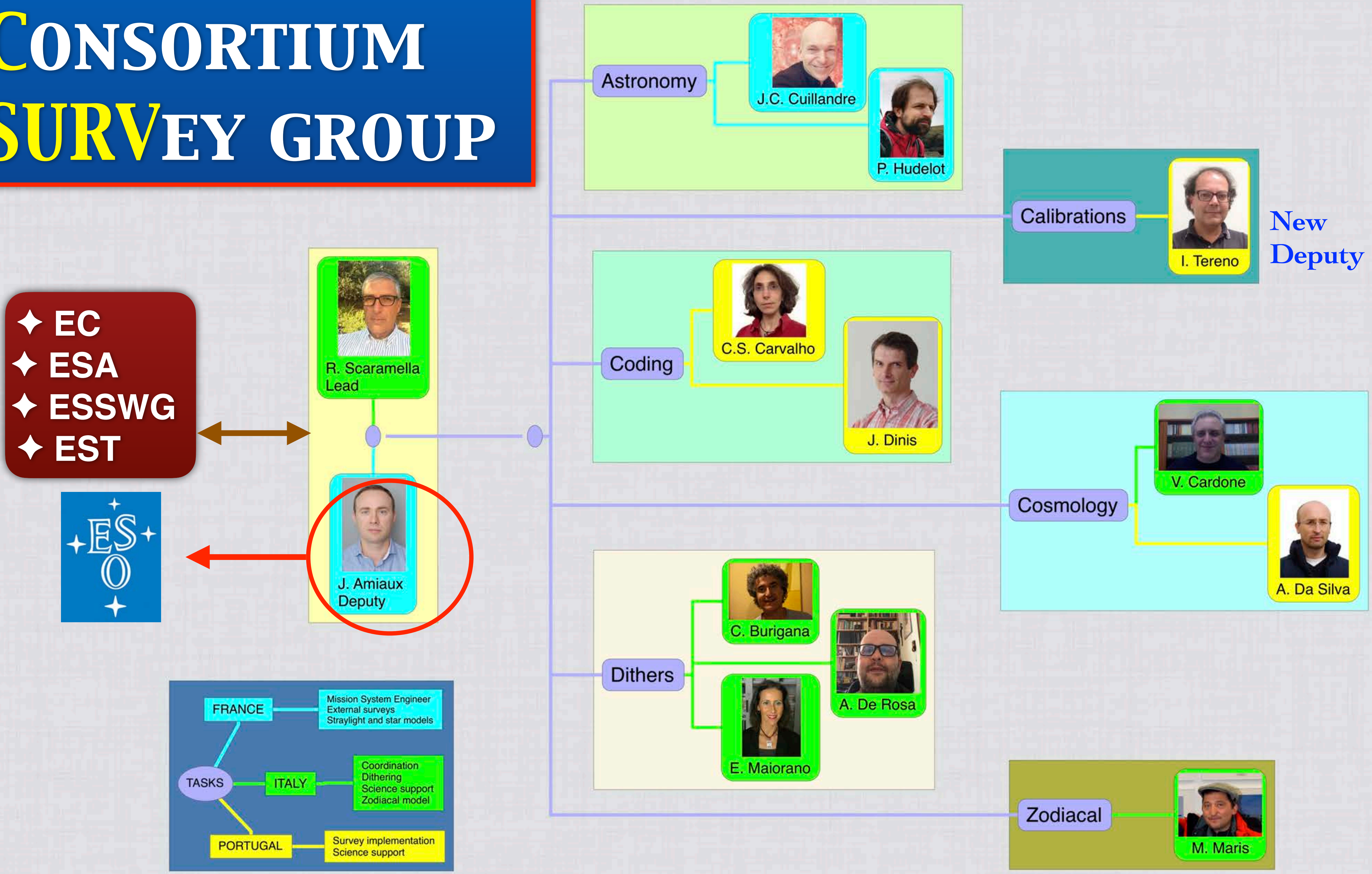

Euclid STAR Prize 2020

Euclid Consortium SURvey Group

Team Scientist Award

INAF

INFN Roma1

Cardone was also awarded the 2019 team star prize for theoretical work on Fisher matrices

~1930 Discovery: the Expansion of the Universe

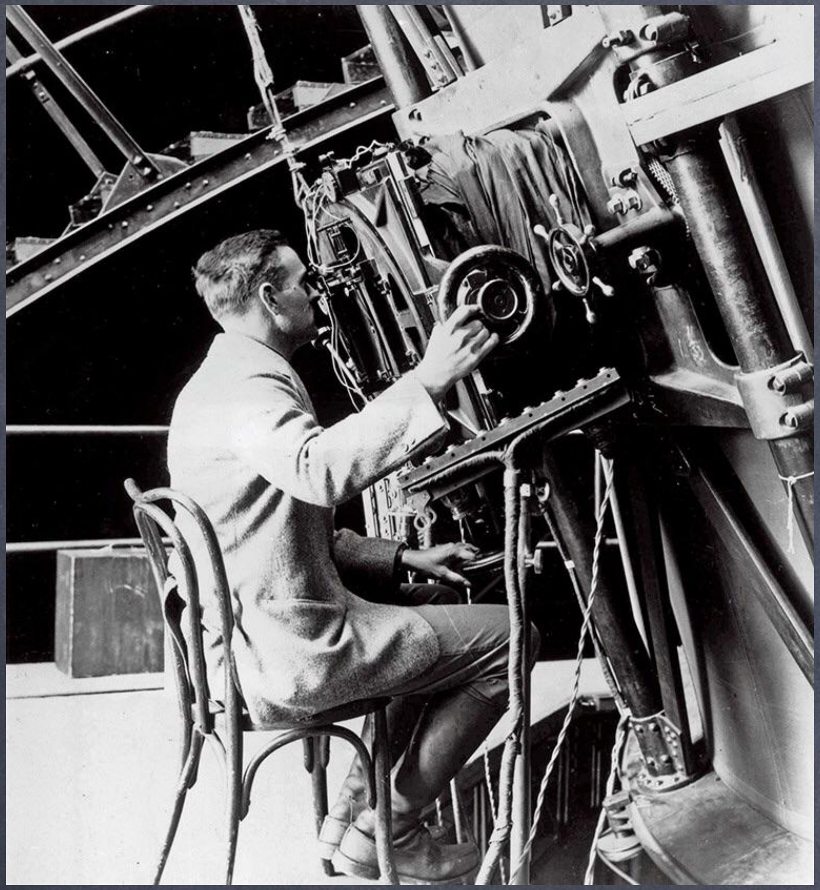

Hubble 1929-1931

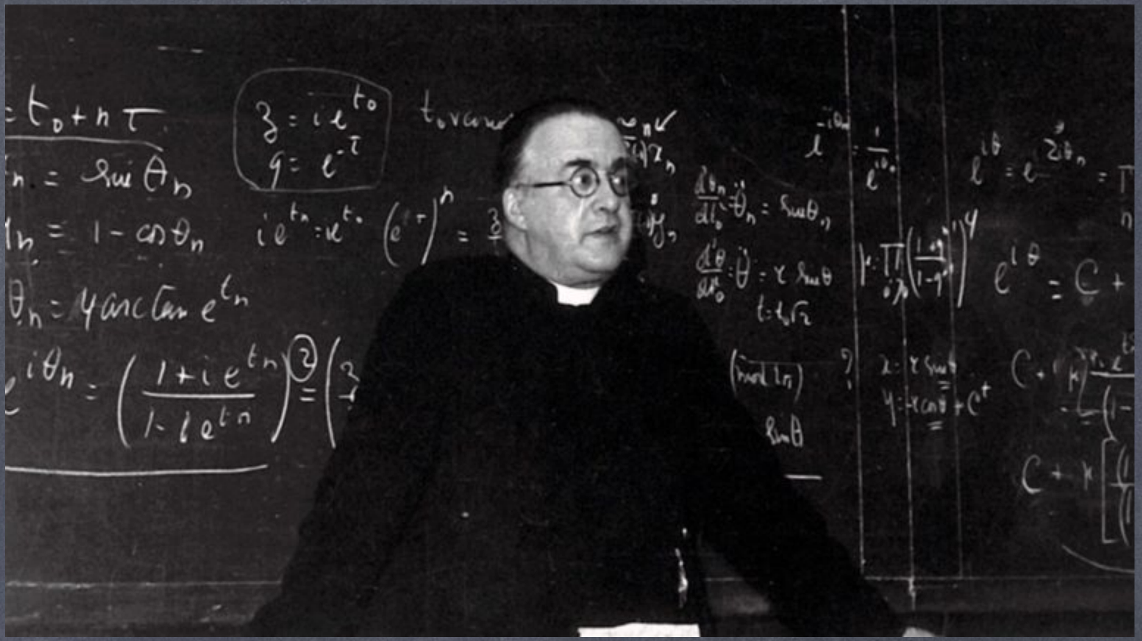

Le Maître 1926

Recession velocity ∝ redshift z is linearly proportional to distance (z<<1)

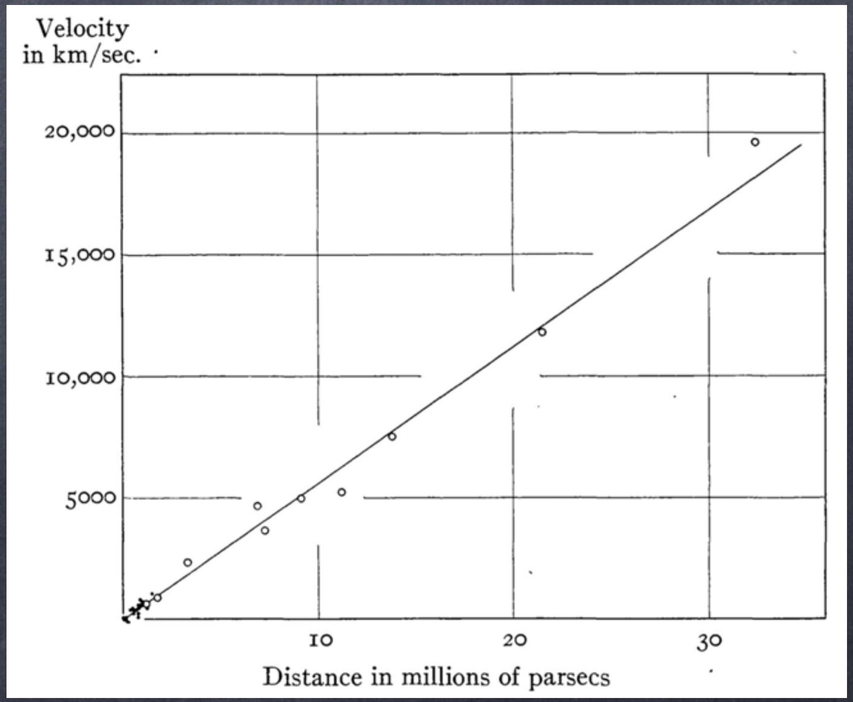

$z \propto d \; ; \; z \cong H_0 d$

The Cosmic Microwave Background is SMOOTH !!

$$\frac{\Delta T}{T} \simeq 10^{-5} = 0.00001$$

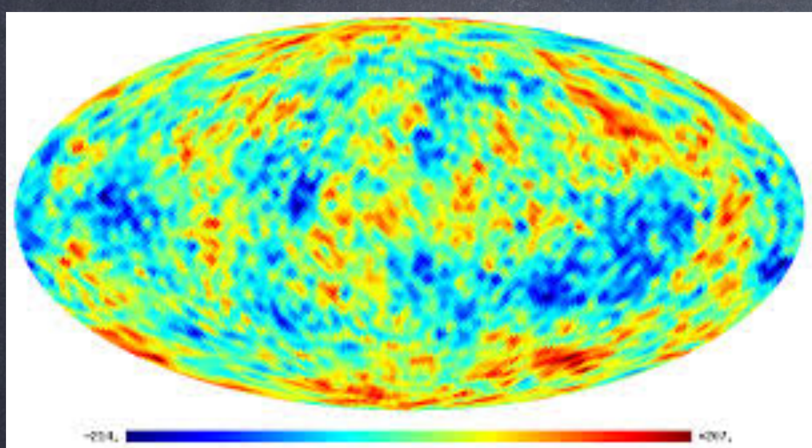

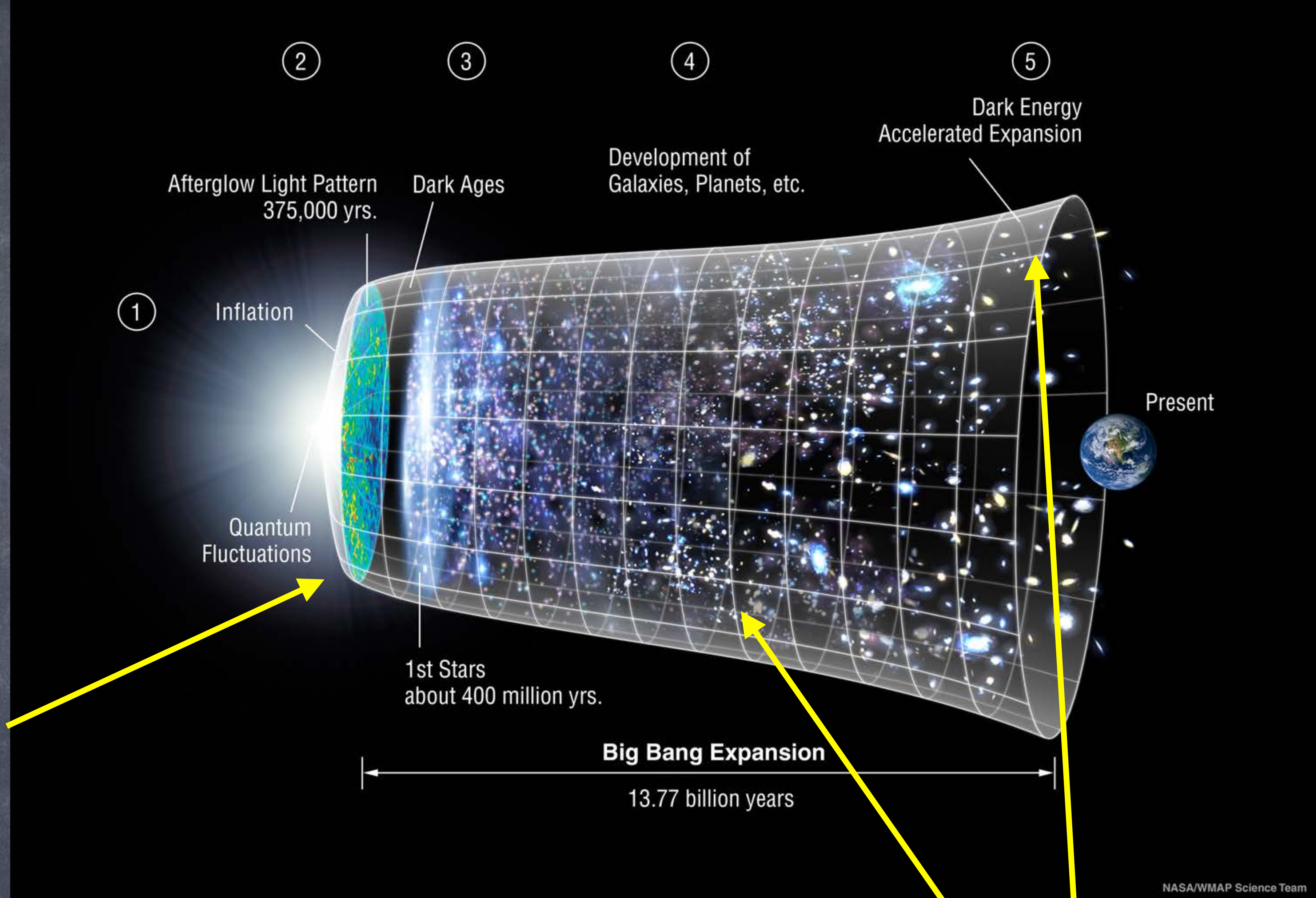

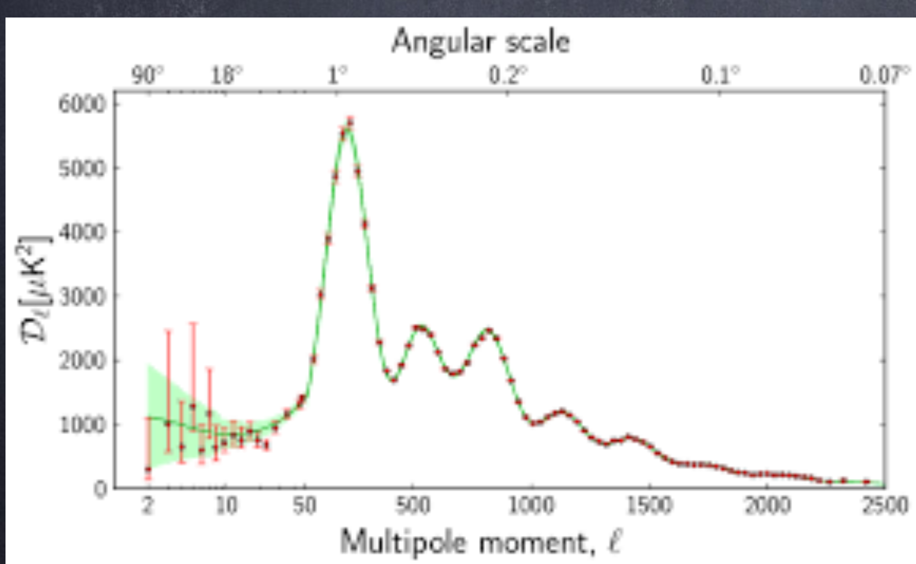

CMB theory (green line) and data (red dots) in excellent agreement

Formation and growth of structures

The ***how*** depends on gravitation and constituents

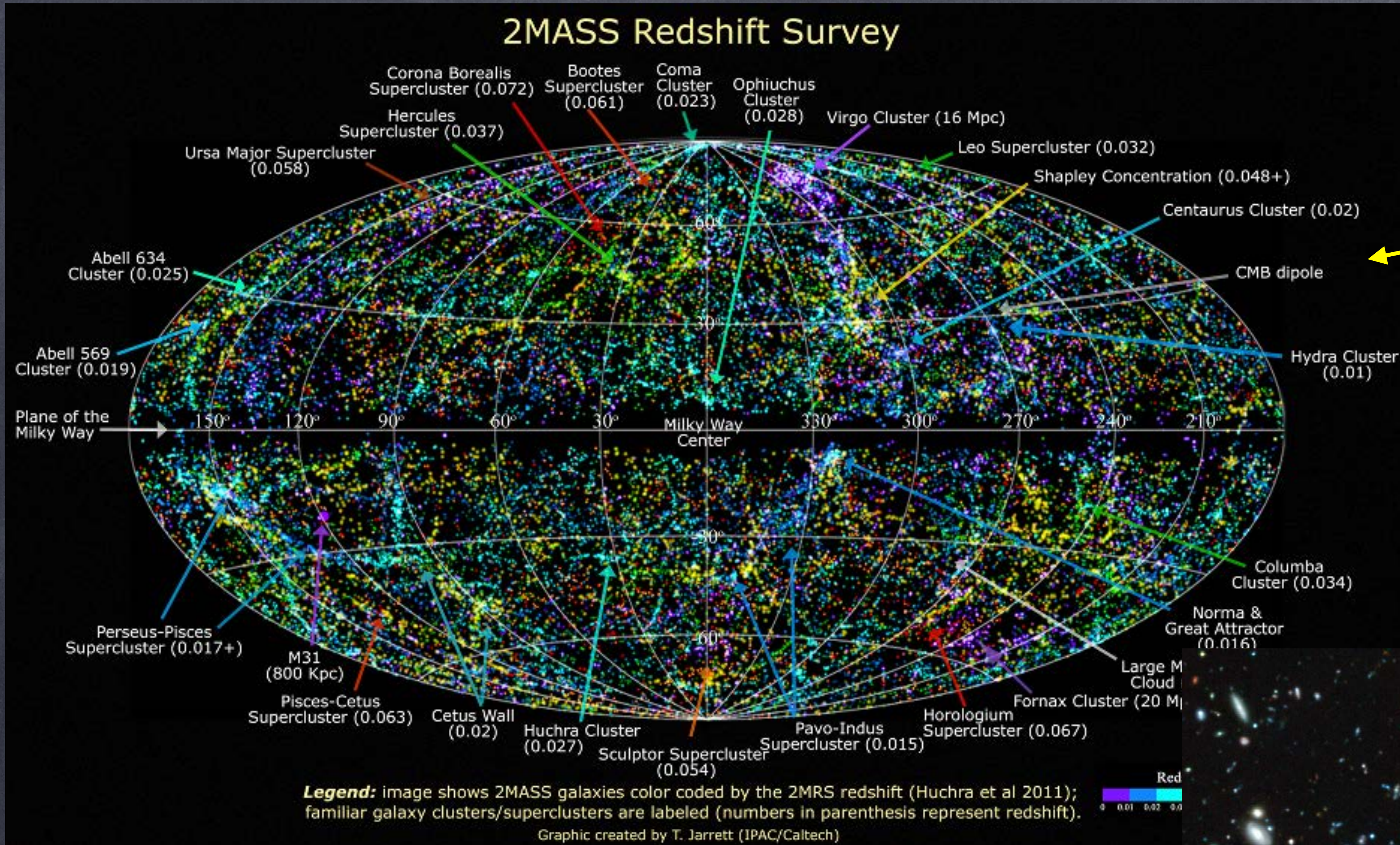

Nearby Universe

SKY IS FULL OF GALAXIES… WHAT ELSE?

Faint, high redshift Universe

Since ~90 years dealing with Dark Matter mystery…..

Die Rotverschiebung von extragalaktischen Nebeln
von **F. Zwicky.**
(16. II. 33.)
Helvetica Physica Acta, 1933, 6, 110

1933

Fritz Zwicky (1933)

was einer Geschwindigkeit von nur 10 m/sek entspricht. Um also auf diese Weise zu einer Erklärung für die grossen Streugeschwindigkeiten zu kommen, müsste man noch eine sehr viel grössere Dichte dunkler Materie zulassen als unter 1. oder 2.

Fritz Zwicky (1937)

2. We must know how much dark matter is incorporated in nebulae in the form of cool and cold stars, macroscopic and microscopic solid bodies, and gases.

1937

IV. NEBULAE AS GRAVITATIONAL LENSES

As I have shown previously,[6] the probability of the overlapping of images of nebulae is considerable. The gravitational fields of a number of "foreground" nebulae may therefore be expected to deflect the light coming to us from certain background nebulae. The observation of such gravitational lens effects promises to furnish us with the simplest and most accurate determination of nebular masses. No thorough search for these effects has as yet been undertaken. It

Finds DM & predicts Grav Lensing from cosmic structures!!

Bullet Cluster: Dark Matter!

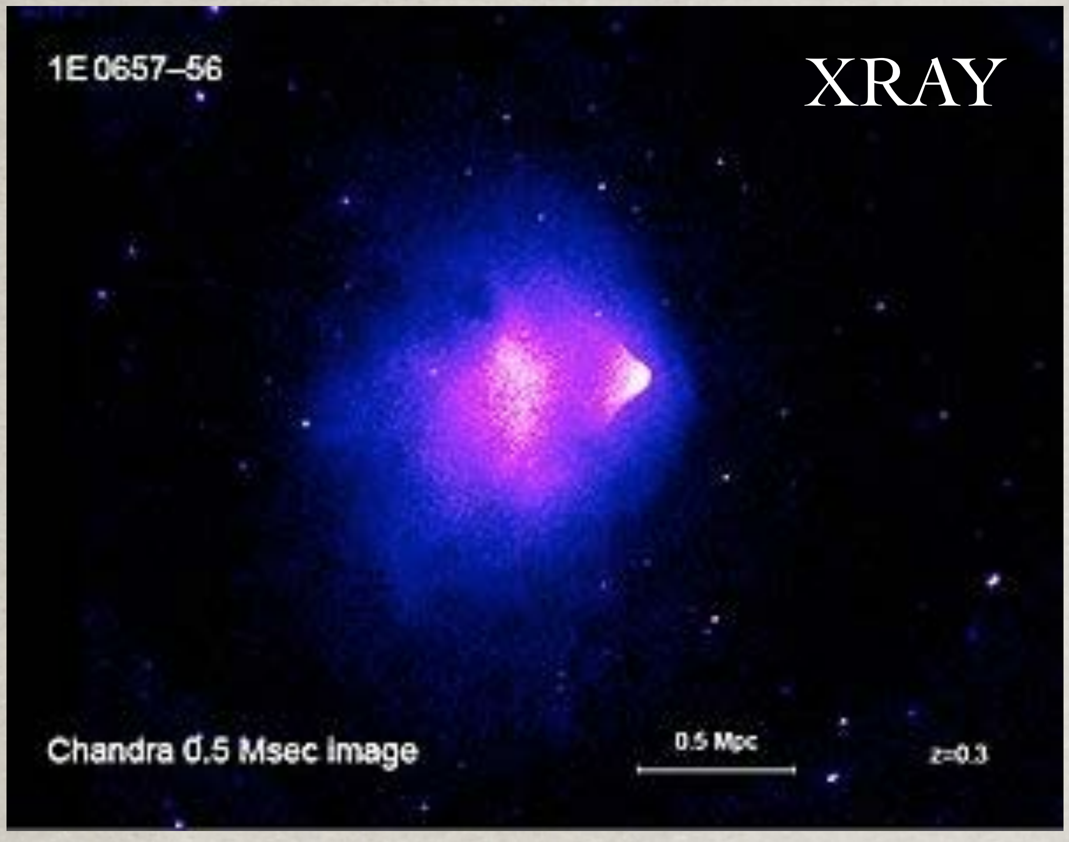

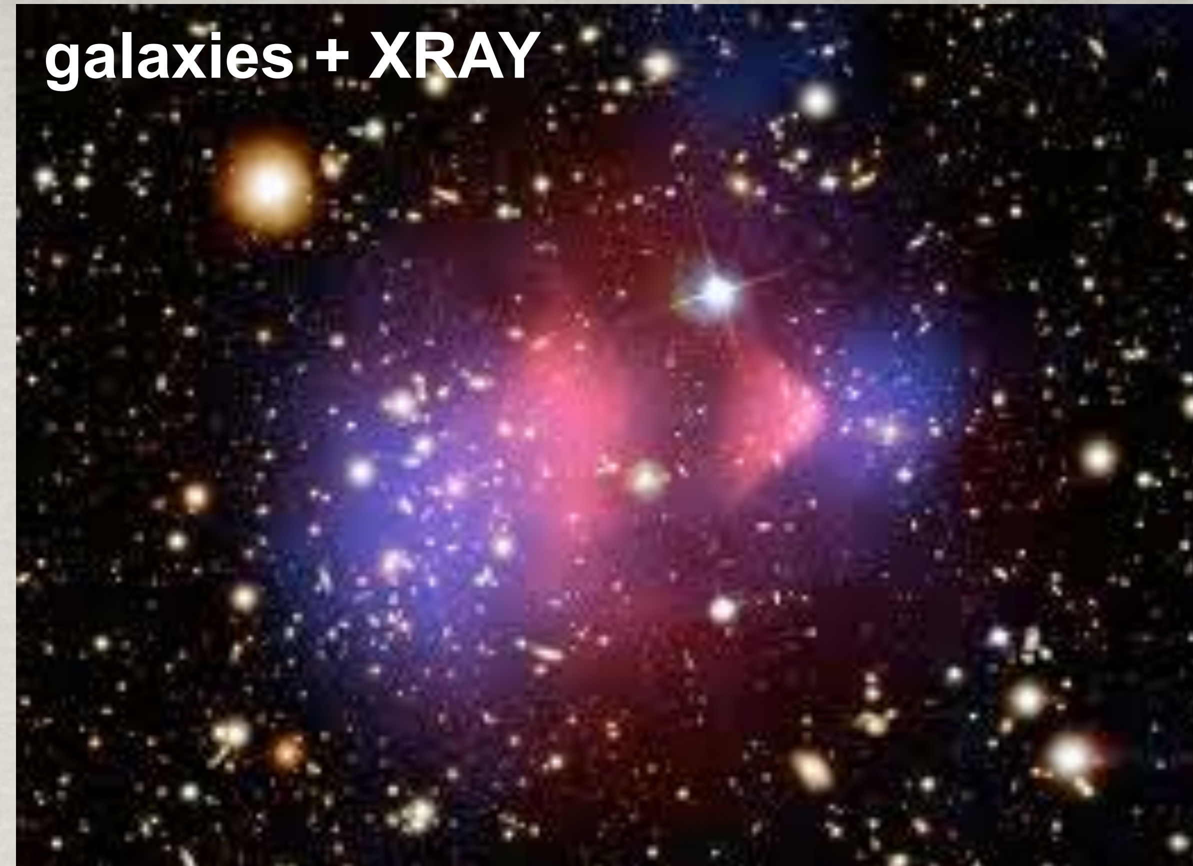

Cluster dominant mass component not hot gas nor (simple) modified gravity: $\rho_T \neq \rho_B$

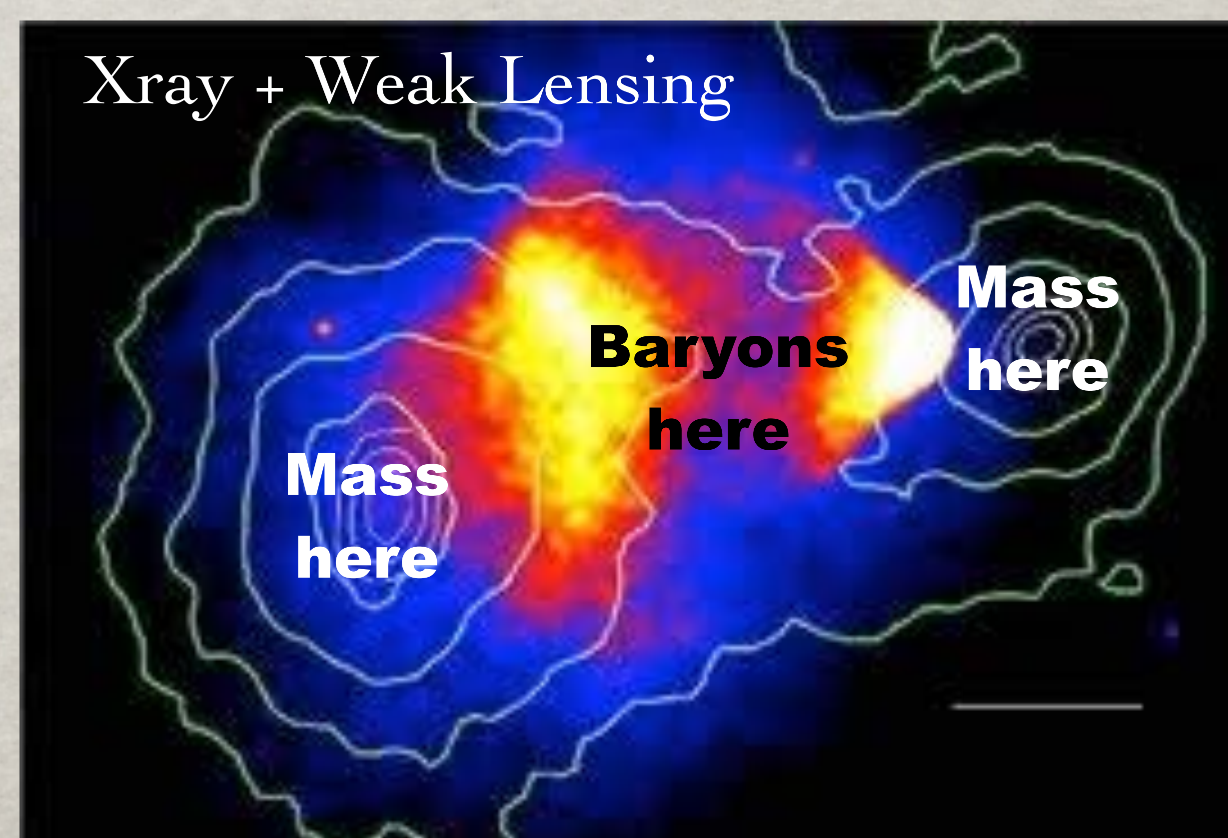

Integrated Sachs Wolfe
(will use Planck)

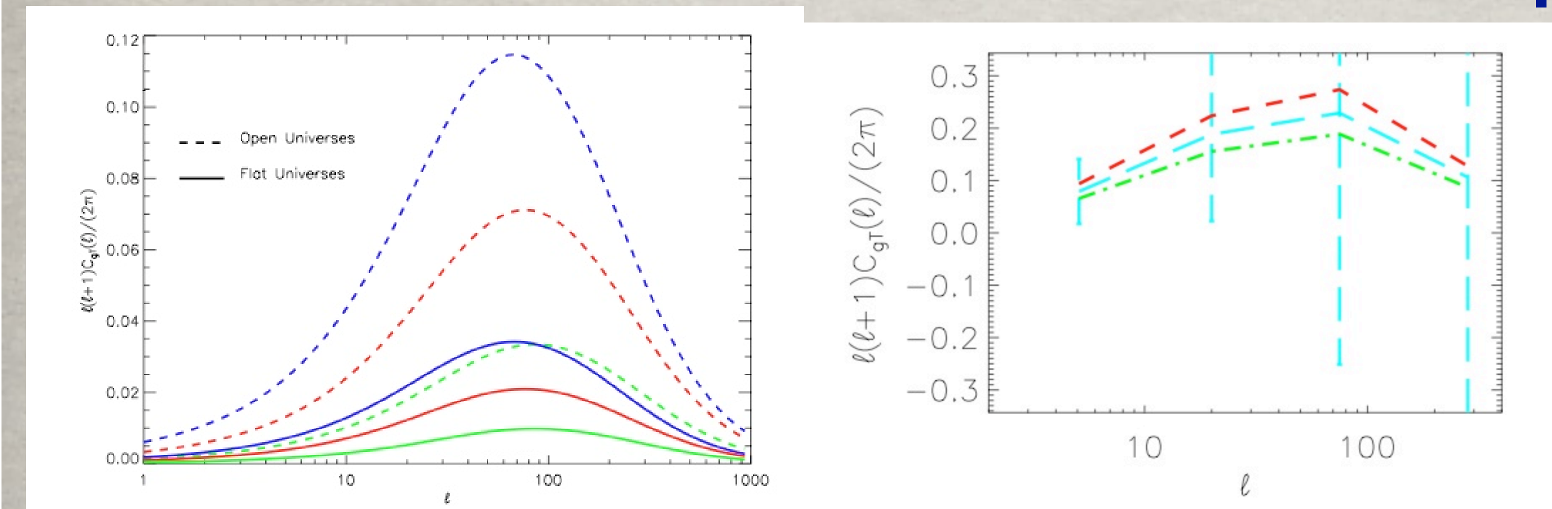

Figure 12.1: *Left Panel*: Prediction of the ISW cross-correlation signal for different values of the dark energy density ($\Omega_{DE} = 0.10$, green line; $\Omega_{DE} = 0.20$, red line; $\Omega_{DE} = 0.30$, blue line) for universes with flat geometry (solid lines) and universes with open geometry and no dark energy. The ISW signal for universes with the same matter density is larger in open universes than in flat universes. The signal is calculated for a Euclid-like photometric survey. *Right panel*: The ISW cross-correlation signal for different values of the growth parameter ($\gamma = 0.44$, green dash-dotted line; $\gamma = 0.55$, blue dashed line; $\gamma = 0.68$, e.g. a DGP model, red short dashed). *Both figures are taken from Rassat (2007).*

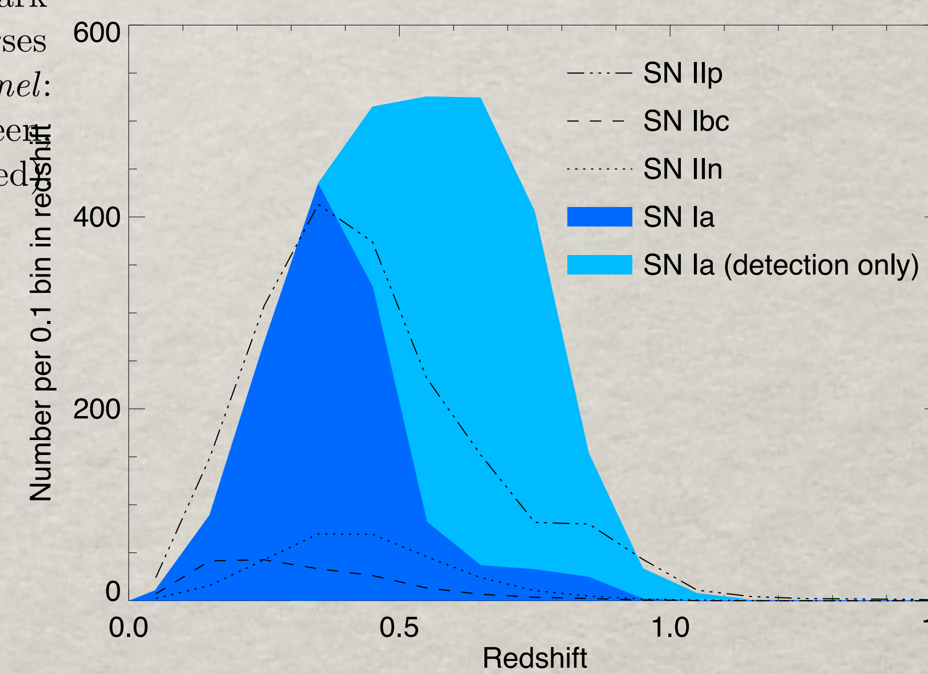

Physics and cosmology from SN [? Feasibility]

Figure 16.2: Number of SNe of various types that are expected to be detected by Euclid in the J band, as a function of redshift. Estimates for SNe of type Ia (dark blue shaded region), Ibc, IIn and IIp were provided by A. Goobar based on assumptions in Goobar *et al.* (2008), using SNe Ia rates from Dahlen *et al.* (2004) and assuming a 5 year survey that monitors a patch of 10sq deg at any time. These histograms represent the $N(z)$ for SNe with sufficient sampling to measure their lightcurve shapes (i.e. reaching 1 magnitude fainter than the peak brightness). The light-blue shaded region shows an independent estimate of the total number of SNe Ia detections including those only detected at peak luminosity, i.e. without full lightcurve measurements.

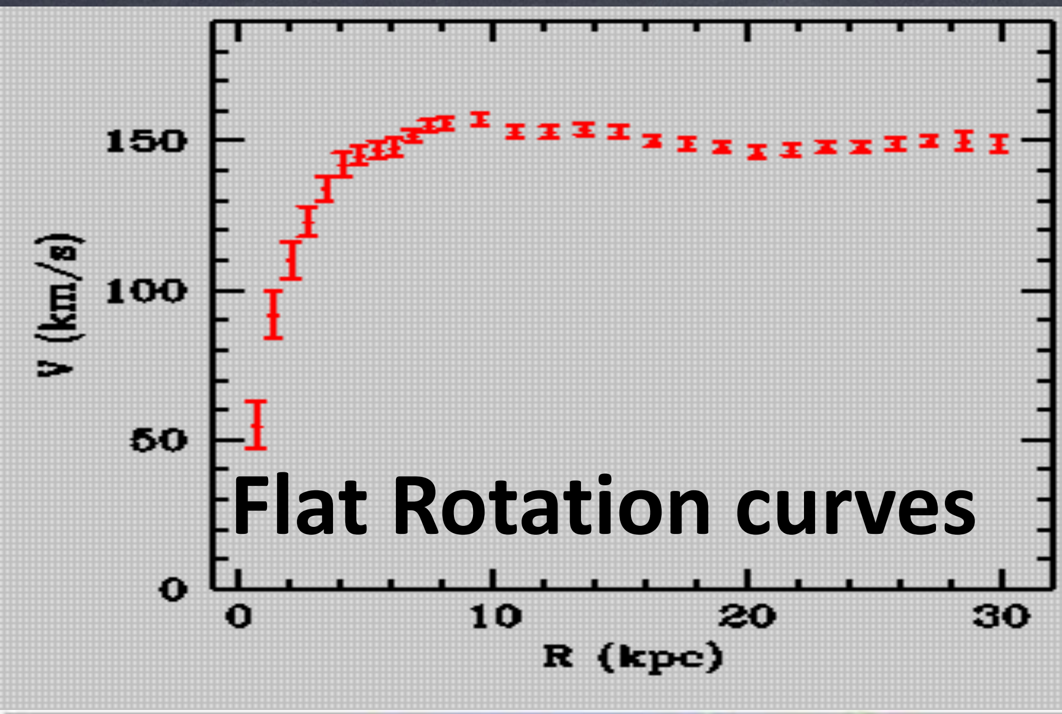

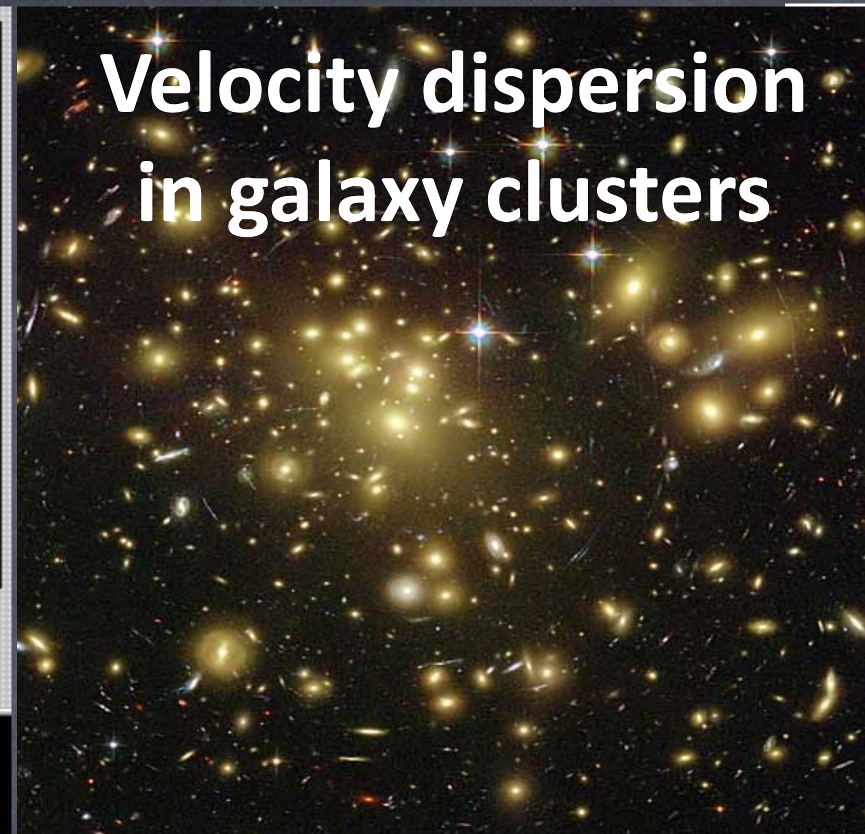

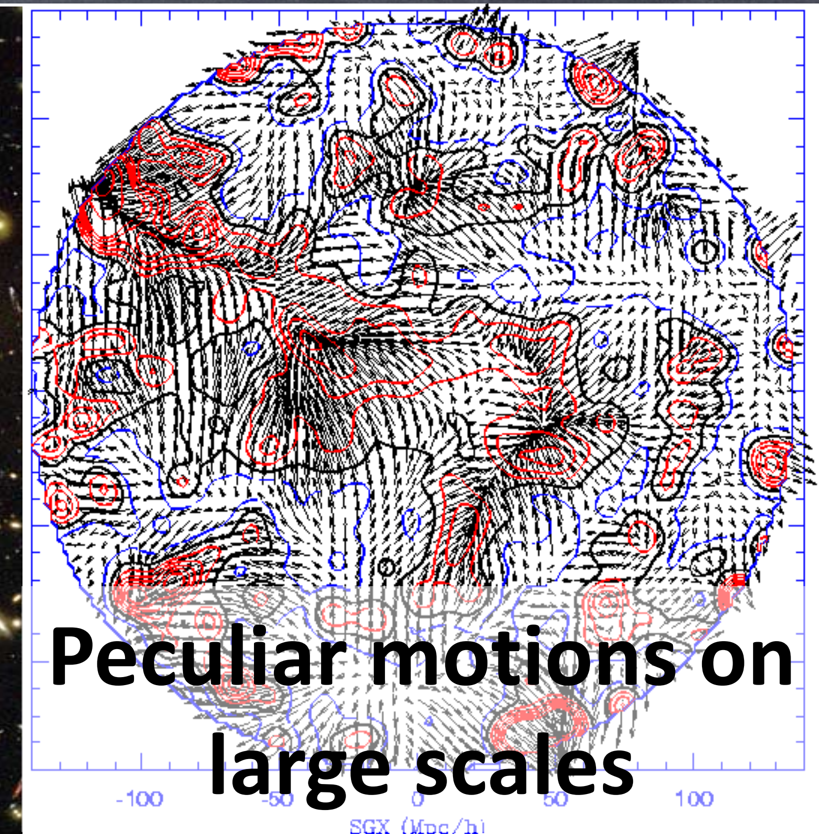

Dark Matter (indirect) evidence comes from gravity

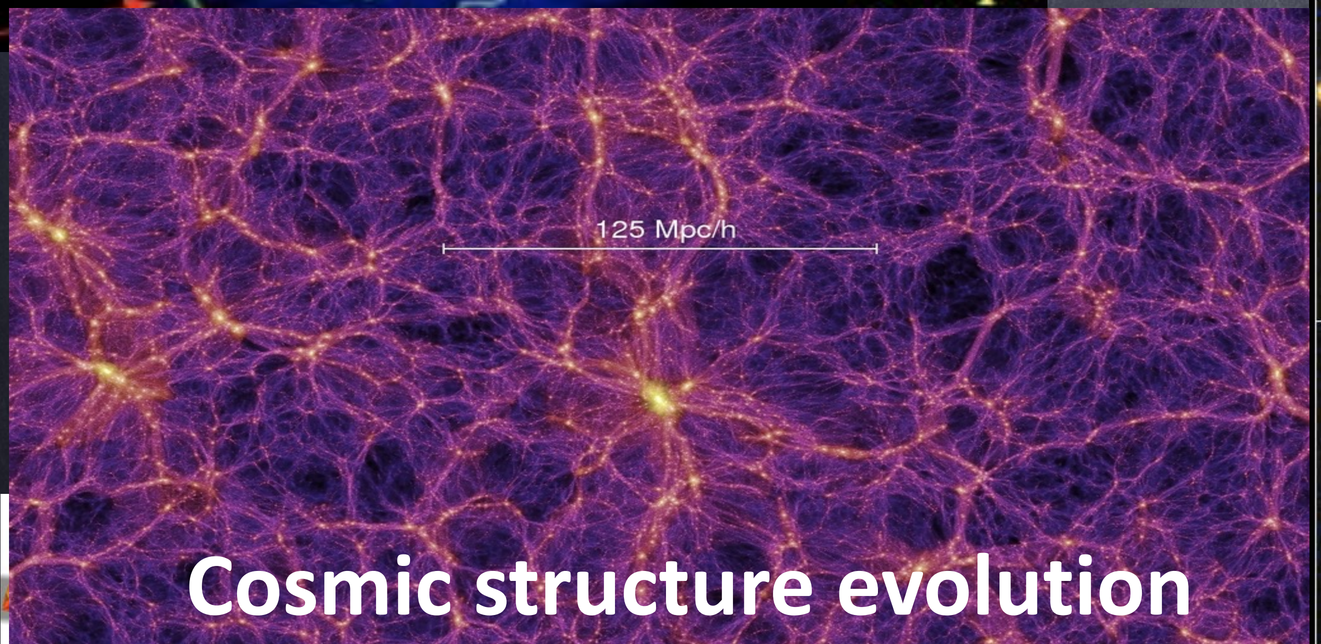

Since ~20 years dealing with another mystery.....

The Nobel Prize in Physics 2011

Photo: U. Montan
Saul Perlmutter
Prize share: 1/2

Photo: U. Montan
Brian P. Schmidt
Prize share: 1/4

Photo: U. Montan
Adam G. Riess
Prize share: 1/4

The Nobel Prize in Physics 2011 was divided, one half awarded to Saul Perlmutter, the other half jointly to Brian P. Schmidt and Adam G. Riess "*for the discovery of the accelerating expansion of the Universe through observations of distant supernovae*".

If so, why ?

What is the Universe made of ?

Current hypothesis

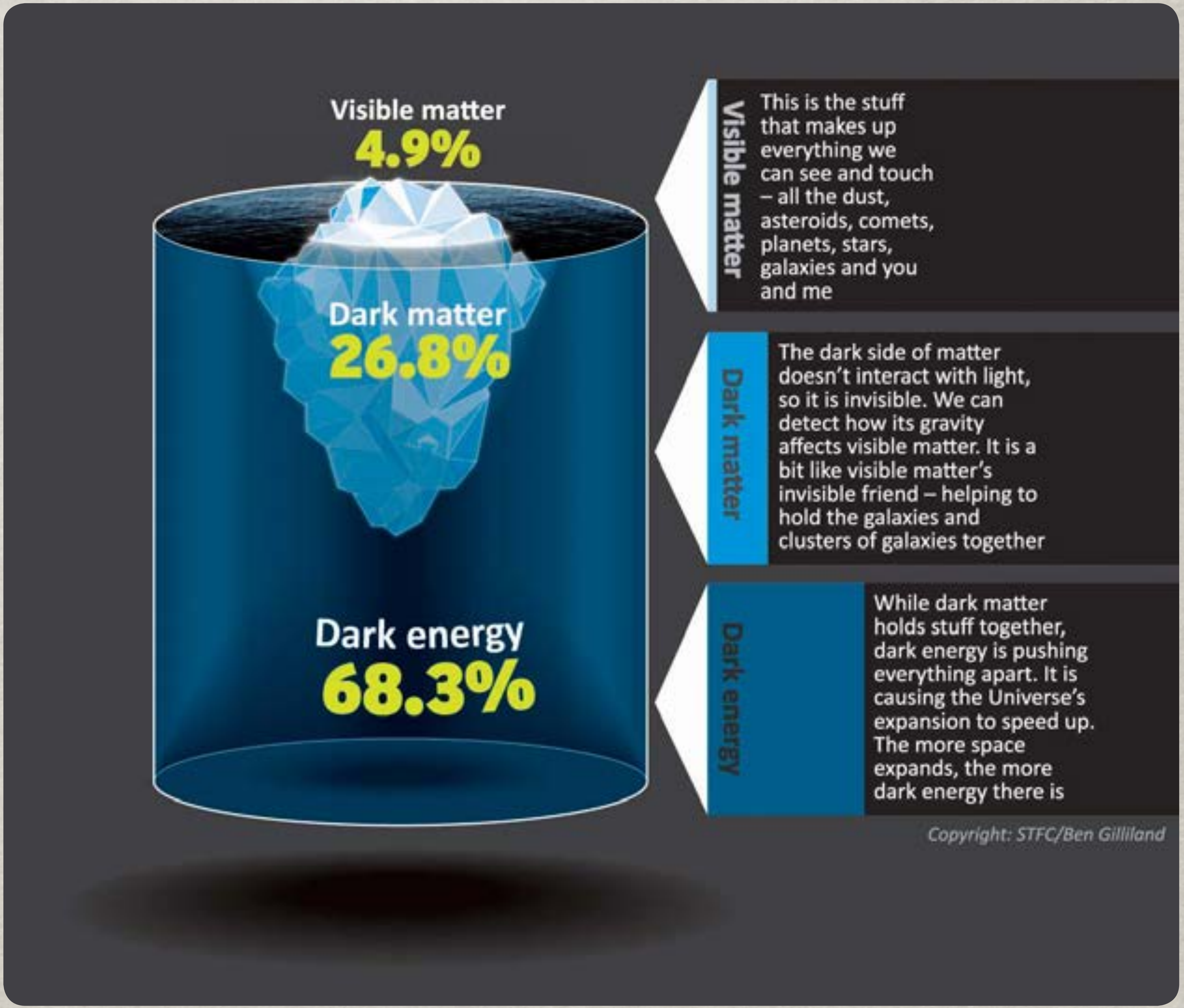

The relative abundances of the three presumed constituents of mass-energy in our Universe: visible matter, dark matter and dark energy (Credit: STFC/Ben Gilliland)

Geometrical tests: H(z)

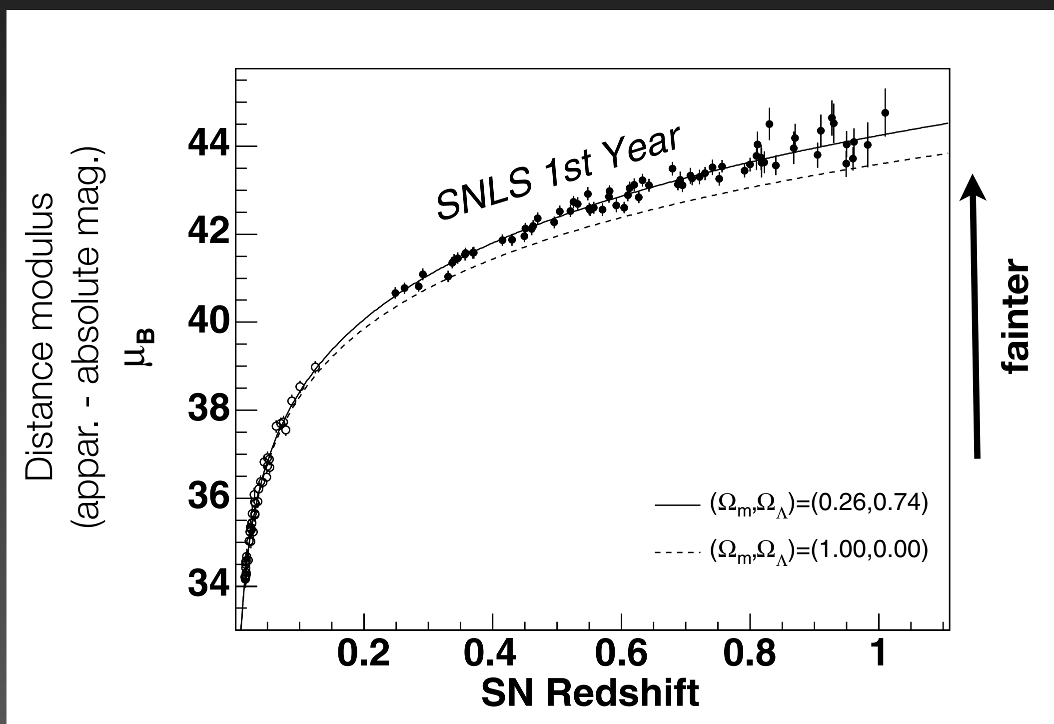

SNIa are standard candles...not!

Kilbinger

- SN have to be "standardized"
- **Brighter SN are slower**
  Origin unknown. (Nickel mass variations? anisotropic explosions?)
- **Brighter SN are bluer**
  Dust: More absorption, more reddening
- Empirical standardization method: add color (at max) and stretch parameters

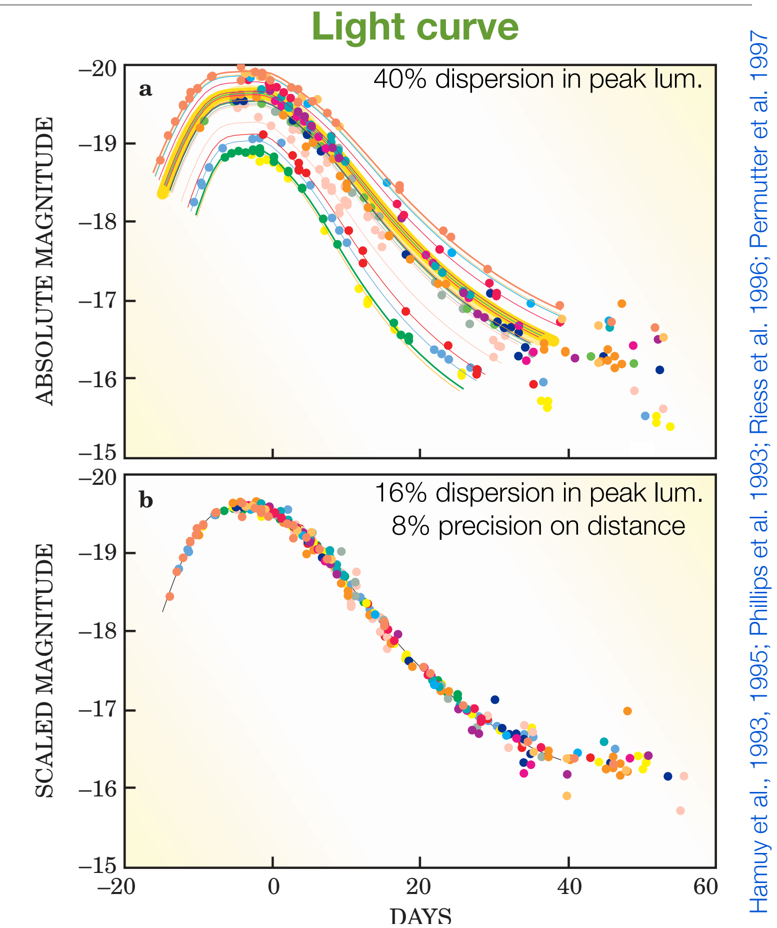

- The universe has always expanded at the current rate
- The universe contains a lot of matter (Ω_m= 6)
- The universe contains less matter (Ω_m= 1)
- The universe contains a mix of matter and "dark energy" (Ω_m= 0.27, Ω_Λ= 0.73)

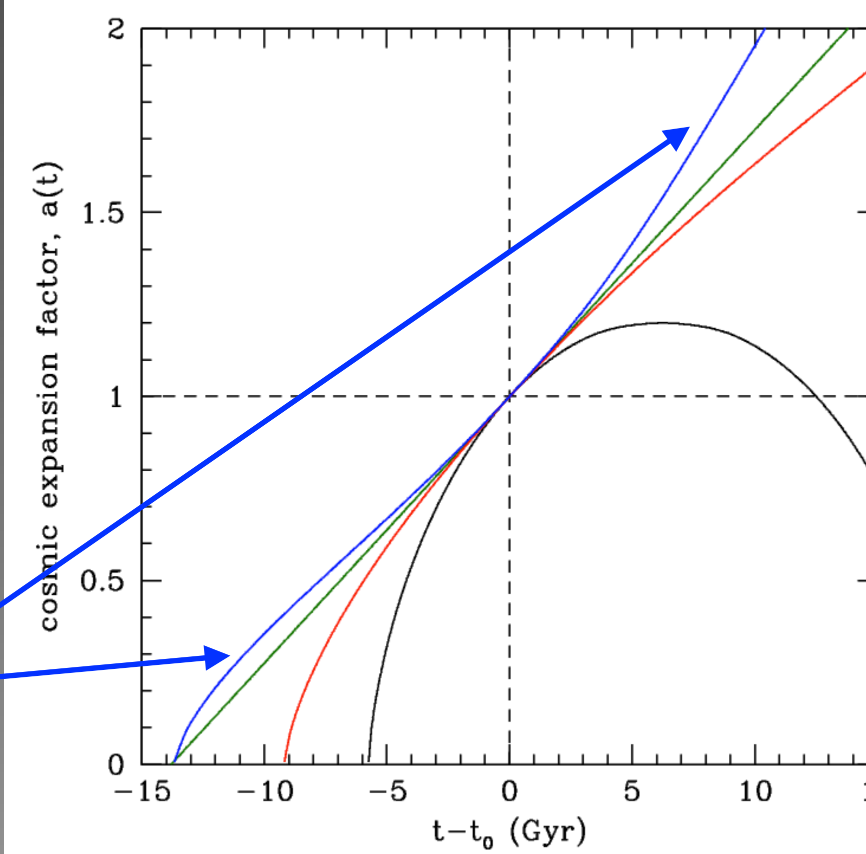

Recall

Redshift: $z=(\lambda_{obs}-\lambda_{em})/\lambda_{em}$

$1+z=a(0)/a(z)$,
$a(t)$ expansion factor

$R_{phys}=a\, r_{comov}$
$H=d[\ln(a)]/dt=\dot{a}/a$

Measure $\lambda_{obs}/\lambda_{em}=1+z$

galaxy spectra have
emission
and
absorption
lines

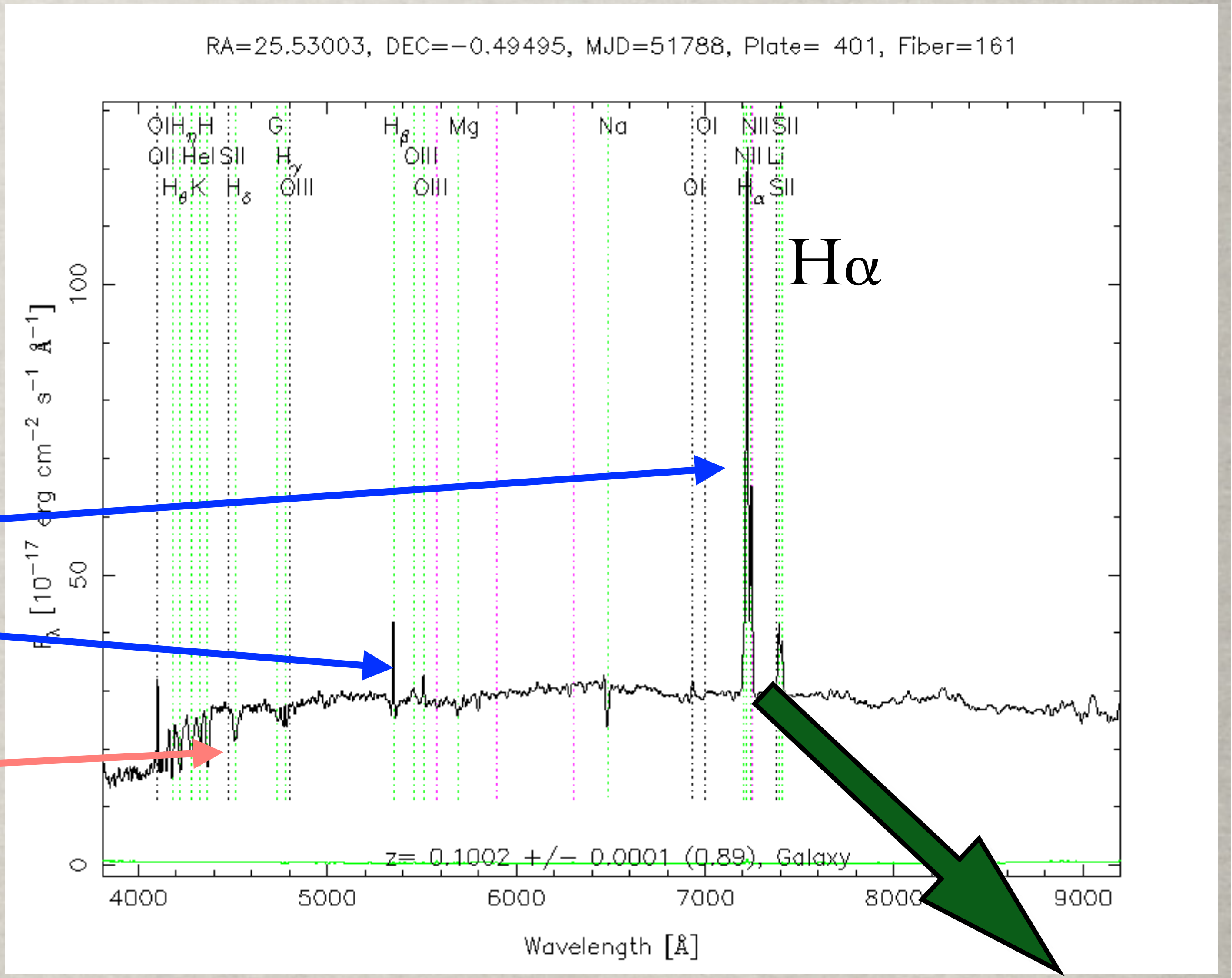

1-2 μm

Also photometric z: less precise, but deeper and easier

BAO as standard ruler

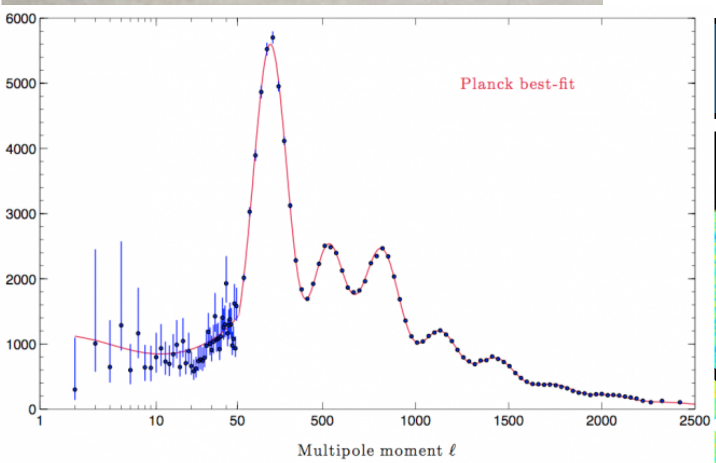

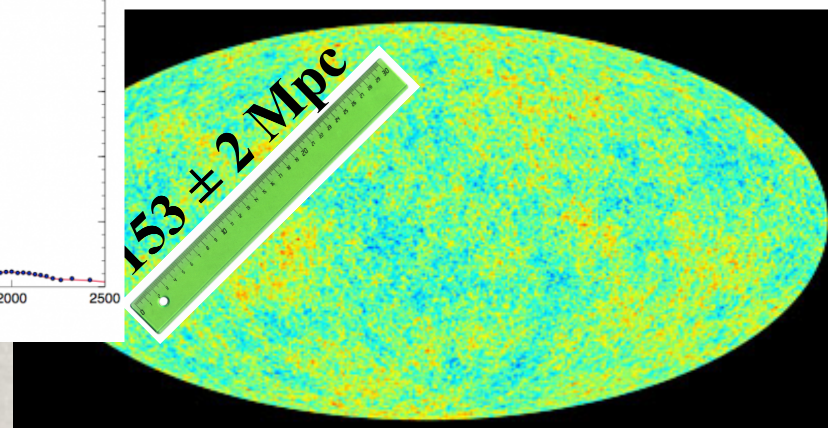

CMB (z≈1000)

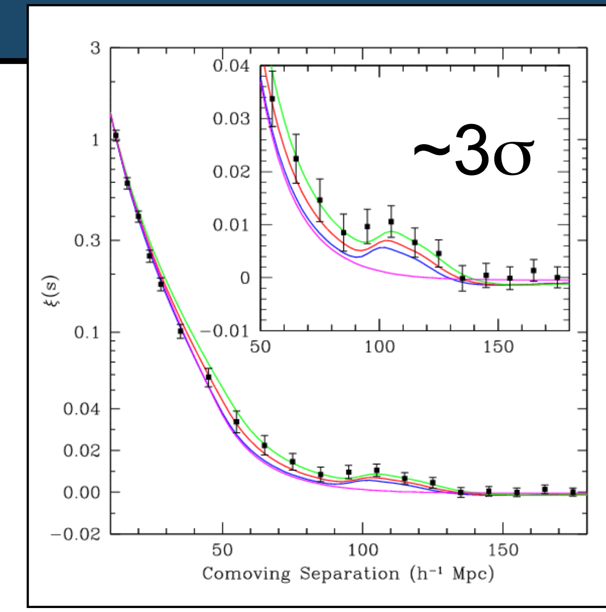

Galaxies (z>1)

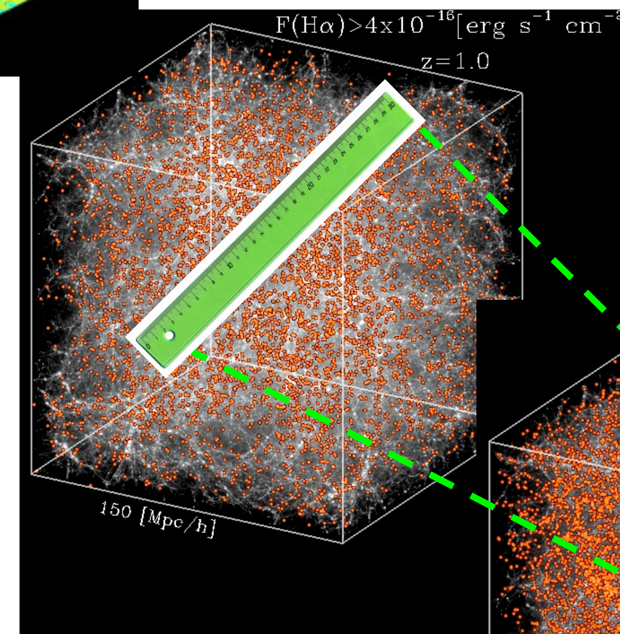

Galaxies (z≈0.35)

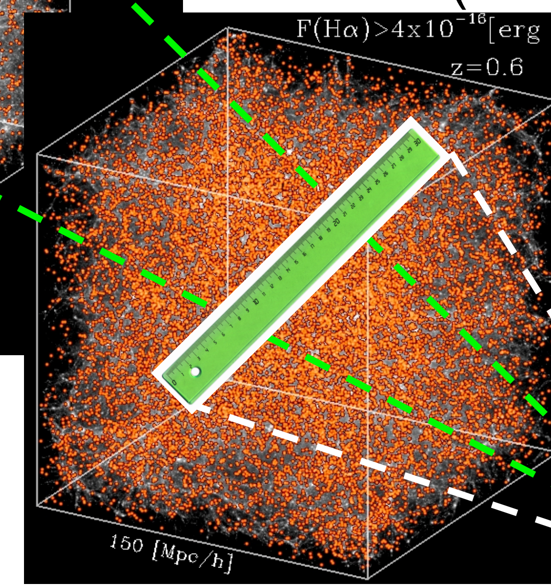

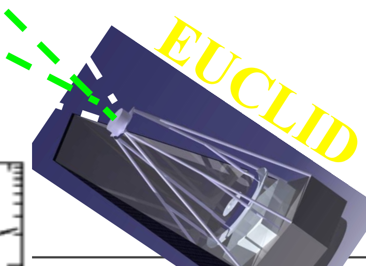

- $H(z)$ (radial)
- $D_A(z)$ (tangential)
- $H(z)$ & $D_A(z)$ depend on $w(z)$

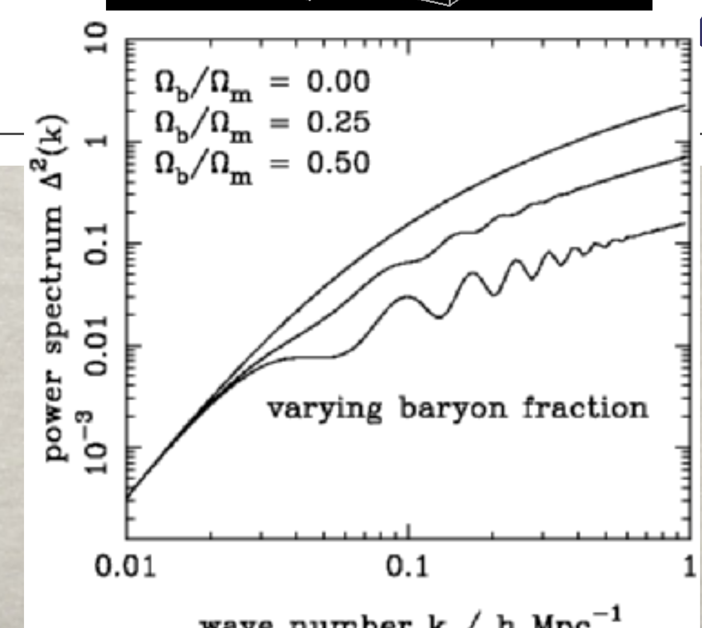

Clustering reveals features in the power spectrum of density perturbations (e.g. Ων, ν masses)

Expansion and Growth Histories through Gravitational Lensing

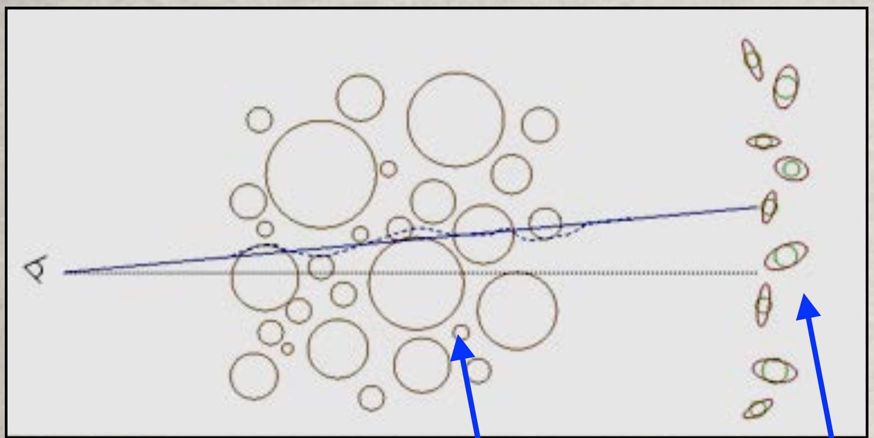

matter (mostly DM)

background galaxies

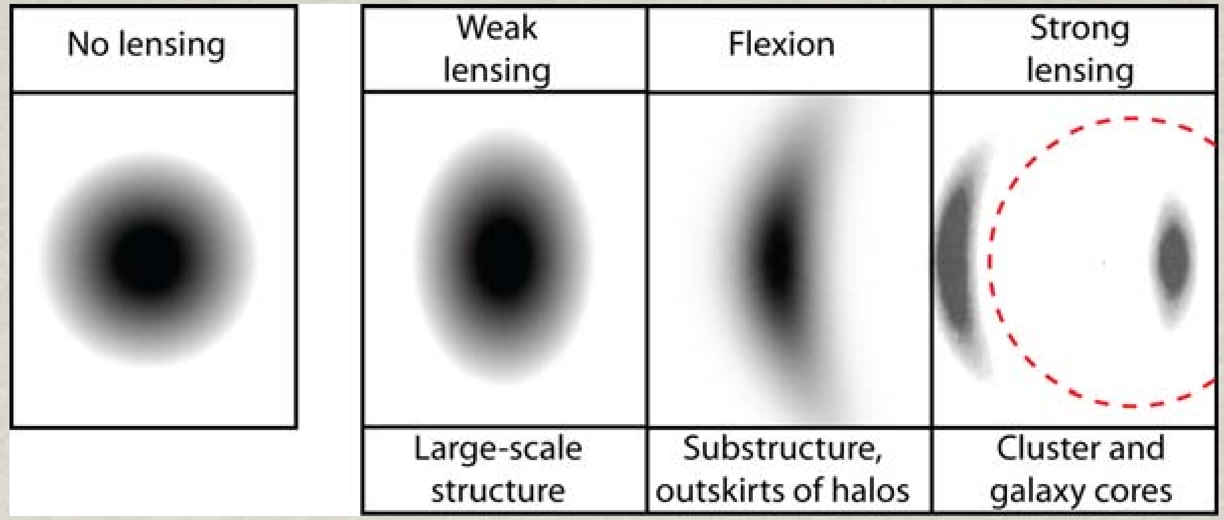

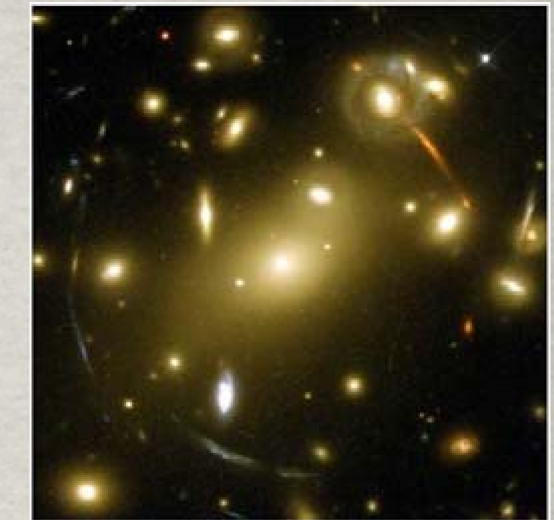

Figure 2.8: a. (Left) Illustrations of the effect of a lensing mass on a circularly symmetric image. Weak lensing elliptically distorts the image, flexion provides an arc-ness and strong lensing creates large arcs

$$\kappa = \frac{3H_0^2\Omega_m}{2c^2}\int_0^{\chi_s} d\chi \frac{D(\chi)D(\chi_s-\chi)}{\chi_s}(1+z)\delta(\chi),$$

observable

distances

density perturbation

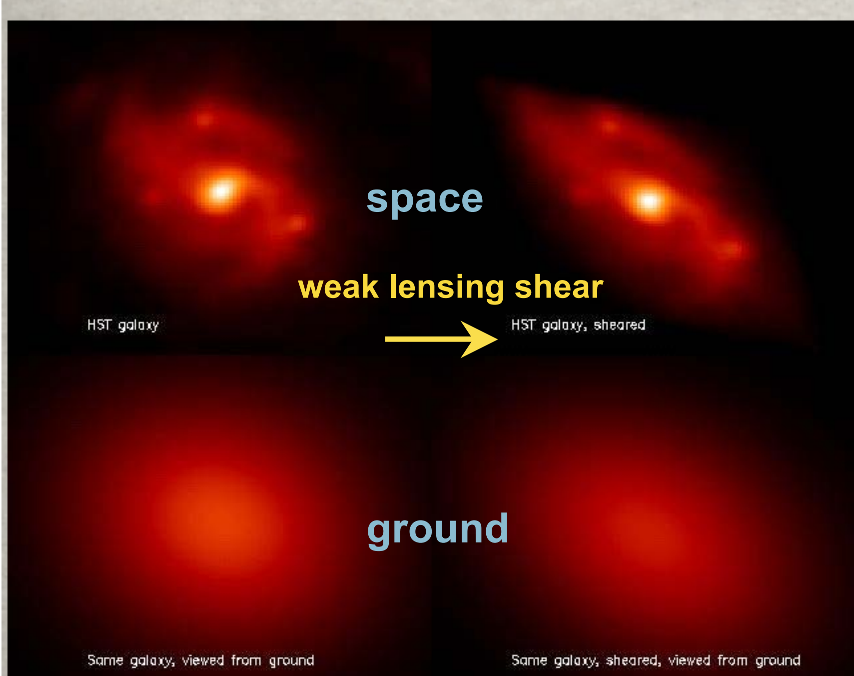

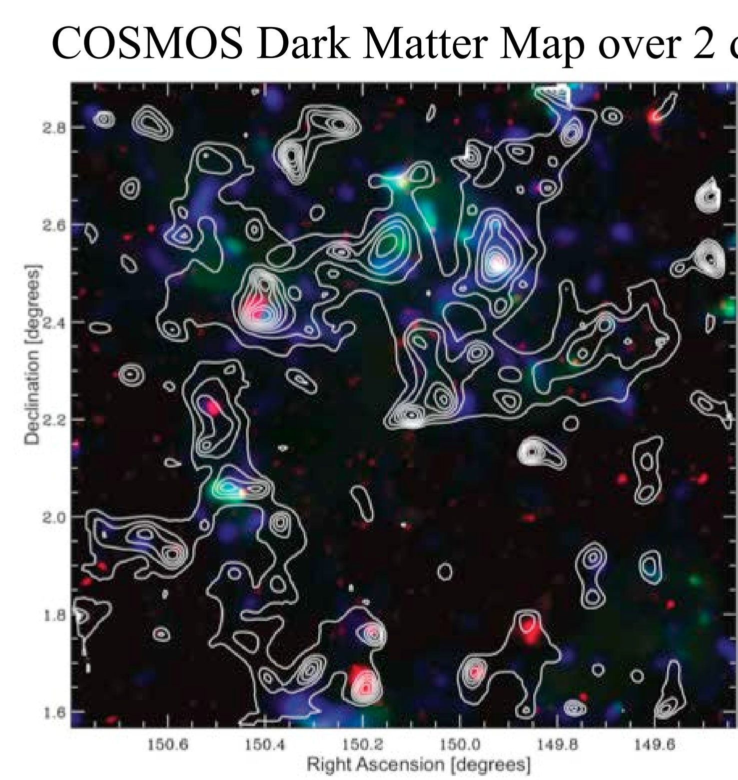

photo z

Massey et al. 2007a, Nature

Synergy with Planck: Universe @z~1000 vs @z~1-3

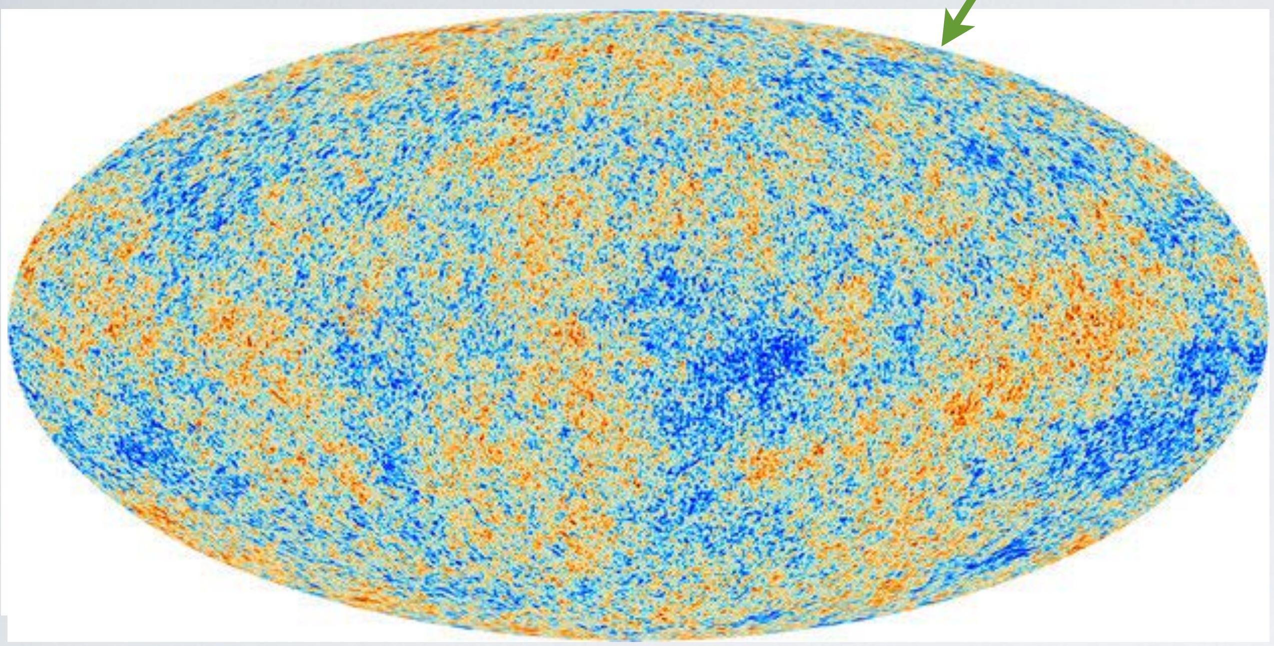

R. Teyssier et al.: Full-sky weak-lensing simulation with 70 billion particles

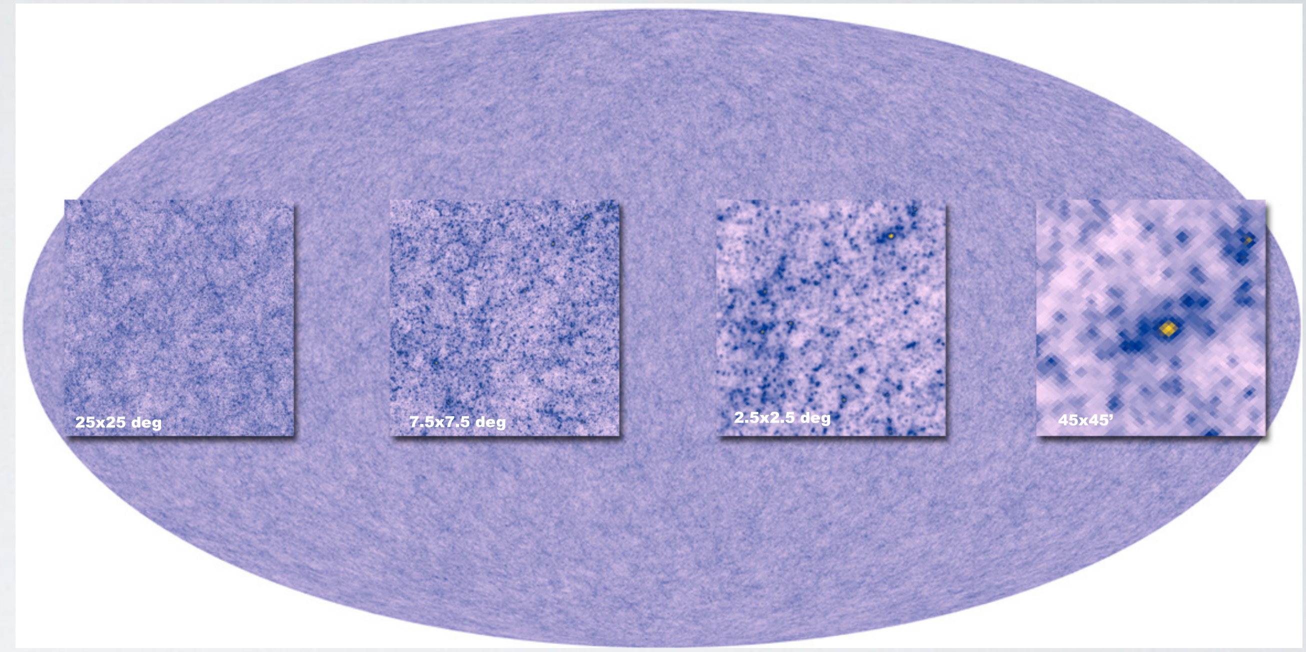

WL sims: <1" pixels

Most of the DE effects happen at z < 3

Need also <u>dynamics</u> to further disentagle

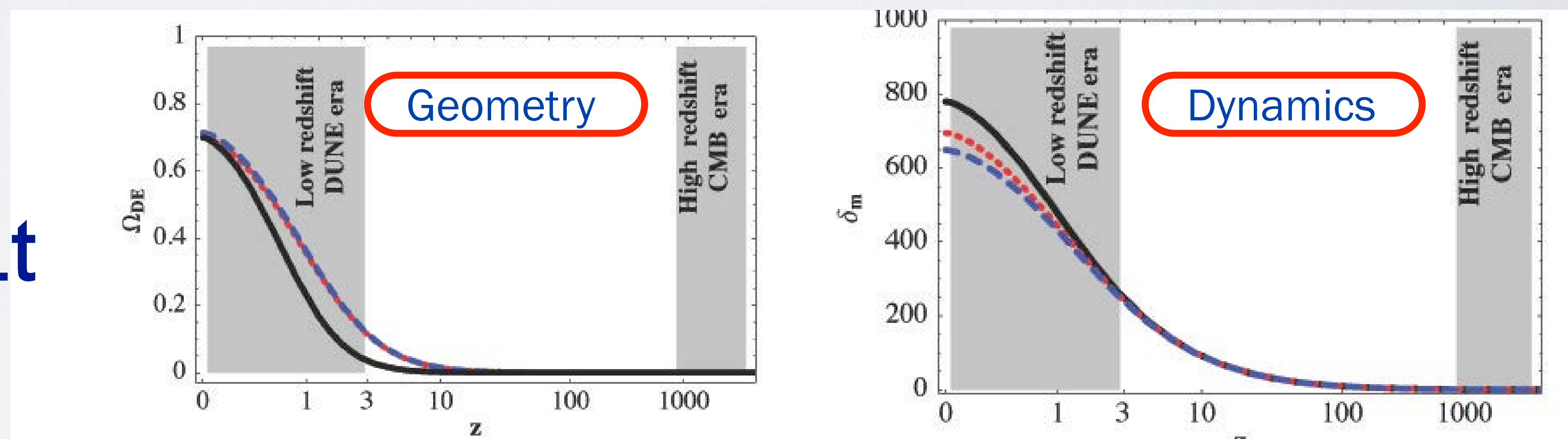

Figure C.1: *Effect of dark energy on the evolution of the Universe.* ***Left:*** *Fraction of the density of the Universe in the form of dark energy as a function of redshift z., for a model with a cosmological constant (w=-1, black solid line), dark energy with a different equation of state (w=-0.7, red dotted line), and a modified gravity model (blue dashed line). In all cases, dark energy becomes dominant in the low redshift Universe era probed by DUNE, while the early Universe is probed by the CMB.* ***Right:*** *Growth factor of cosmic structures for the same three models. Only by measuring the geometry (left panel) and the growth of structure (right panel) at low redshifts can a modification of dark energy be distinguished from that of gravity. Weak lensing measures both effects.*

ΛCDM model

Many parameters, lots of Physics

Planck Collaboration Cosmological parameters[14]

	Description	Symbol	Value
Independent parameters	Physical baryon density parameter[a]	$\Omega_b h^2$	0.022 30 ±0.000 14
	Physical dark matter density parameter[a]	$\Omega_c h^2$	0.1188 ±0.0010
	Age of the universe	t_0	13.799 ±0.021 × 10^9 years
	Scalar spectral index	n_s	0.9667 ±0.0040
	Curvature fluctuation amplitude, $k_0 = 0.002\ \mathrm{Mpc}^{-1}$	Δ^2_R	$2.441^{+0.088}_{-0.092} \times 10^{-9}$[17]
	Reionization optical depth	τ	0.066 ±0.012
Fixed parameters	Total density parameter[b]	Ω_{tot}	1
	Equation of state of dark energy	w	−1
	Sum of three neutrino masses	Σm_ν	0.06 eV/c^2[c][13]:40
	Effective number of relativistic degrees of freedom	N_{eff}	3.046[d][13]:47
	Tensor/scalar ratio	r	0
	Running of spectral index	$d\,n_s / d \ln k$	0
Calculated values	Hubble constant	H_0	67.74 ±0.46 km s^{-1} Mpc^{-1}
	Baryon density parameter[b]	Ω_b	0.0486 ±0.0010[e]
	Dark matter density parameter[b]	Ω_c	0.2589 ±0.0057[f]
	Matter density parameter[b]	Ω_m	0.3089 ±0.0062
	Dark energy density parameter[b]	Ω_Λ	0.6911 ±0.0062
	Critical density	ρ_{crit}	(8.62 ±0.12) × 10^{-27} kg/m^3[g]
	Fluctuation amplitude at $8h^{-1}$ Mpc	σ_8	0.8159 ±0.0086
	Redshift at decoupling	z_*	1 089.90 ±0.23
	Age at decoupling	t_*	377 700 ±3200 years[17]
	Redshift of reionization (with uniform prior)	z_{re}	$8.5^{+1.0}_{-1.1}$[18]

Parameter values listed below are from the Planck Collaboration Cosmological parameters 68% confidence limits for the base ΛCDM model from Planck CMB power spectra, in combination with lensing reconstruction and external data (BAO+JLA+H_0).[13] See also Planck (spacecraft).

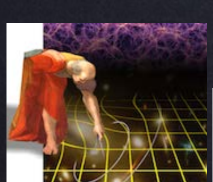

Open Questions in Cosmology

"precise" Cosmology

- Nature of the Dark Energy
- Nature of the Dark Matter
- Initial conditions (Inflation Physics)
- Modifications to Gravity
- Formation and Evolution of Galaxies

Large ignorance on ~95% of Universe content !!

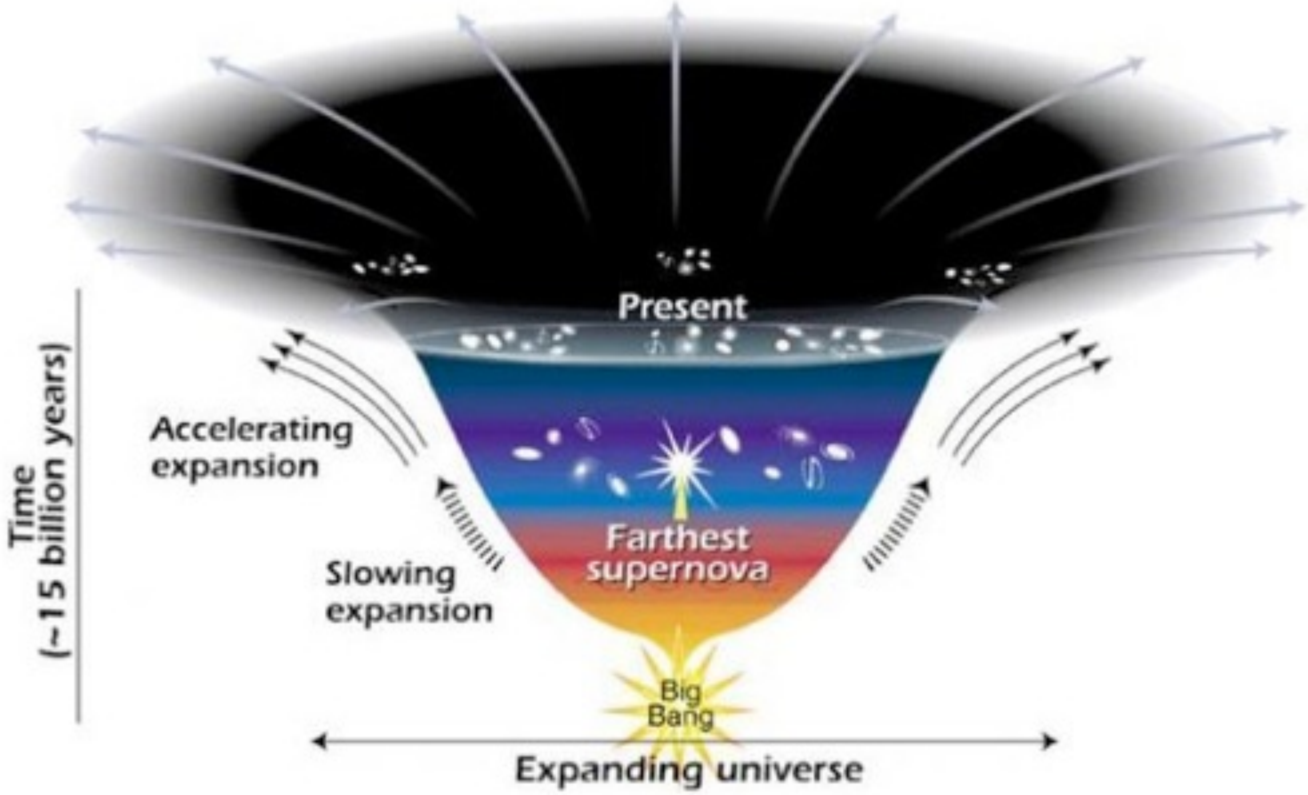

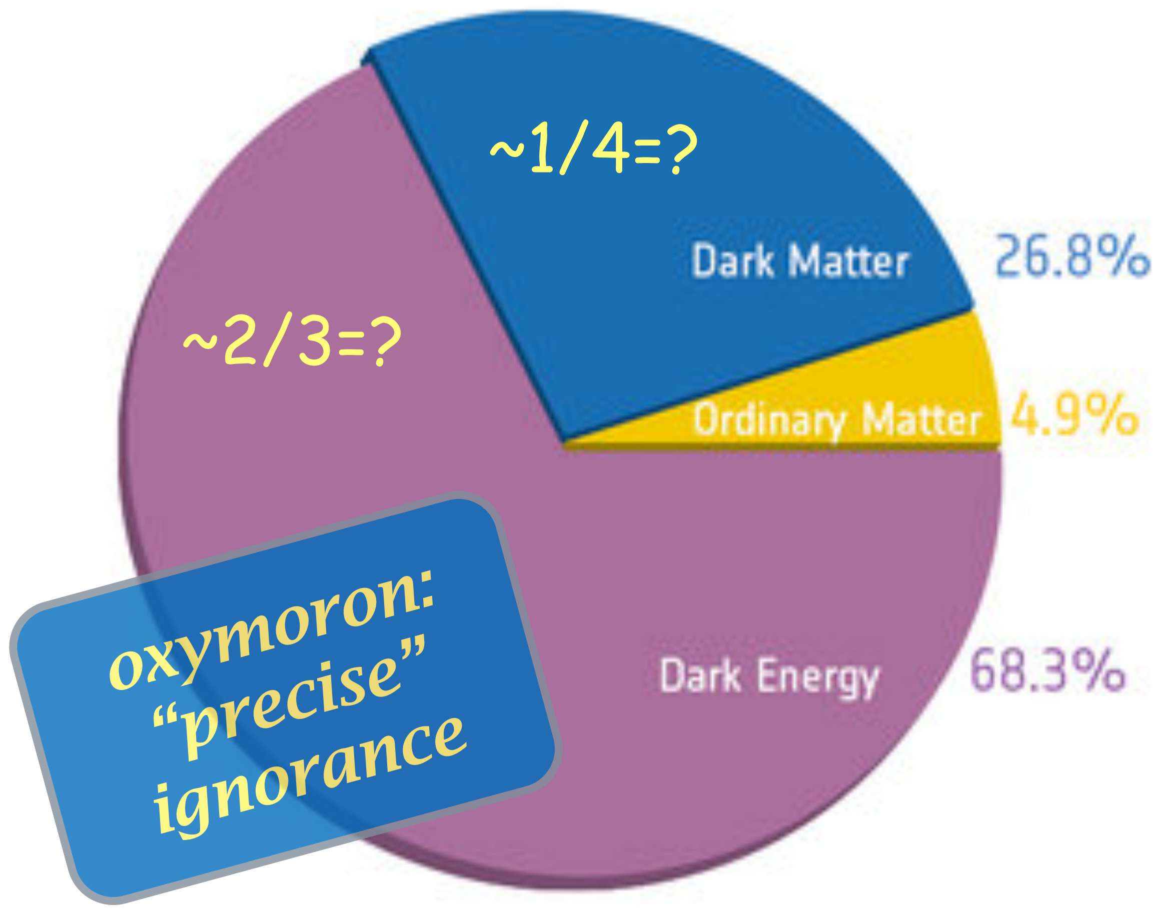

New Worlds, New Horizons in Astronomy and Astrophysics (Decadal Survey 2010)

Ground Projects – Large – in Rank Order

Large Synoptic Survey Telescope (LSST)

LSST is a multipurpose observatory that will explore the nature of dark energy and the behavior of dark matter and will robustly explore aspects of the time-variable universe that will certainly lead to new discoveries. LSST addresses a large number of the science questions highlighted in this report. An 8.4-meter optical telescope to be sited in Chile, LSST will image the entire available sky every 3 nights.

TABLE ES.3 Ground: Recommended Activities—Large Scale (Priority Order)

Recommendation[b]	Science	Technical Risk[c]	Appraisal of Costs Through Construction[a] (U.S. Federal Share 2012-2021)	Appraisal of Annual Operations Costs[d] (U.S. Federal Share)	Page Reference
1. LSST - Science late 2010s - NSF/DOE	Dark energy, dark matter, time-variable phenomena, supernovas, Kuiper belt and near-Earth objects	Medium low	\$465M (\$421M)	\$42M (\$28M)	7-29

Space Projects – Large – in Rank Order

Wide Field Infrared Survey Telescope (WFIRST)

A 1.5-meter wide-field-of-view near-infrared-imaging and low-resolution-spectroscopy telescope, WFIRST will settle fundamental questions about the nature of dark energy, the discovery of which was one of the greatest achievements of U.S. telescopes in recent years. It will employ three distinct techniques—measurements of weak gravitational lensing, supernova distances, and baryon acoustic oscillations—to determine the effect of dark energy on the evolution of the universe. An equally

TABLE ES.5 Space: Recommended Activities—Large-Scale (Priority Order)

Recommendation	Launch Date[b]	Science	Technical Risk[c]	Appraisal of Costs[a]: Total (U.S. share)	Appraisal of Costs[a]: U.S. share 2012-2021	Page Reference
1. WFIRST - NASA/DOE collaboration	2020	Dark energy, exoplanets, and infrared survey-science	Medium low	\$1.6B	\$1.6B	7-17

DE as TOP priority both for Ground and Space also across the Atlantic

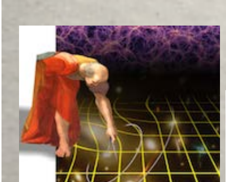

9. Dark Energy

Together with Dark Matter, Dark Energy – the hypothetical form of energy behind the Universe's accelerated expansion – constitutes the least-understood component of the cosmos. It is studied via large galaxy-survey campaigns (both satellite-based and ground-based) that combine spectroscopic, photometric and weak-lensing techniques to reconstruct the growth of cosmic structures.

APPEC supports the forthcoming ESA Euclid satellite mission, which will establish clear European leadership in space-based Dark Energy research. Because of their complementarity to Euclid, APPEC encourages continued European participation in the US-led DESI and LSST ground-based research projects. To benefit fully from the combined power of satellite-based and ground-based experiments, the exchange of data is essential.

In a number of countries, the scope of astroparticle physics has recently been expanded to include experiments targeted at a better, more detailed understanding of Dark Energy and the CMB. These are important topics in their own right, but each also provides independent and often complementary information on subjects such as neutrino properties and the overall composition and evolution of our Universe. With upcoming Dark Energy facilities on the ground (DESI and LSST) and in space (Euclid) offering performance improvements of an order of magnitude compared with their precursors, and with next-generation CMB research directed specifically at the discovery of B-mode polarisation – the tell-tale signal of the period of inflation in the very early Universe – ground-breaking discoveries are anticipated.

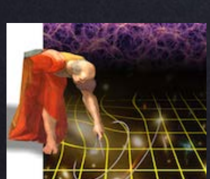

Giga structures/years/pc/samples....

Giga €...

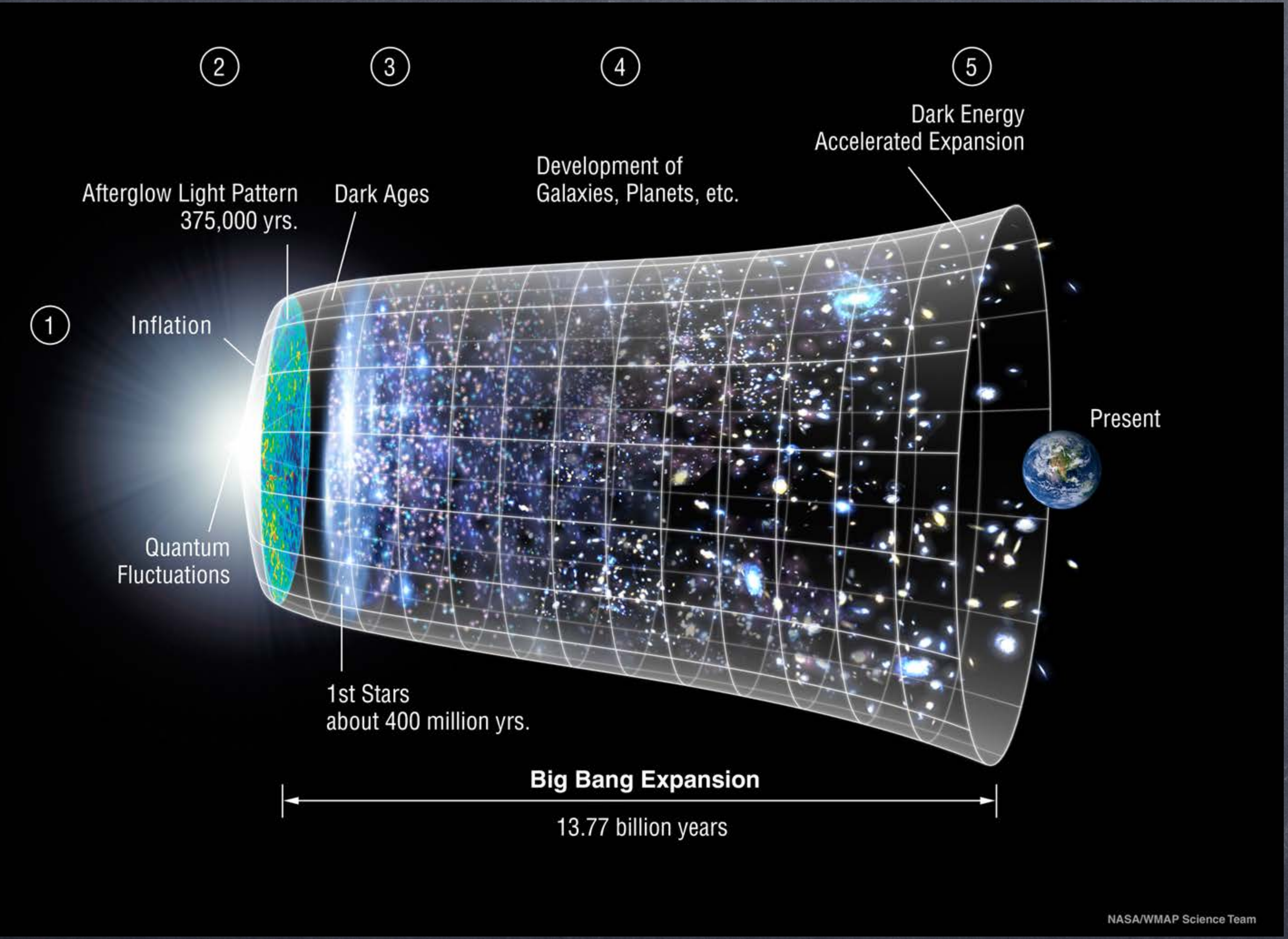

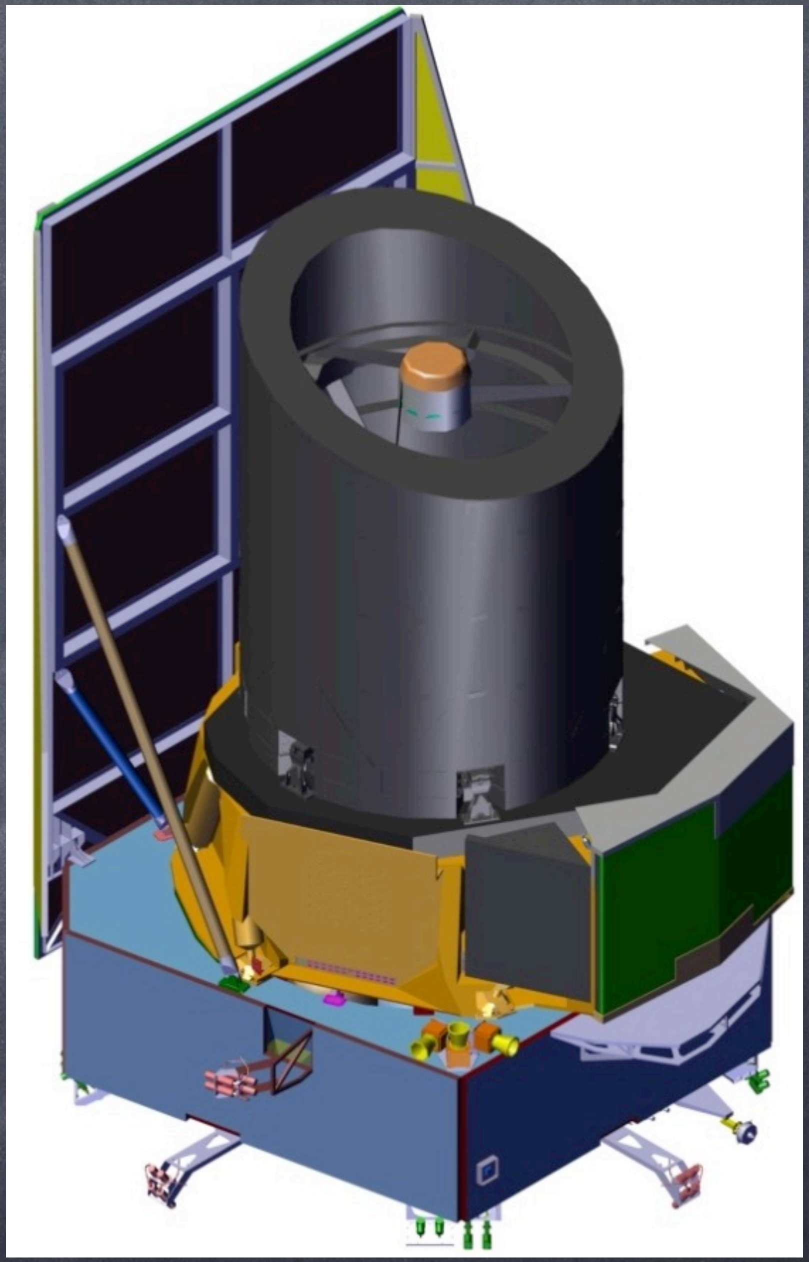

Observed with a **mini** structure: mirror ~1.2 m ∅

EUCLID

1. Why
2. How
3. When

1. Dark Energy & Dark Matter (Cosmology) ; Legacy science
2. Space imaging (morphology & NIR) + Spectra: Grav. Lensing & Clustering
3. 2023-2029+ (6y mission +)

Main Scientific Objectives
Understand the nature of Dark Energy and Dark Matter by: • Reach a dark energy *FoM* > 400 using only weak lensing and galaxy clustering; this roughly corresponds to 1 sigma errors on w_p and w_a of 0.02 and 0.1, respectively. • Measure γ, the exponent of the growth factor, with a 1 sigma precision of < 0.02, sufficient to distinguish General Relativity and a wide range of modified-gravity theories • Test the Cold Dark Matter paradigm for hierachical structure formation, and measure the sum of the neutrino masses with a 1 sigma precision better than 0.03eV. • Constrain n_s, the spectral index of primordial power spectrum, to percent accuracy when combined with Planck, and to probe inflation models by measuring the non-Gaussianity of initial conditions parameterised by f_{NL} to a 1 sigma precision of ~2.

SURVEYS		
	Area (deg2)	Description
Wide Survey	15,000 (required) 20,000 (goal)	Step and stare with 4 dither pointings per step.
Deep Survey	40	In at least 2 patches of > 10 deg^2 2 magnitudes deeper than wide survey

PAYLOAD					
Telescope	1.2 m Korsch, 3 mirror anastigmat, f=24.5 m				
Instrument	VIS	NISP			
Field-of-View	0.787×0.709 deg^2	0.763×0.722 deg^2			
Capability	Visual Imaging	NIR Imaging Photometry			NIR Spectroscopy
Wavelength range	550– 900 nm	Y (920-1146nm),	J (1146-1372 nm)	H (1372-2000nm)	1100-2000 nm
Sensitivity	24.5 mag 10σ extended source	24 mag 5σ point source	24 mag 5σ point source	24 mag 5σ point source	$3\ 10^{-16}$ erg cm-2 s-1 3.5σ unresolved line flux
Detector Technology	36 arrays 4k×4k CCD	16 arrays 2k×2k NIR sensitive HgCdTe detectors			
Pixel Size Spectral resolution	0.1 arcsec	0.3 arcsec			0.3 arcsec R=250

SPACECRAFT	
Launcher	Soyuz ST-2.1 B from Kourou
Orbit	Large Sun-Earth Lagrange point 2 (SEL2), free insertion orbit
Pointing	25 mas relative pointing error over one dither duration 30 arcsec absolute pointing error
Observation mode	Step and stare, 4 dither frames per field, VIS and NISP common FoV = 0.54 deg^2
Lifetime	7 years
Operations	4 hours per day contact, more than one groundstation to cope with seasonal visibility variations;
Communications	maximum science data rate of 850 Gbit/day downlink in K band (26GHz), steerable HGA

Budgets and Performance				
	Mass (kg)		*Nominal Power (W)*	
industry	TAS	Astrium	TAS	Astrium
Payload Module	897	696	410	496
Service Module	786	835	647	692
Propellant	148	232		
Adapter mass/ Harness and PDCU losses power	70	90	65	108
Total (including margin)	[illegible]	**2160**	**1368**	**1690**

All data you need to know (Red Book, some changes)

- Wide Area (>10^4 sq deg)
- Wide Field (FoV > 0.5 sq deg)
- Opt. imaging
- NIR photom
- NIR slitless

Two instruments:

VIS: optical imager &

NISP: NIR imager + grisms

- *Unique* **legacy survey**: 2 billion galaxies imaged in optical/NIR to mag >24 Million NIR galaxy spectra, full extragalactic sky coverage, Galactic sources
- Unique database for **various fields in astronomy**: galaxy evolution, search for high-z objects, clusters, strong lensing, brown dwarfs, exo-planets, etc
- **Synergies with other facilities**: JWST, Planck, Erosita, GAIA, DES, Pan-STARSS, LSST, E-ELT etc (e.g. to do NIR from the ground would take several x 10^3 yr)
- **All data publicly available** through a legacy archive

Enormous database to harvest

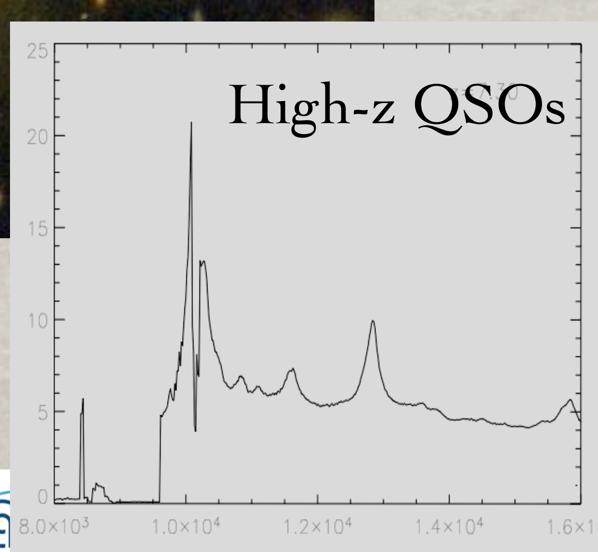

Euclid in context

	VISTA	SASIR	Euclid
Wide survey	680 years	66 years	5 years
Deep survey	72 years	7 years	“5 years”

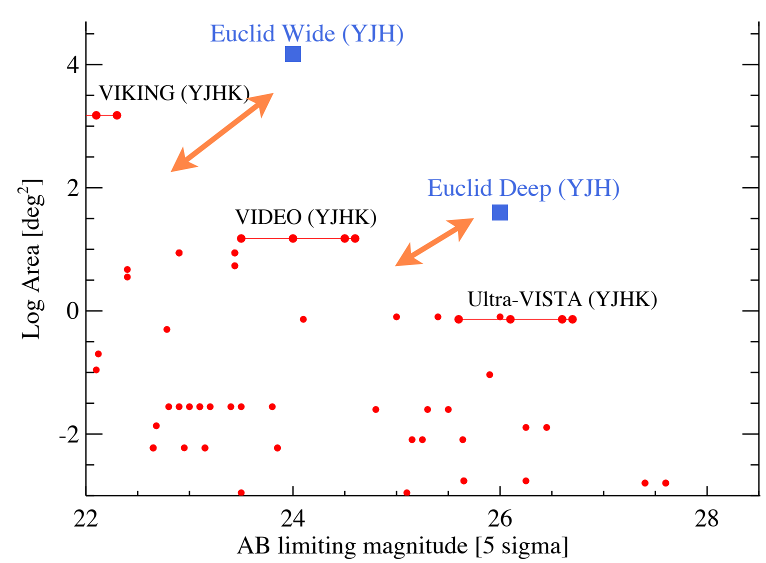

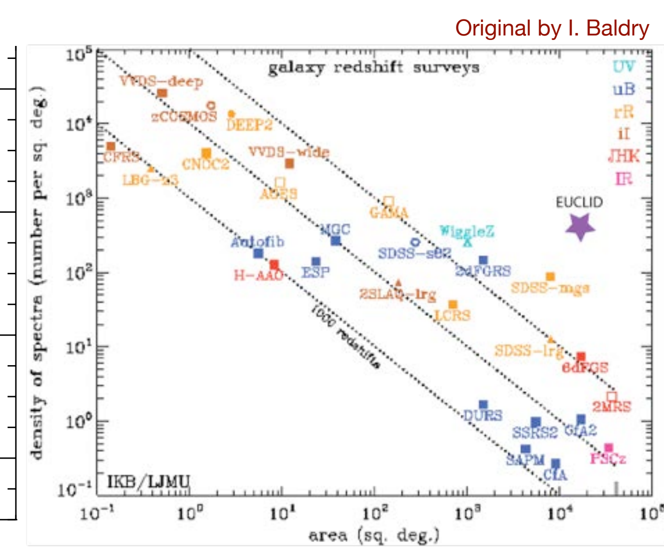

Public data releases:

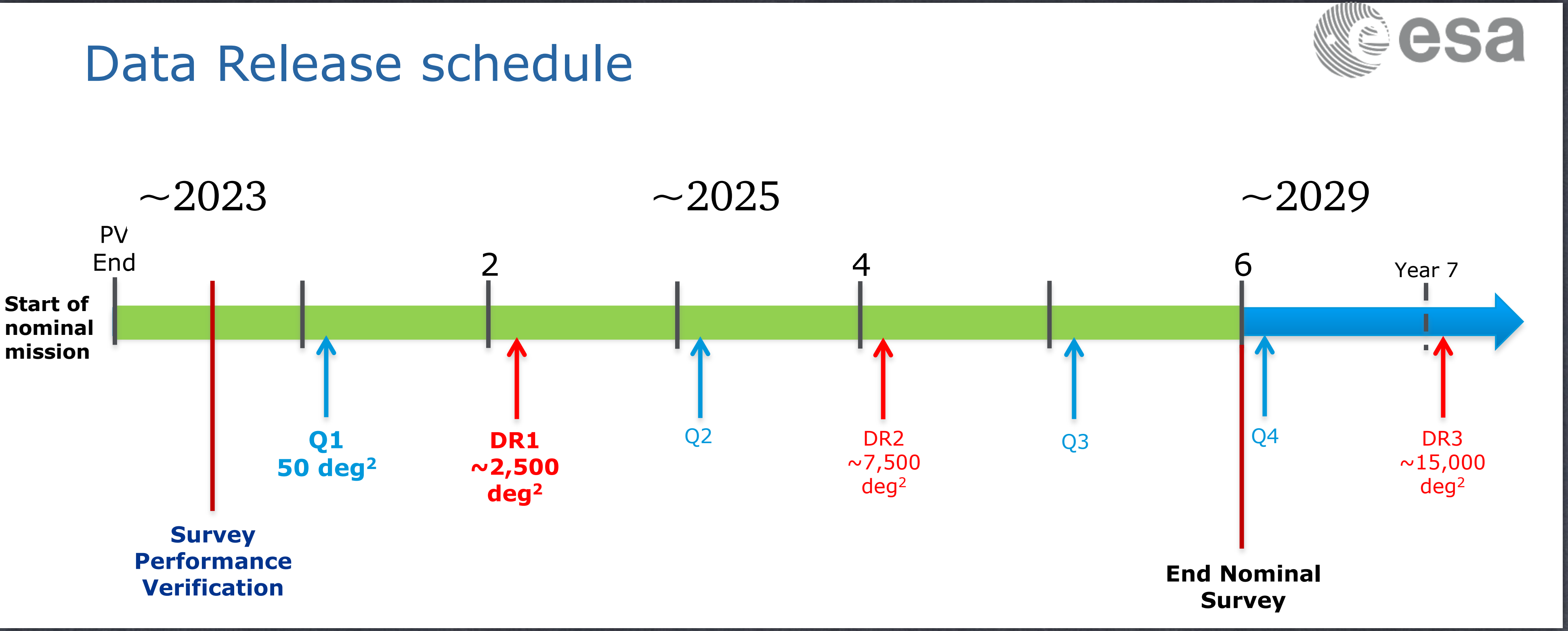

Two kind:

Q's = small area prerelease for the community to get acquainted

DR = data release (three DR of increasing areas: early -2500-, intermediate -7500-, final -15000 sq degs)

Q1: 14 months after start of the nominal mission — data released: one visit on the deep fields [50 sq deg]

DR1: one year after Q1 — data released: 2500 sq deg

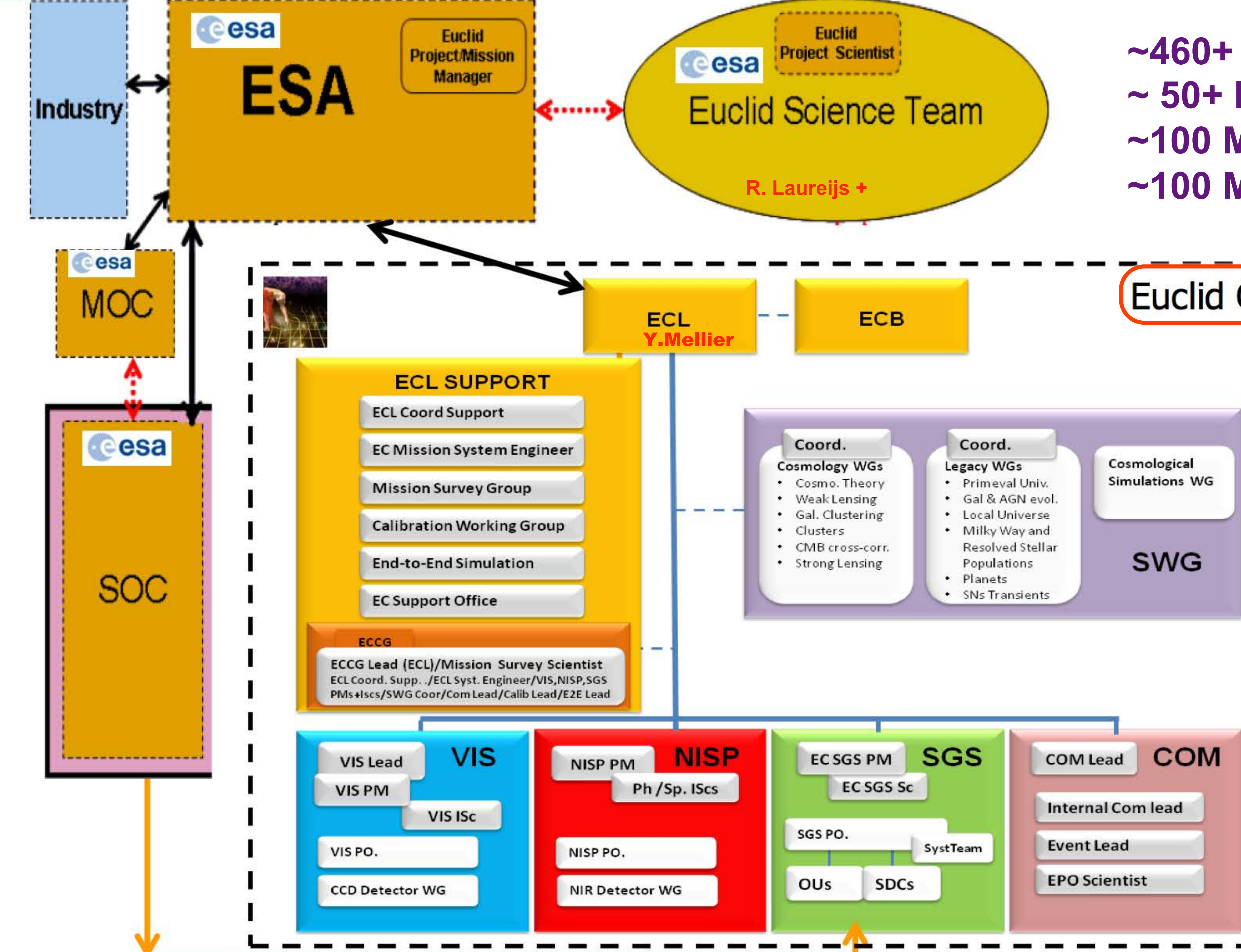

~460+ M€ (ESA)
~ 50+ M$ (NASA)
~100 M€ EC instr
~100 M€ EC Gnd Seg

Euclid Consortium

- 1500 members,
- 120 Labs
- 13 European countries:

Austria, Denmark, France, Finland,, Germany, Italy, The Netherlands, Norway, Portugal, Romania, Spain, Switzerland, UK

+ US/NASA and Berkeley labs.

Canada, Japan

Italy (ASI, INAF, INFN) contributes to the instruments (electronics and mechanical parts), leads the Ground Segment and the Survey, coordinates several Science Working Groups, two members in the ESA Science Team.

~300 italian scientists are members of the EC

Italy in Euclid

L. Stanco

"Euclid-Italy" Team

- ~320 members
- Financial support from ASI, partly from MIUR (PRIN), INFN
- Universities : Bo, Mi, Na, Pd, RM1, RM2, RM3, TS, SISSA, SNS
- INAF : OABo, OABrera, OACt, OAA, OANa, OAPd, OARM, OATo, OATs, IASFBO, IASFMII, IAPS
- INFN: Bologna, Genova,Lecce, Milano, Padova, Roma1

"Euclid-INFN" Team

~44+7 members

- Bologna: 16 members
- Genova: ≈ 7
- Lecce: 5
- Milano: 3
- Padova: 11
- Roma1: 9

Year 2018, still growing

Note: partial overlap between INFN-INAF-UNI

The ubiquitous symbol.. (hex U+039B)

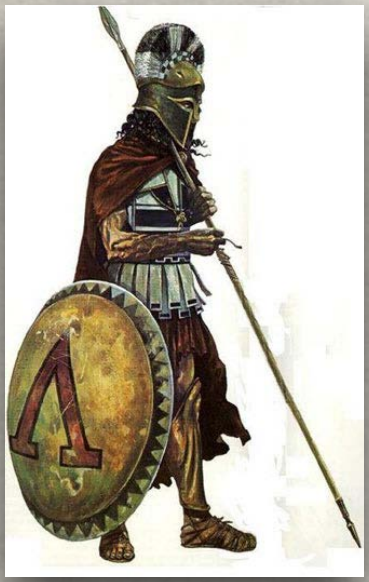

SAMSUNG

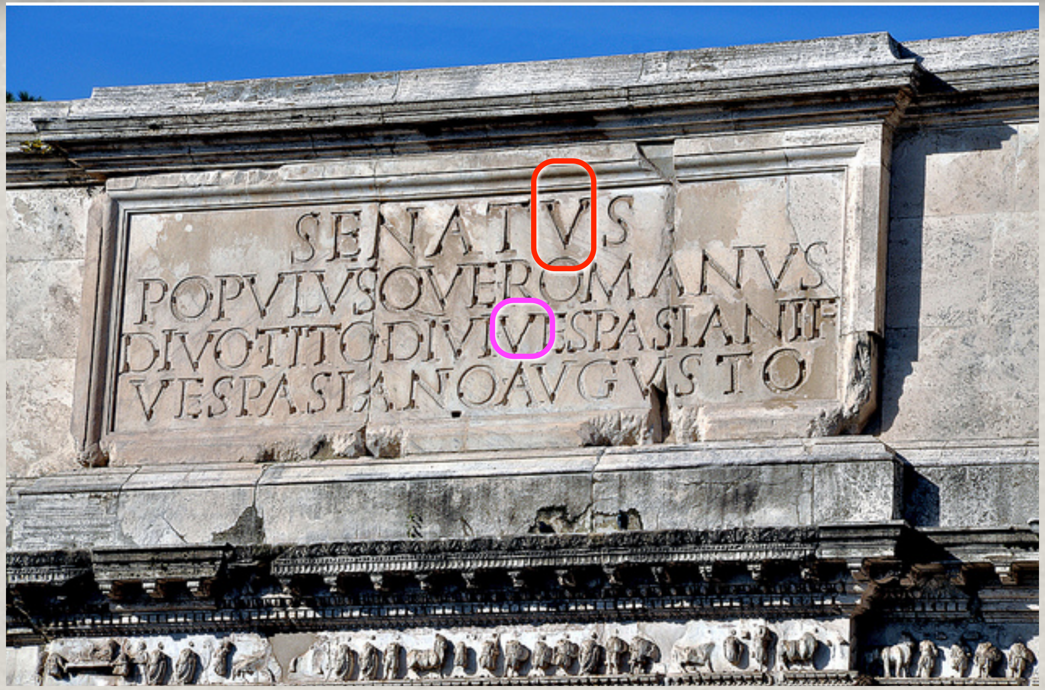

one vowel (u),
one consonant (v),
one number (5)

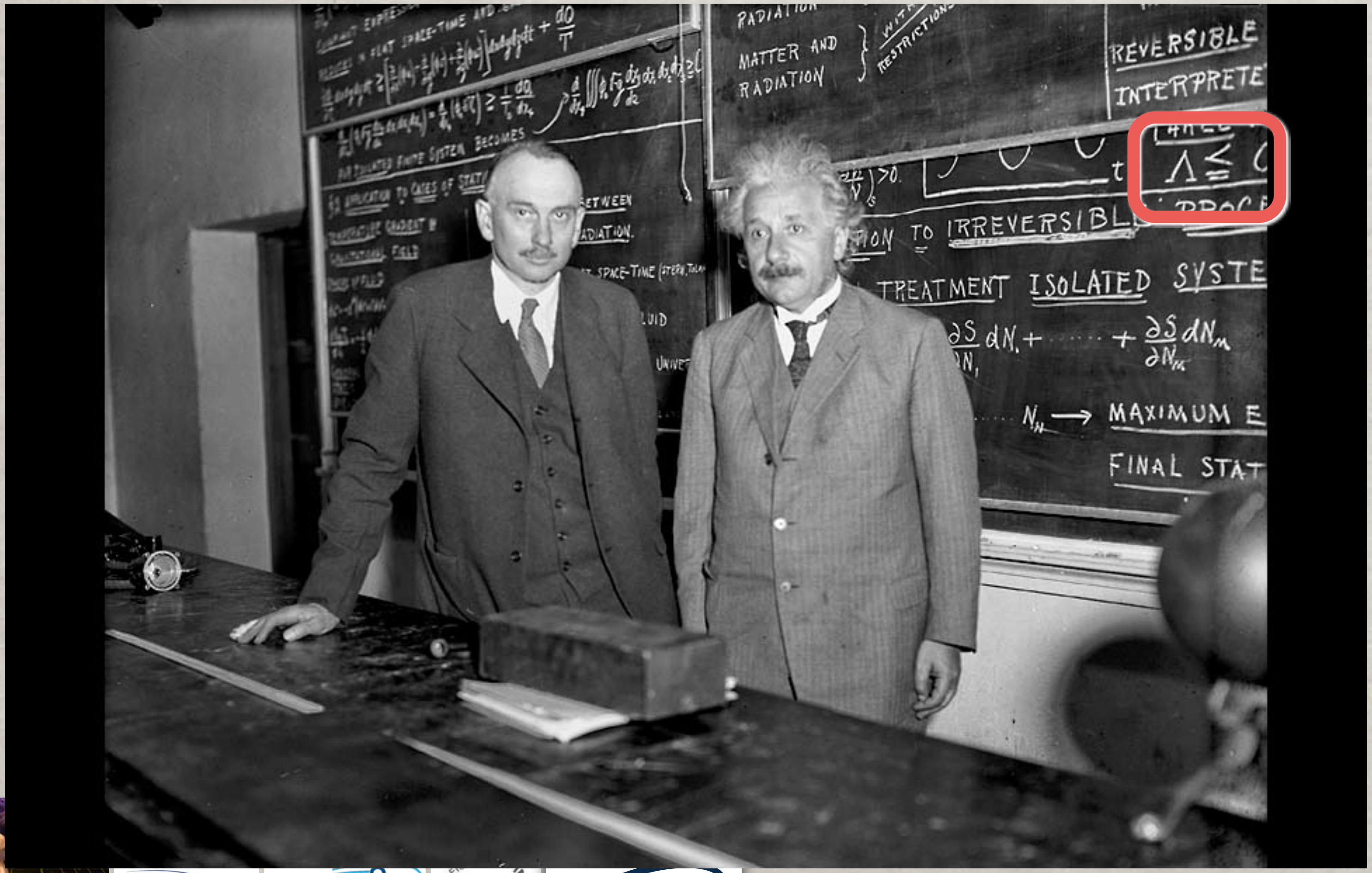

$$R_{\mu\nu} - \frac{1}{2} R\, g_{\mu\nu} + \Lambda\, g_{\mu\nu} = \frac{8\pi G}{c^4} T_{\mu\nu}$$

$\varrho_{vac} = \Lambda / 8\pi \quad \sim 10^{-29}\ \mathrm{g/cm^3}$

$t_{pl} = (Gh/2\pi c^5)^{1/2} = 5.4 \times 10^{-44}\mathrm{s}$

$t_U \sim 8 \times 10^{60}$

$\Lambda \sim t^{-2} \sim 10^{-122}$

Λ or ?

A simple equation: $A = B \longrightarrow A - B = 0$

At general level one has: $\boxed{F = S}$

Field equations (laws): gravity, electromagnetism..

Sources: masses, charges..

$F = 0 \longrightarrow$ no source case: propagation of waves

Assume F=S works but not quite: $F \simeq S \longrightarrow$ Need to change the description

Can change:

$\boxed{F = S'} = S + T$ by **adding a new source**, T, (F laws unchanged)

$F + J = \boxed{F' = S}$ by **modifying the laws** with new parts, J, (S sources unchanged)

Does gravity follow standard G.R.? Need experiments with high sensitivity/precision....

(cf. L. Amendola, M. Kuntz, et al Theory SWG, Living reviews)

The most general (linear, scalar) metric at first-order

$$ds^2 = a^2[(1+2\Psi)dt^2 - (1+2\Phi)(dx^2+dy^2+dz^2)]$$

Weak limit

At the linear perturbation level and sub-horizon scales

Full metric reconstruction at first order requires 3 functions

$$H(z) \quad \Phi(k,z) \quad \Psi(k,z)$$

- modified Poisson's equation $\quad k^2\Psi = -4\pi G a^2 Q(k,a)\rho_m\delta_m$
- non-zero anisotropic stress $\quad \eta(k,a) = \dfrac{\Phi+\Psi}{\Psi}$

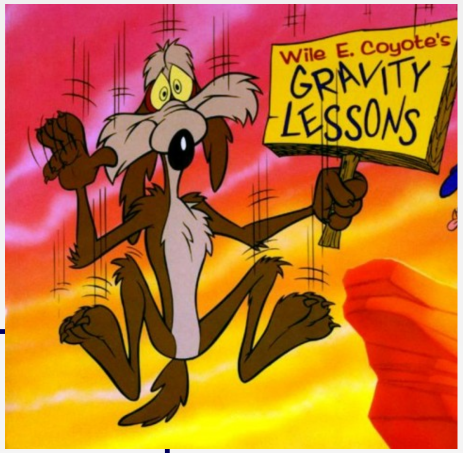

std matter

$$G_{\mu\nu} = -8\pi G T_{\mu\nu} - Y_{\mu\nu}$$

Std gravity,

new matter

$$Y_{\mu\nu} = X_{\mu\nu} - G_{\mu\nu}$$

New gravity,

std matter

$$X_{\mu\nu} = -8\pi G T_{\mu\nu}$$

$$T^{\nu}_{\mu\,;\nu} = 0.$$

Modified Gravity at linear level

standard gravity	$Q(k,a)=1$ $\eta(k,a)=0$	
scalar-tensor models	$Q(a)=\frac{G^*}{FG_{cav,0}}\frac{2(F+F'^2)}{2F+3F'^2}$ $\eta(a)=\frac{F'^2}{F+F'^2}$	Boisseau et al. 2000 Acquaviva et al. 2004 Schimd et al. 2004 L.A., Kunz &Sapone 2007
f(R)	$Q(a)=\frac{G^*}{FG_{cav,0}}\frac{1+4m\frac{k^2}{a^2R}}{1+3m\frac{k^2}{a^2R}}, \quad \eta(a)=\frac{m\frac{k^2}{a^2R}}{1+2m\frac{k^2}{a^2R}}$	Bean et al. 2006 Hu et al. 2006 Tsujikawa 2007
DGP	$Q(a)=1-\frac{1}{3\beta}; \quad \beta=1+2Hr_c w_{DE}$ $\eta(a)=\frac{2}{3\beta-1}$	Lue et al. 2004; Koyama et al. 2006
coupled Gauss-Bonnet	$Q(a)=...$ $\eta(a)=...$	see L. A., C. Charmousis, S. Davis 2006

Galaxies, BAO **COMPLEMENTARITY** Photons, WL

massive particles respond to Ψ

massless particles respond to Φ-Ψ

Need to break degeneracy: *use growth of fluctuations*

$$\delta'' + (1+\frac{H'}{H})\delta = \frac{k^2}{a^2}\Psi$$

$$\alpha = \int \nabla_{perp}(\Psi-\Phi)dz$$

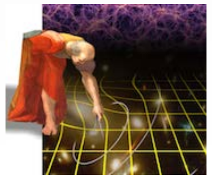

Galaxies, BAO **COMPLEMENTARITY** **Photons, WL**

massive particles respond to Ψ

$$\delta''+(1+\frac{H'}{H})\delta=\frac{k^2}{a^2}\Psi$$

massless particles respond to Φ-Ψ

$$\alpha=\int\nabla_{perp}(\Psi-\Phi)dz$$

Correlation of galaxy ellipticities:
galaxy weak lensing

$$P_{ellipt}(k,z)\propto(\Phi-\Psi)^2$$

DGP

(Dvali, Gabadadze, Porrati 2000)

$$S=\int d^5x\sqrt{-g^{(5)}}\;R^{(5)}\;+\;L\int d^4x\sqrt{-g}\,R$$

$$H^2-\frac{H}{L}=\frac{8\pi G}{3}\rho$$

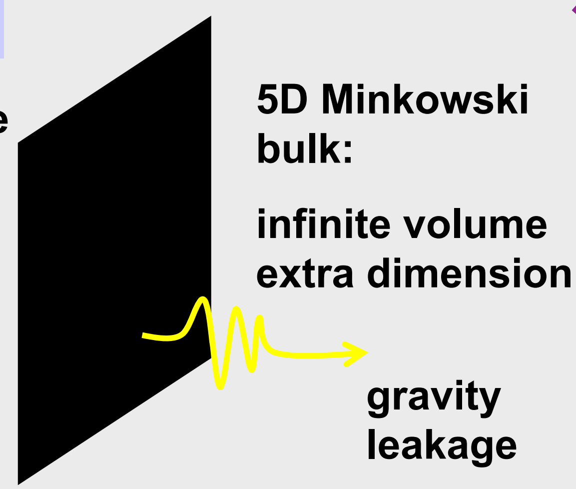

L = crossover scale:

$$r \ll L \Rightarrow V \propto \frac{1}{r}$$

$$r \gg L \Rightarrow V \propto \frac{1}{r^2}$$

- **5D gravity dominates at low energy/late times/large scales**
- **4D gravity recovered at high energy/early times/small scales**

ESTEC 2009

γ: perturbation growth index under gravity

$$\frac{d\log\delta}{d\log a}=\Omega_m(a)^\gamma$$

$$\gamma_s=\frac{3(1-w)}{6w-5}\approx 0.55$$ Standard

DG

$$\gamma\approx\gamma_s\left(1+\frac{1-Q}{(1-w)(1-\Omega_m)}\right)\approx 0.65-0.70$$

f(R)

$$\gamma\approx\gamma_s\left(1+\frac{k^2a^2}{M(f)^2+k^2a^2}\right)\approx 0.40-0.55$$

FoM = Figure of Merit

An important step in the field was done in a report by the U.S. Dark Energy Task Force [DETF], which defined a hierarchy of future experiments, increasingly more precise (stages I—IV) [Albrecht et al 2006]

In the report a simple metric was proposed to rank the future experiments, that is the inverse of the area enclosing the 95% c.l. in the w_0—w_a plane.

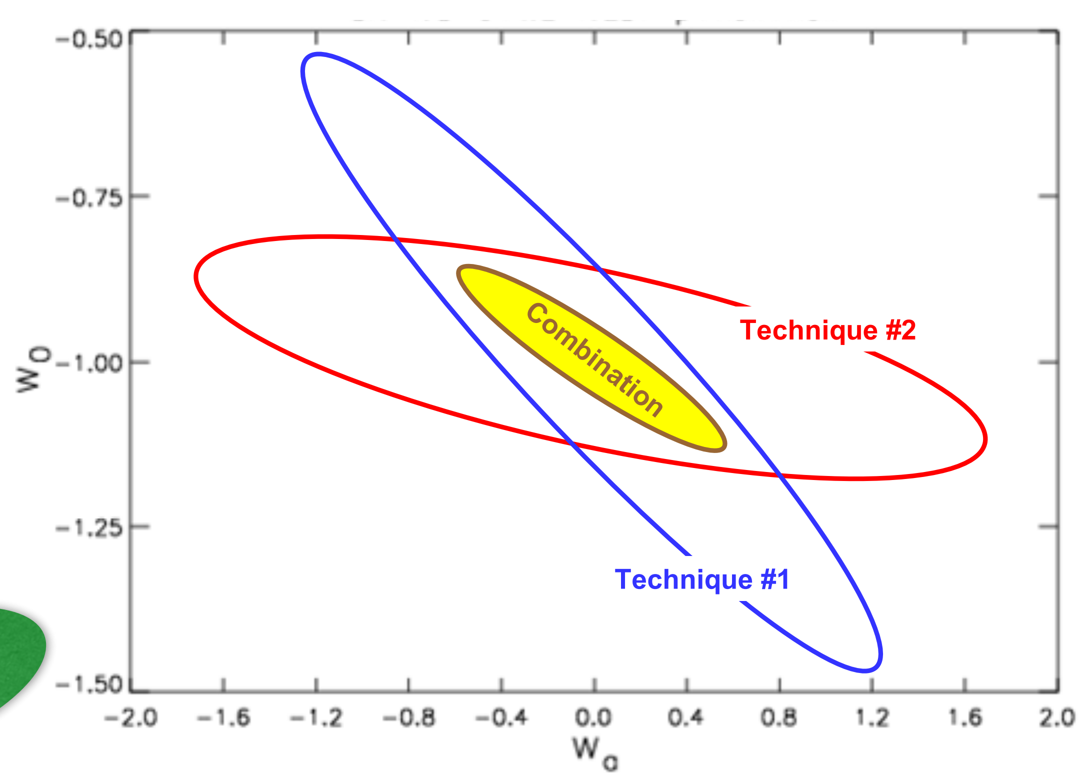

Illustration of the power of combining techniques. Technique #1 and Technique #2 have roughly equal DETF figure of merit. When results are combined, the DETF figure of merit is substantially improved.

FoM[A] < FoM[B]

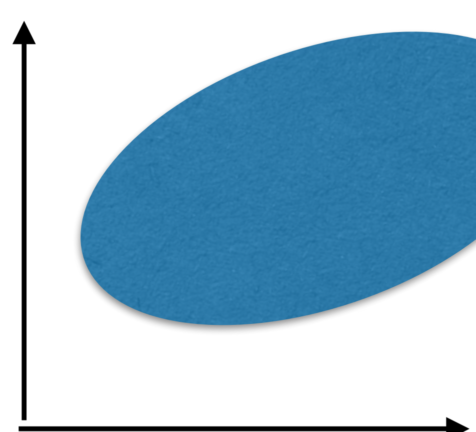

Experiment A

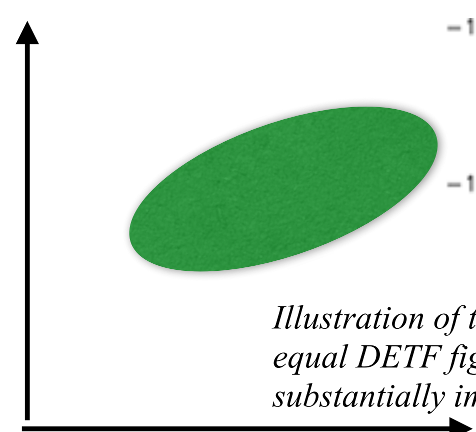

Experiment B

Wolz et al 2012

$$F_{ij} = -\left\langle \frac{\partial^2 \ln \mathscr{L}}{\partial \theta_i \partial \theta_j} \right\rangle$$

For geometrical cosmological probes Fisher has problems
Use MCMC

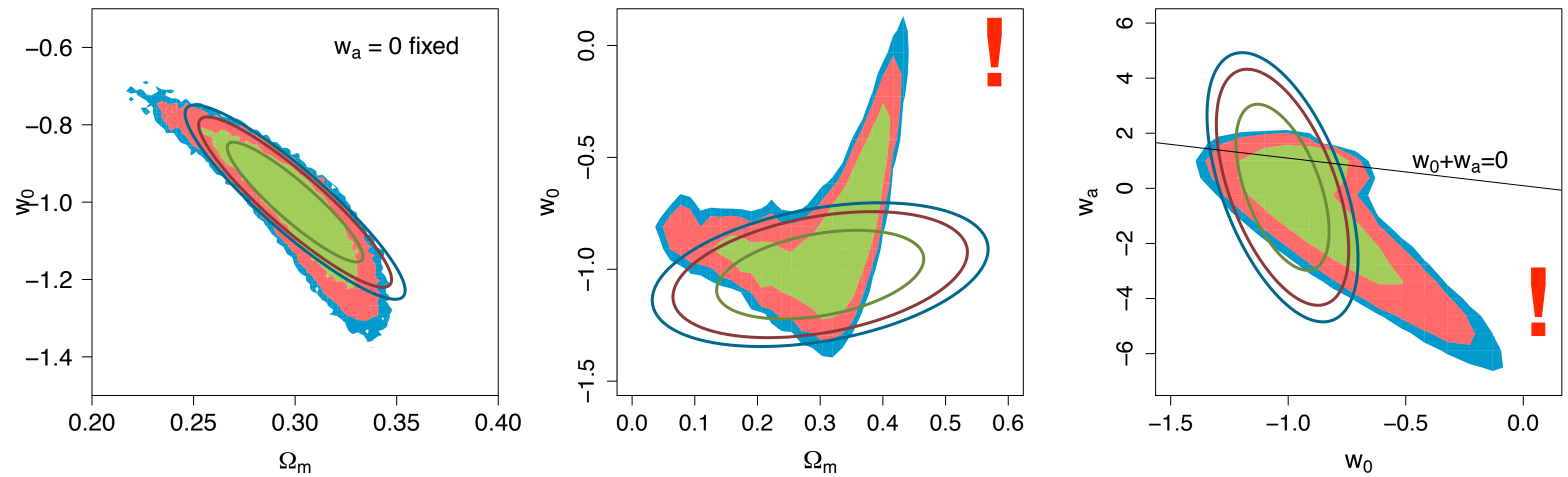

Figure 1. 68%, 90% and 95% confidence regions for a supernova survey. Filled contours correspond to the full posterior sampled with MCMC, while the solid lines represent the Fisher matrix results. The parameter spaces are $\{\Omega_\mathrm{m}, w_0, M_\mathrm{int}\}$ with fixed $w_a = 0$ (*left panel*), and $\{\Omega_\mathrm{m}, w_0, w_a, M_\mathrm{int}\}$ (*middle and right panels*). The parameters which are not shown have been marginalised in all panels.

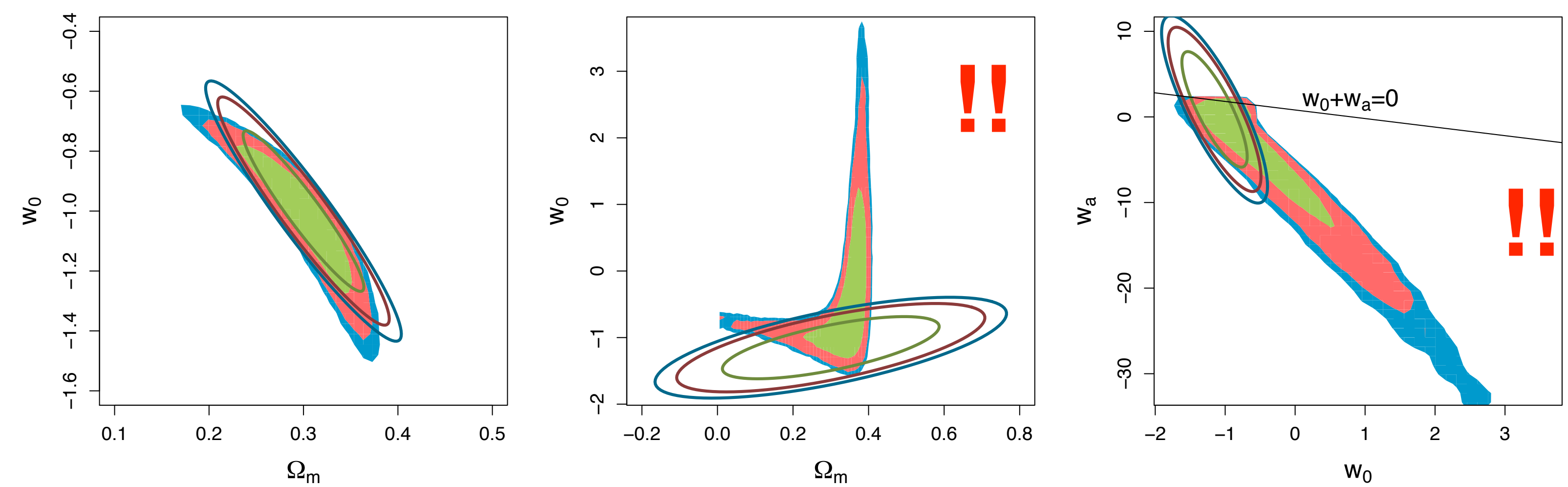

Figure 2. Confidence regions for a SKA-like BAO survey. Filled contours correspond to the MCMC, while the solid lines represent the Fisher matrix results. The parameter space is $\{\Omega_\mathrm{m}, w_0\}$ (*left panel*), and $\{\Omega_\mathrm{m}, w_0, w_a\}$ (*middle and right panels*). In the latter cases, we marginalise over the hidden parameter.

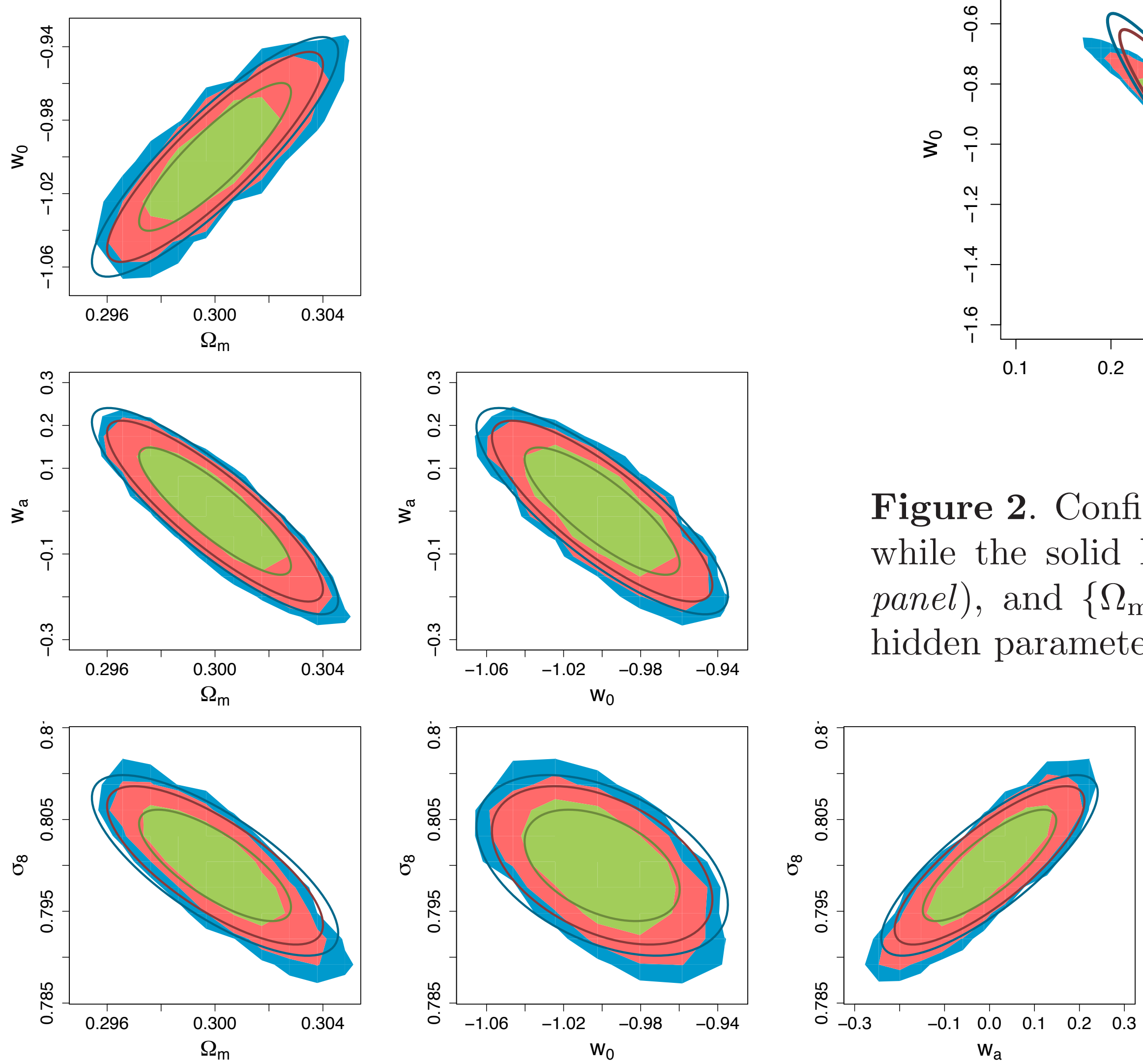

Fisher for Weak Lensing not bad

Figure 7. Marginalised 68%, 90% and 95% confidence regions for a Euclid-like weak lensing survey.

A legion of papers combining different probes/ samples, myriads of plots with isocontours..

Table 2: Best-fit values and 1σ uncertainties for the cosmological free parameters in each model and data set.

Model	Data set	$\Omega_{M,0}$	$\Omega_{\Lambda,0}$	w_0	w_a
Flat ΛCDM	SNe+QSO	$0.295^{+0.013}_{-0.012}$			
	BAO	$0.373^{+0.056}_{-0.048}$			
	SNe+QSO+BAO	0.300 ± 0.012			
Non-flat ΛCDM	SNe+QSO	0.504 ± 0.029	$1.107^{+0.051}_{-0.052}$		
	BAO	$0.376^{+0.057}_{-0.049}$	$0.638^{+0.071}_{-0.079}$		
	SNe+QSO+BAO	$0.364^{+0.022}_{-0.021}$	0.829 ± 0.035		
Flat wCDM	SNe+QSO	$0.403^{+0.022}_{-0.024}$		$-1.494^{+0.132}_{-0.143}$	
	BAO	$0.381^{+0.057}_{-0.050}$		$-1.049^{+0.098}_{-0.116}$	
	SNe+QSO+BAO	$0.369^{+0.022}_{-0.023}$		$-1.283^{+0.094}_{-0.108}$	
Non-flat wCDM	SNe+QSO	$0.280^{+0.041}_{-0.037}$	$1.662^{+0.041}_{-0.048}$	$-0.667^{+0.024}_{-0.027}$	
	BAO	$0.301^{+0.080}_{-0.072}$	$0.463^{+0.072}_{-0.058}$	$-2.850^{+1.459}_{-1.441}$	
	SNe+QSO+BAO	$0.224^{+0.018}_{-0.017}$	$1.667^{+0.040}_{-0.047}$	$-0.626^{+0.012}_{-0.013}$	
CPL	SNe+QSO	$0.447^{+0.023}_{-0.027}$		$-1.267^{+0.196}_{-0.191}$	$-3.771^{+2.113}_{-2.496}$
	BAO	$0.420^{+0.073}_{-0.070}$		$-0.821^{+0.469}_{-0.349}$	$-1.269^{+1.835}_{-2.608}$
	SNe+QSO+BAO	$0.354^{+0.032}_{-0.030}$		$-1.323^{+0.103}_{-0.112}$	$0.745^{+0.483}_{-0.974}$
JBP	SNe+QSO	$0.441^{+0.025}_{-0.028}$		$-1.250^{+0.223}_{-0.209}$	$-4.282^{+2.680}_{-3.283}$
	BAO	$0.384^{+0.103}_{-0.098}$		$-1.091^{+0.923}_{-0.727}$	$0.235^{+4.922}_{-6.612}$
	SNe+QSO+BAO	$0.354^{+0.032}_{-0.030}$		-1.371 ± 0.141	$1.127^{+1.293}_{-1.547}$
Exponential	SNe+QSO	$0.395^{+0.023}_{-0.026}$		$-1.481^{+0.141}_{-0.147}$	
	BAO	$0.371^{+0.058}_{-0.051}$		$-1.067^{+0.102}_{-0.119}$	
	SNe+QSO+BAO	$0.359^{+0.023}_{-0.024}$		$-1.271^{+0.092}_{-0.107}$	
Rational	SNe+QSO	$0.452^{+0.022}_{-0.025}$		$-1.316^{+0.172}_{-0.168}$	$-2.654^{+1.329}_{-1.626}$
	BAO	$0.410^{+0.086}_{-0.081}$		$-0.930^{+0.464}_{-0.333}$	$-0.423^{+1.064}_{-1.671}$
	SNe+QSO+BAO	$0.307^{+0.044}_{-0.055}$		$-1.303^{+0.115}_{-0.106}$	$1.010^{+0.152}_{-0.466}$

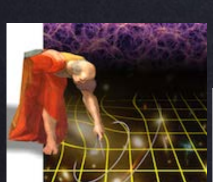

HUNTING DOWN HORIZON-SCALE EFFECTS WITH MULTI-WAVELENGTH SURVEYS

José Fonseca,[1*] Stefano Camera,[2] Mário G. Santos[1,3,4], Roy Maartens[1,5]

Multitracer techniques useful and informative

Measuring cosmic velocities with 21 cm intensity mapping and galaxy redshift survey cross-correlation dipoles

Alex Hall[1,*] and Camille Bonvin[2,†]

$$C^{CD}_{AB}(d,d') = \frac{1}{V}\int \frac{k^2 \mathrm{d}k}{2\pi^2} \sum_{\ell,\ell'} i^{\ell'-\ell} w_\ell w_{\ell'} j_\ell(kd) j_{\ell}(kd') \sum_{L,L'} G^{L'L}_{\ell'\ell} \left[P^{AC}_L(k)P^{DB}_{L'}(k) + (-1)^{\ell'} P^{AD}_L(k) P^{CB}_{L'}(k)\right]$$
$$+ \int \frac{k^2 \mathrm{d}k}{2\pi^2} \sum_{\ell,\ell'} i^{\ell'-\ell} w_\ell w_{\ell'} j_\ell(kd) j_\ell(kd') \sum_L \begin{pmatrix} L & \ell & \ell' \\ 0 & 0 & 0 \end{pmatrix}^2 \left[\frac{\delta^K_{AC}}{\bar{n}_A V} P^{DB}_L(k) + \frac{\delta^K_{BD}}{\bar{n}_B V} P^{CA}_L(k)\right.$$
$$\left. + (-1)^{\ell'} \frac{\delta^K_{AD}}{\bar{n}_A V} P^{BC}_L(k) + (-1)^{\ell'} \frac{\delta^K_{BC}}{\bar{n}_B V} P^{DA}_L(k)\right]$$
$$+ \frac{\delta^K_{AC}\delta^K_{BD}}{\bar{n}_A \bar{n}_B V} \frac{\delta^K_{d,d'}}{4\pi d^2 L_p} \sum_\ell \frac{w_\ell^2}{2\ell+1} + \frac{\delta^K_{BC}\delta^K_{AD}}{\bar{n}_A \bar{n}_B V} \frac{\delta^K_{d,d'}}{4\pi d^2 L_p} \sum_\ell (-1)^\ell \frac{w_\ell^2}{2\ell+1}. \quad (17)$$

the estimator noise. The quantity $G^{L'L}_{\ell'\ell}$ arising from the integral of four Legendre polynomials is expressible in terms of Wigner $3j$ symbols as

$$G^{L'L}_{\ell'\ell} \equiv \sum_{L''} (2L''+1) \begin{pmatrix} \ell & \ell' & L'' \\ 0 & 0 & 0 \end{pmatrix}^2 \begin{pmatrix} L & L' & L'' \\ 0 & 0 & 0 \end{pmatrix}^2, \quad (18)$$

Statistics, + statistics, and even more statistics….

What about Physics ?

Recall a few basics

$$H^2(a) \equiv \left(\frac{\dot{a}}{a}\right)^2 = H_0^2\left[\Omega_m a^{-3} + \Omega_r a^{-4} + \Omega_k a^{-2} + \Omega_X a^{-3(1+w)}\right]$$

Evolution governed by components: H(z) ⇔ Ω_X, w

$$H^2(a) = H_0^2\left[\Omega_R a^{-4} + \Omega_M a^{-3} + \Omega_k a^{-2} + \Omega_{DE}\exp\left\{3\int_a^1 \frac{da'}{a'}\left[1+w(a')\right]\right\}\right]$$

Ellipses: uncertainty in parameters via Fisher matrix. An useful *approximation* (curse of dimensionality; also different definitions). Importance of ***Priors***

Usually use Figure of Merit= 1/Area

FoM= 1/(Δw_0 x Δw_a)

$a=(1+z)^{-1}$ expansion factor

δ = density fluctuation

P(k) = power spectrum of $\delta(\mathbf{x},z)$

w = p/ϱ, γ=growth index

$$f_{\mathrm{GR}}(z) \equiv \frac{d\ln G_{\mathrm{GR}}}{d\ln a} \approx [\Omega_m(z)]^\gamma$$

$w(z)=w_0 + w_a\,(1-a)$

Λ: $w_0 = -1$, $w_a = 0$, $\gamma \sim 0.55$

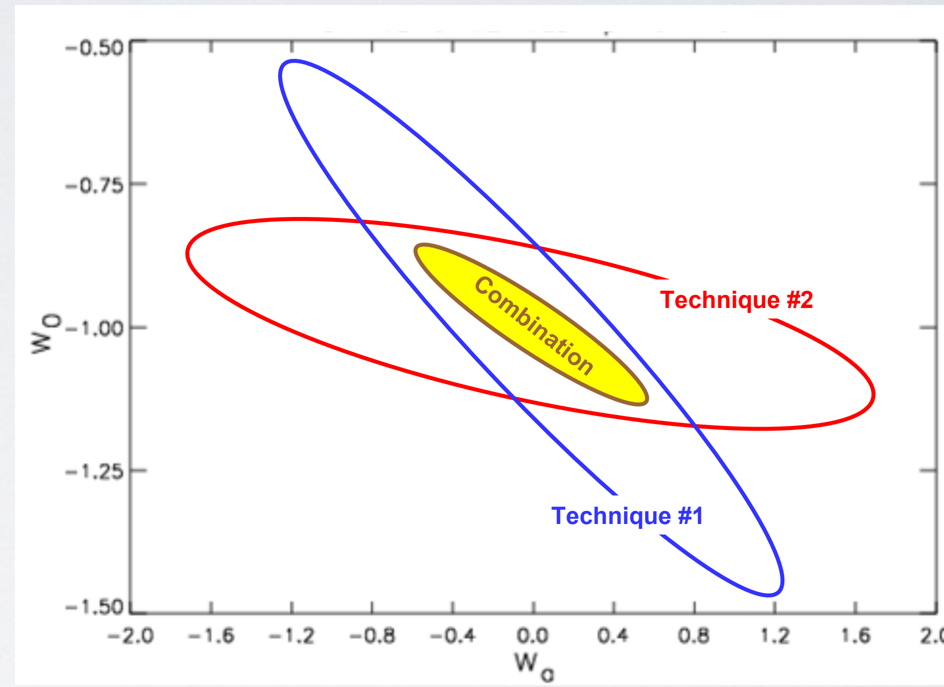

to get a small uncertainty on power spectrum need:

$$\frac{\sigma}{P} = \sqrt{\frac{2}{n_{\mathrm{modes}}}}\left(1+\frac{1}{P\bar{n}}\right)$$

accurate/adequate sampling in number of objects

large volumes to accomodate several Fourier modes

Cosmic Variance ⇔ Volume

Poisson ⇔ Number of galaxies

[un]known systematics

	Modified Gravity	Dark Matter	Initial Conditions	Dark Energy		
Parameter	γ	m_ν/eV	f_{NL}	w_p	w_a	FoM
Euclid Primary	0.01	0.027	5.5	0.015	0.150	430
Euclid All	0.009	0.02	2	0.013	0.048	1540
Euclid +Planck	0.007	0.019	2	0.007	0.035	4020
Current	0.2	0.58	100	0.1	1.5	~10
Improv. Factor	**30**	**30**	**50**	**>10**	**>50**	**>300**

$$\boxed{\mathrm{FoM} = 1/(\Delta w_p \times \Delta w_a)}$$

Goals

500 CBE

6000 Current Best Estimate

IMPROVE ~
× 10 ON W
× 20 ON γ

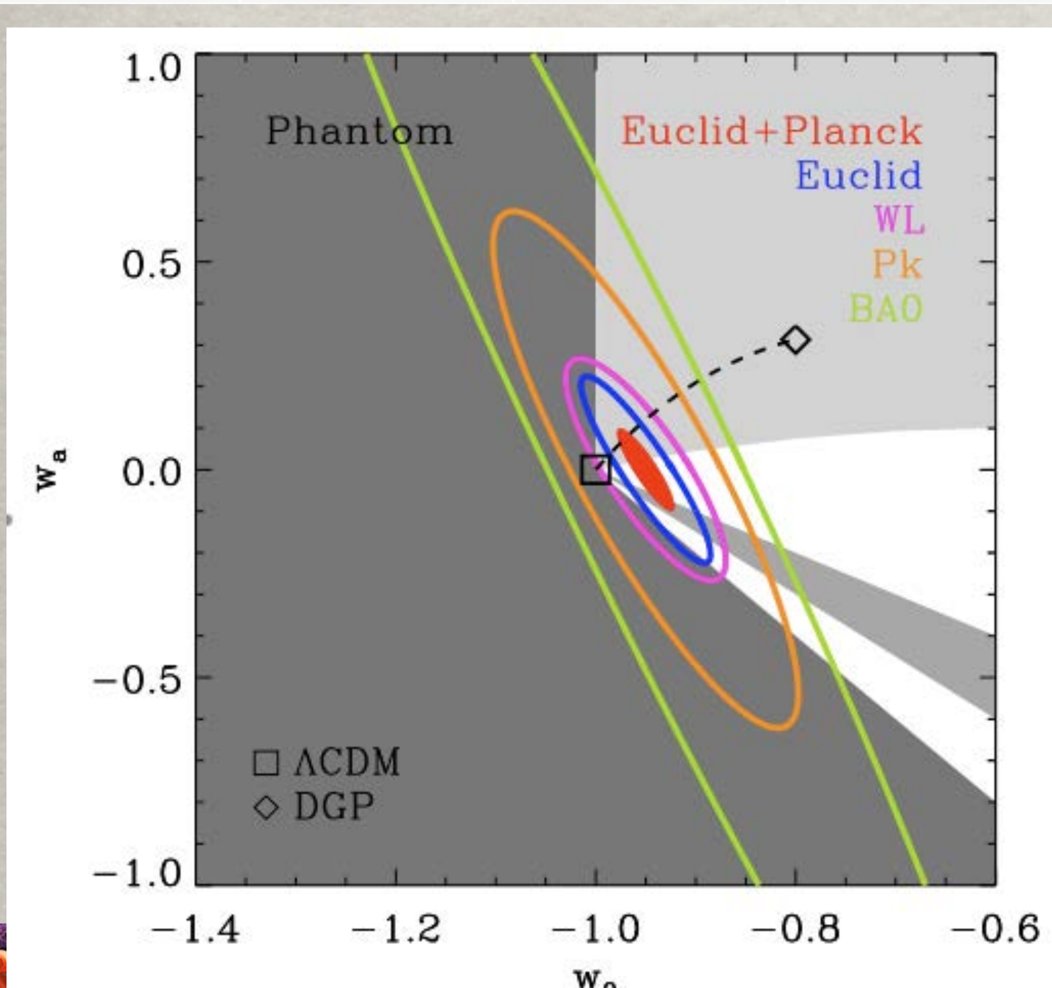

Euclid will challenge all sectors of the cosmological model:

- **Dark Energy**: w_p and w_a with an error of 2% and 13% respectively (no prior)
- **Dark Matter**: test of CDM paradigm, precision of 0.04eV on sum of neutrino masses (with Planck)
- **Initial Conditions**: constrain shape of primordial power spectrum, primordial non-gaussianity
- **Gravity**: test GR by reaching a precision of 2% on the growth exponent γ ($d\ln\delta_m/d\ln a \propto \Omega_m^\gamma$)

Uncover new physics and map LSS at 0<z<2: Low redshift counterpart to CMB surveys

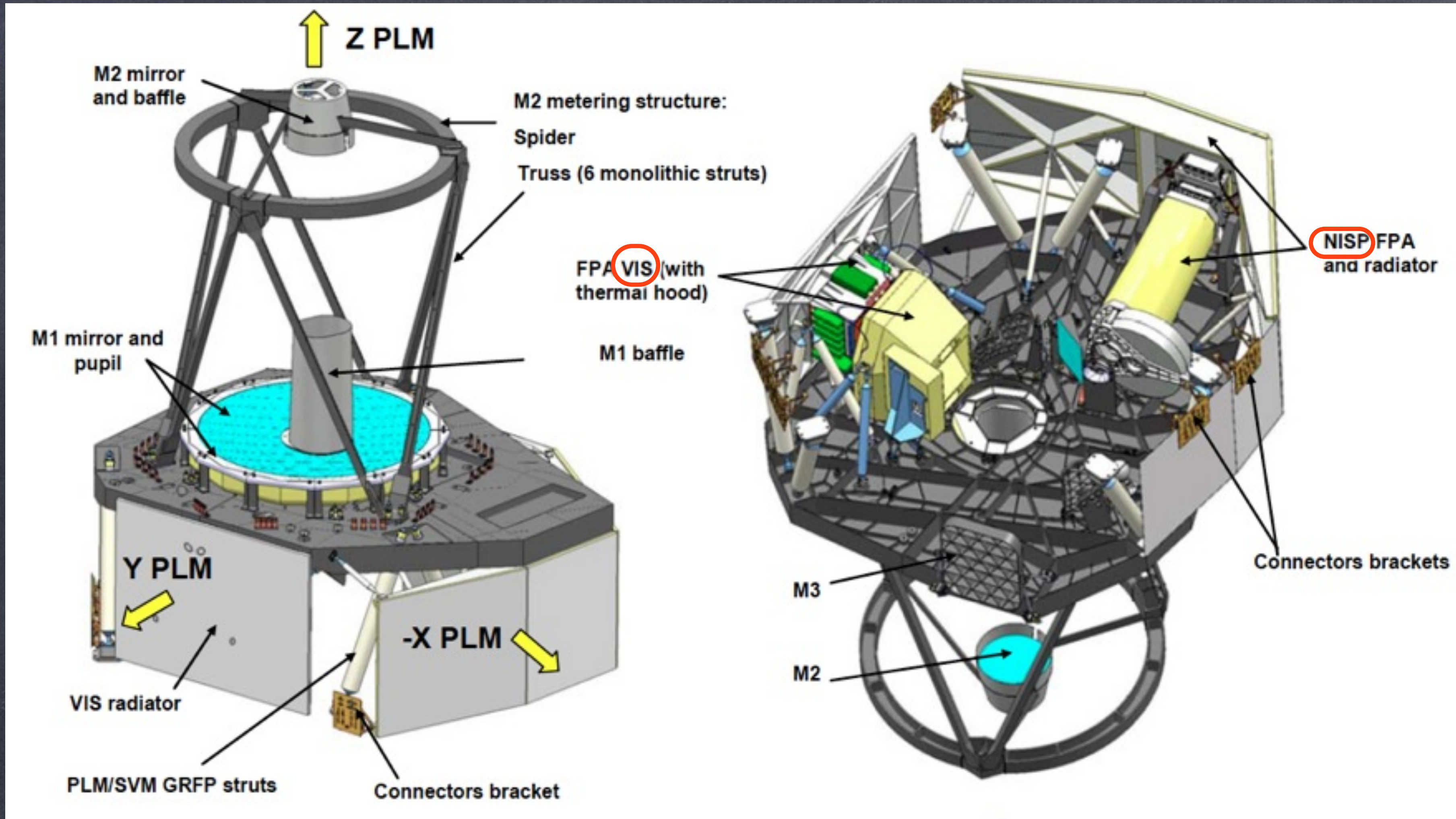

Two instruments:

VIS: optical imager

NISP: NIR imager + grisms

Ground Segment

A few Petabytes...

instruments costs ≈ GS costs

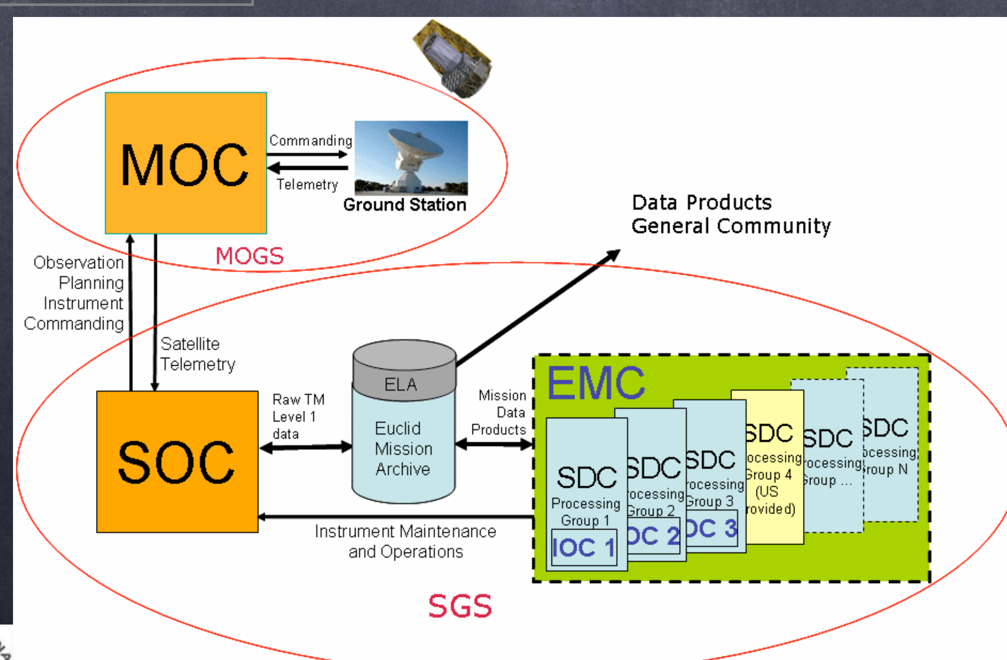

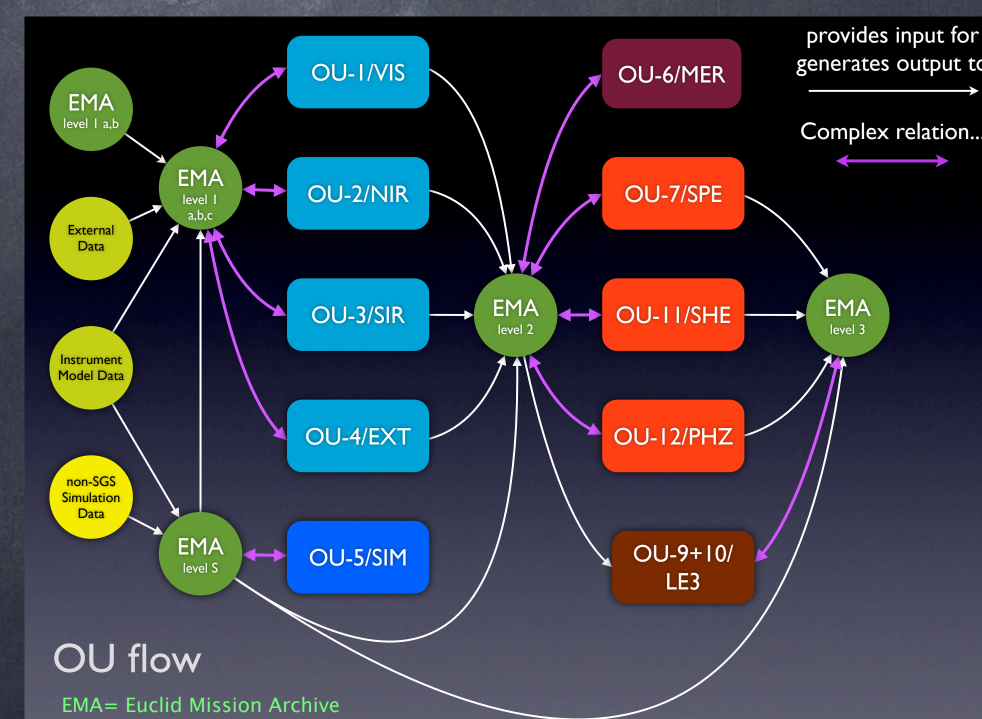

Euclid – Payload Module - hardware

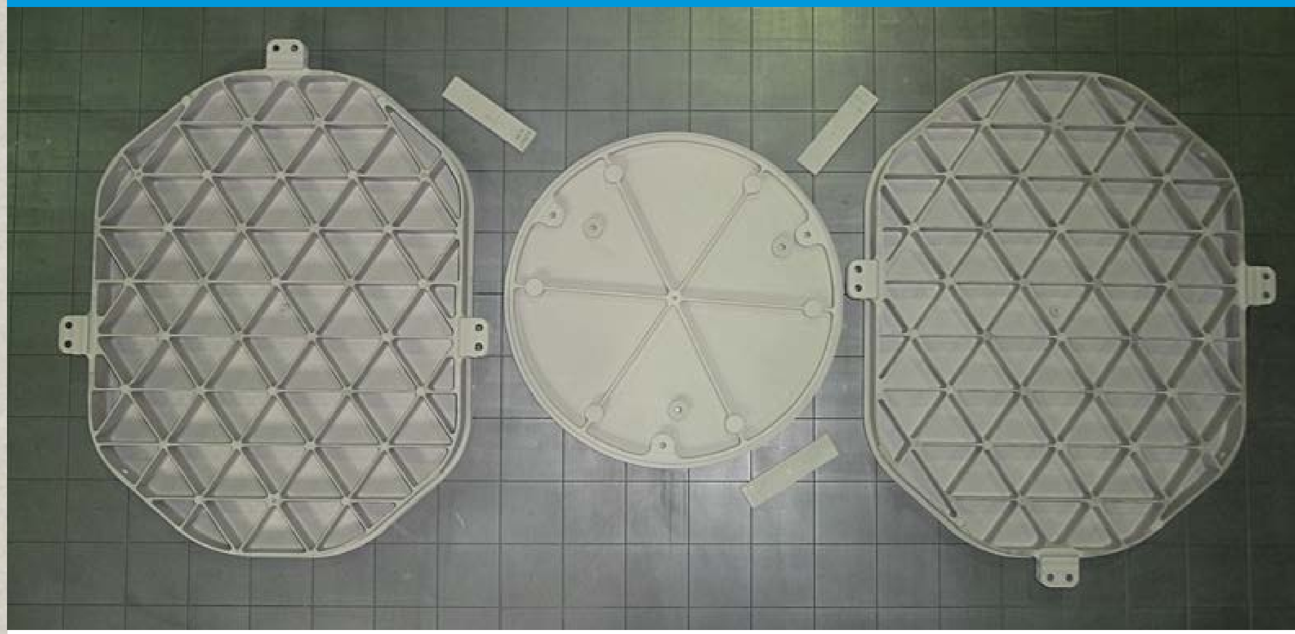

FoM 1, M2 and FoM 3

FoM2

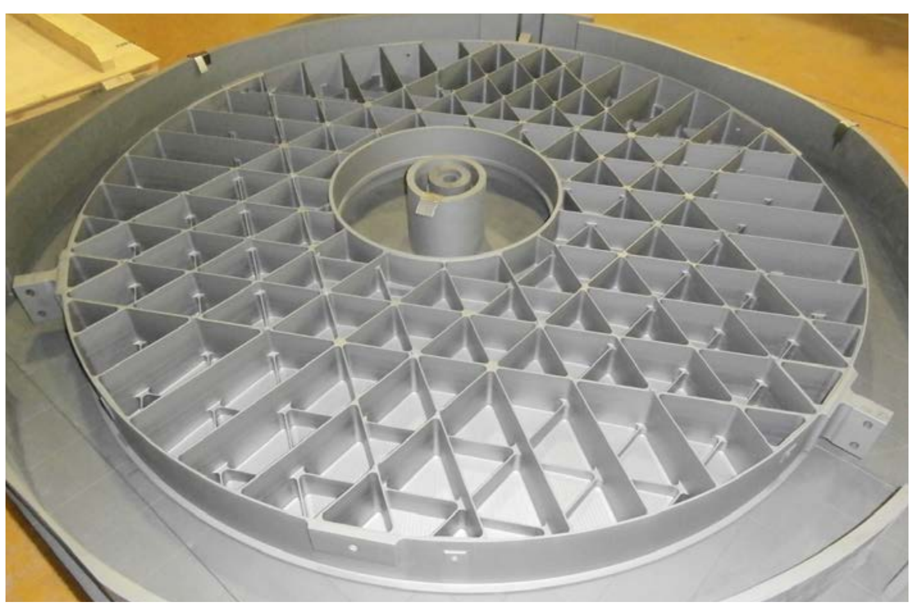

M1

M3

Dichroic plate

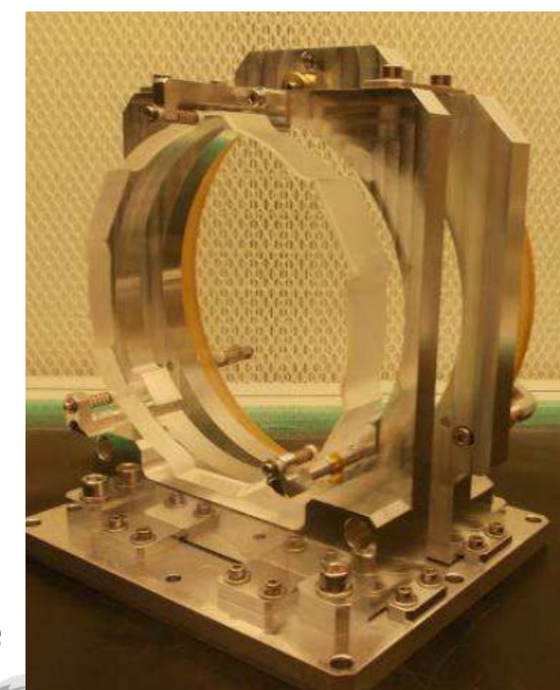

Euclid: small (1m) but powerful telescope

Built and almost assembled, launch in ~18 months, 6y mission

Flight model

October 2021 at Thales—Alenia in Turin

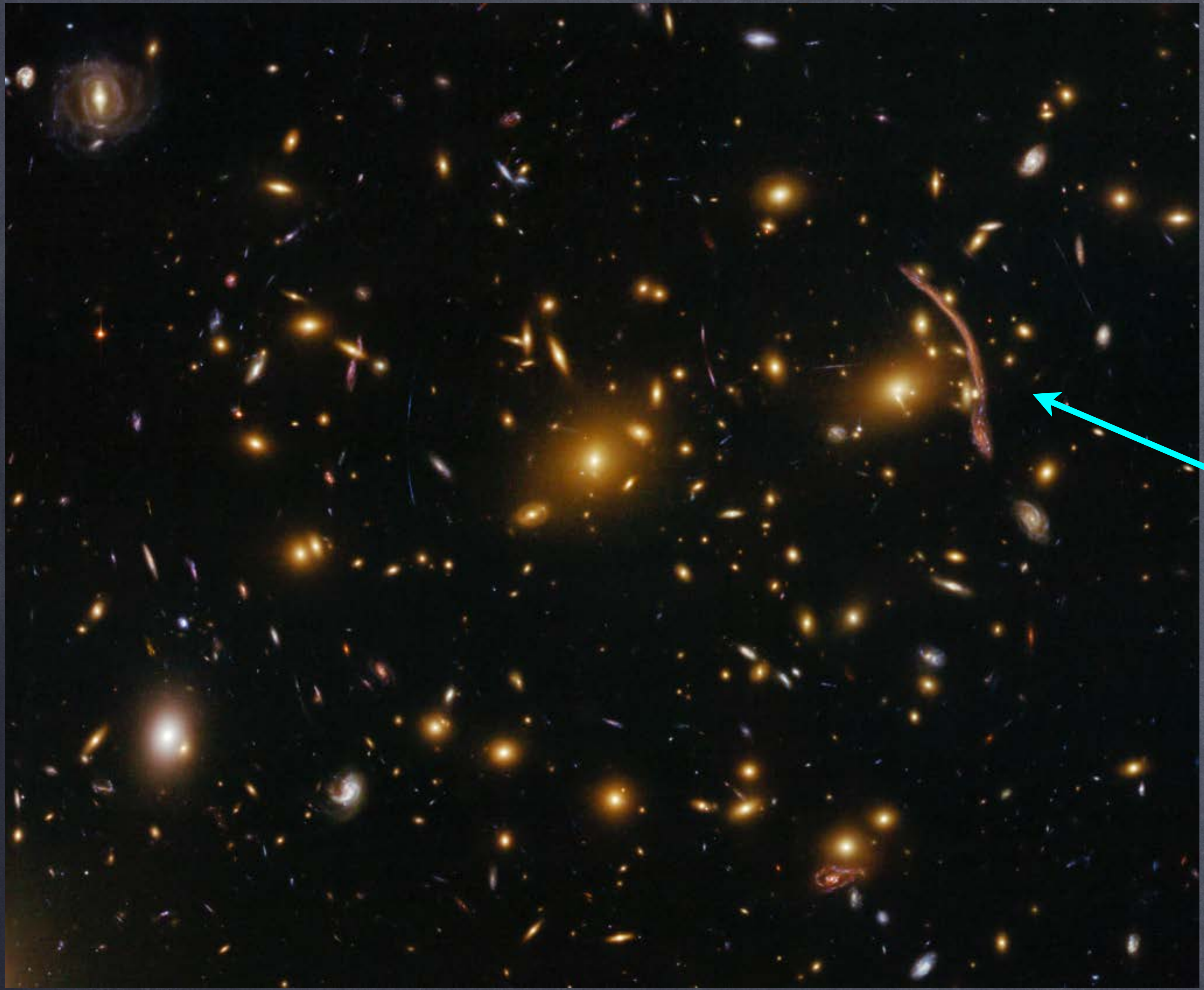

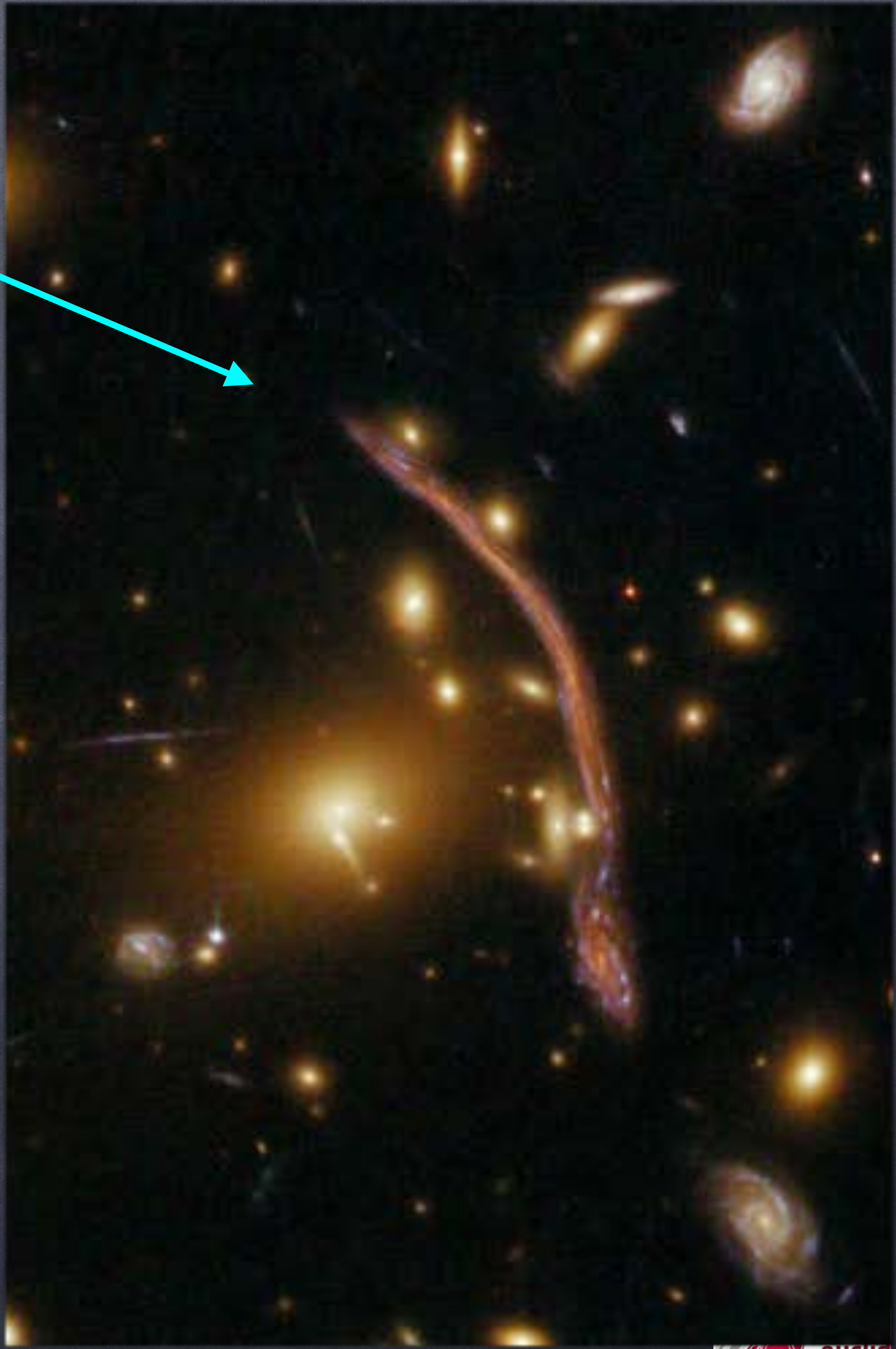

A370 ACS

w.r.t. HST will lose a factor of ~2 in resolution, but get all xgal sky!

EUCLID Mission

- Launcher: Soyuz ST2-1B from Kourou
- Direct injection into tranfer orbit
  - Transfer time: 30 days
  - Transfer orbit inclination: 5.3 deg
- Launch vehicle capacity:
  - 2160 kg (incl. adapter)
  - 3.86 m diameter fairing
- Launch ≈ 2023
- Mission duration: 6 years

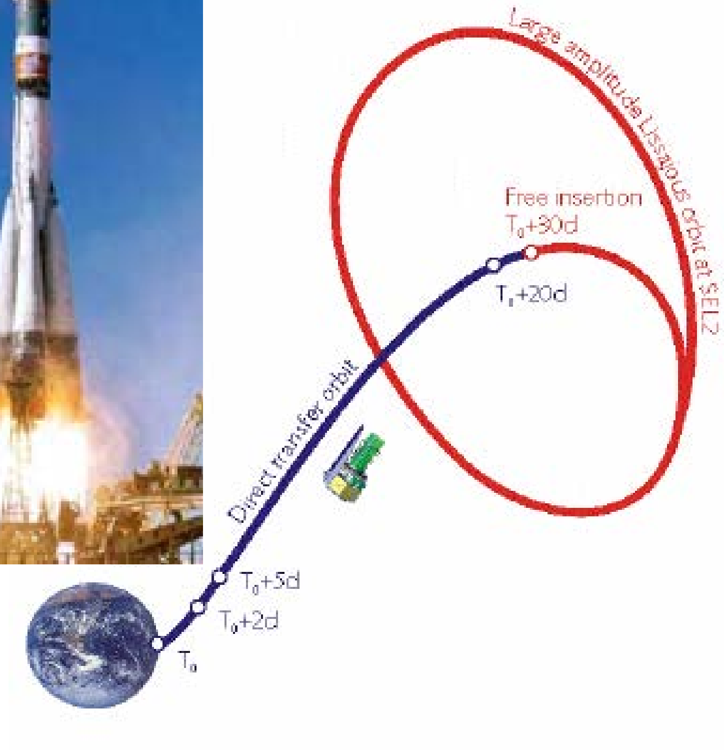

Advanced Studies and Technology Preparation Division

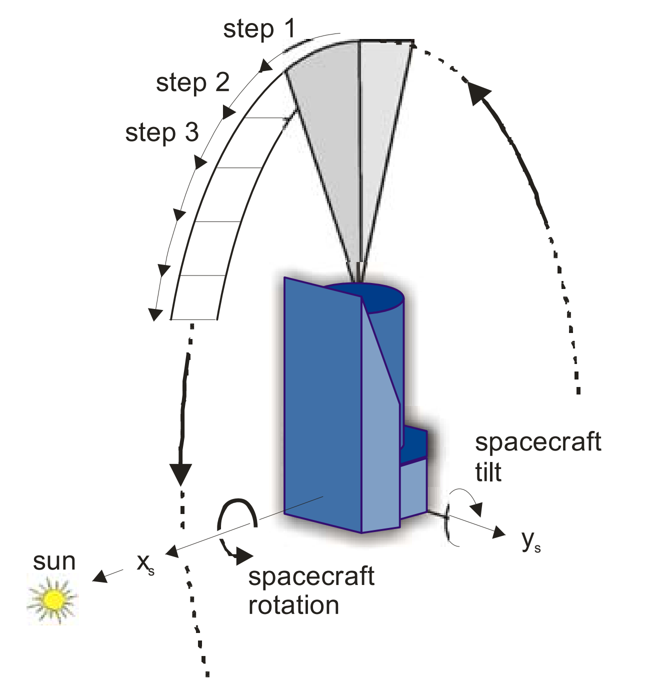

STEP & STARE

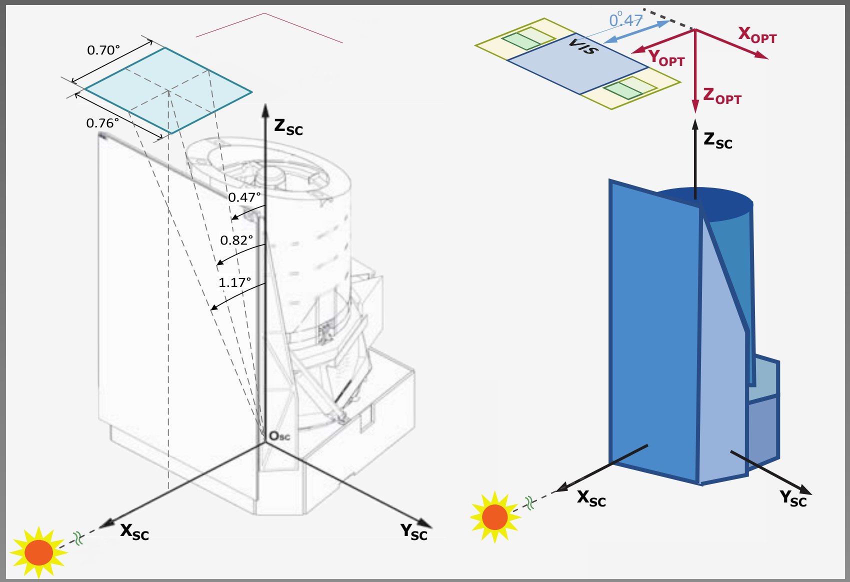

For stability need to always observe almost orthogonally to the sun

Minimal target visibility every six months

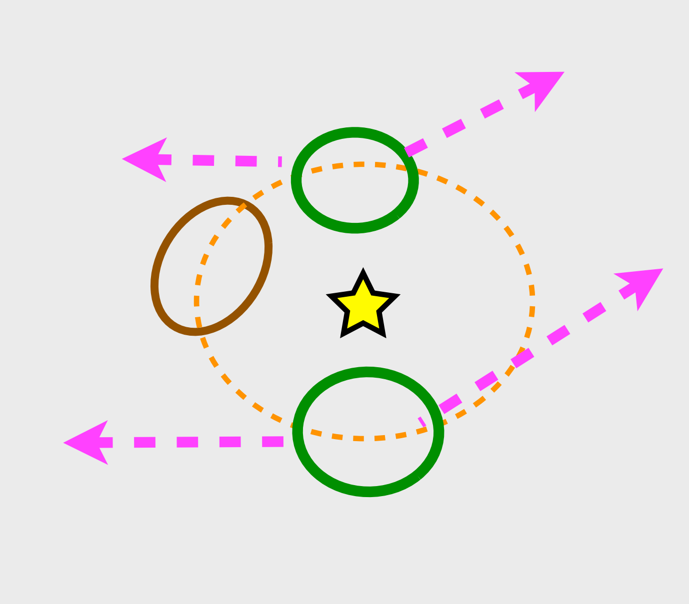

The core: ~0.5 sq/degs, VIS & NIR Focal Planes, lots of pixels !!!

The geometrical Field of View is the sky area limited by the contour of the focal plane array of a given instrument (VIS or NISP) projected onto the sky. The contour is defined by the first pixel line or columns of the detectors on the edge of the FPA as indicated on the next figure.

36 (0.1” pix) Visible FPA: 36 VIS CCD

NIR FPA: 16 H2RG 16 (0.3” pix)

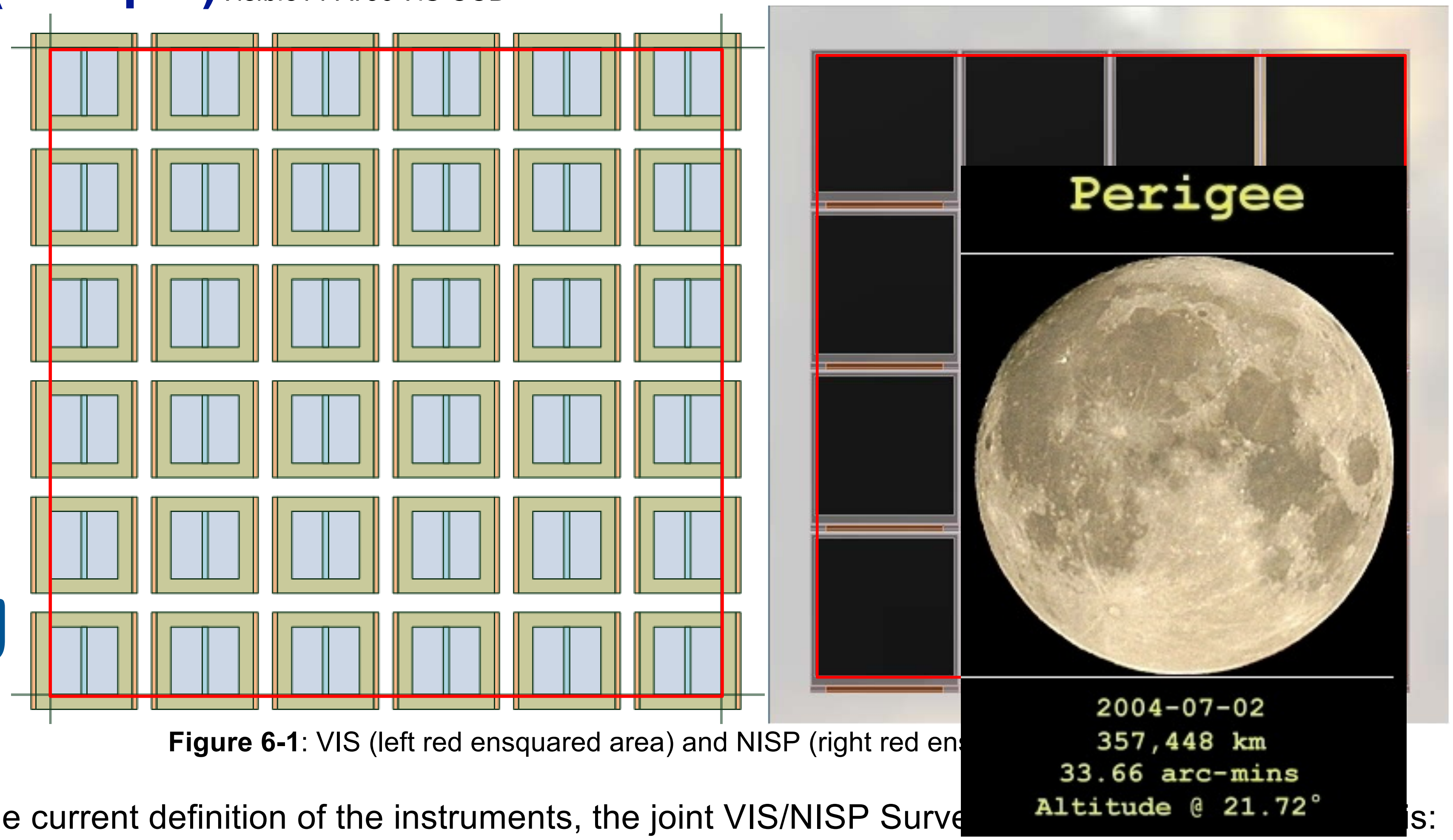

VIS: imaging

NISP: y, J, H photom + slitless

Figure 6-1: VIS (left red ensquared area) and NISP (right red en…

With the current definition of the instruments, the joint VIS/NISP Surve… is:

- JOINT_FOV_x= 0.763°
- JOINT_FOV_y= 0.709°

~44’ side

The x and y field orientations are defined in the figure 6-2.

cf Planck: here ~ O(billion) of pixels for field, plan ~ 30,000 fields

Cosmic rays

M. Cropper, A. Ealet, K. Jahnke, S. Niemi

NIR array

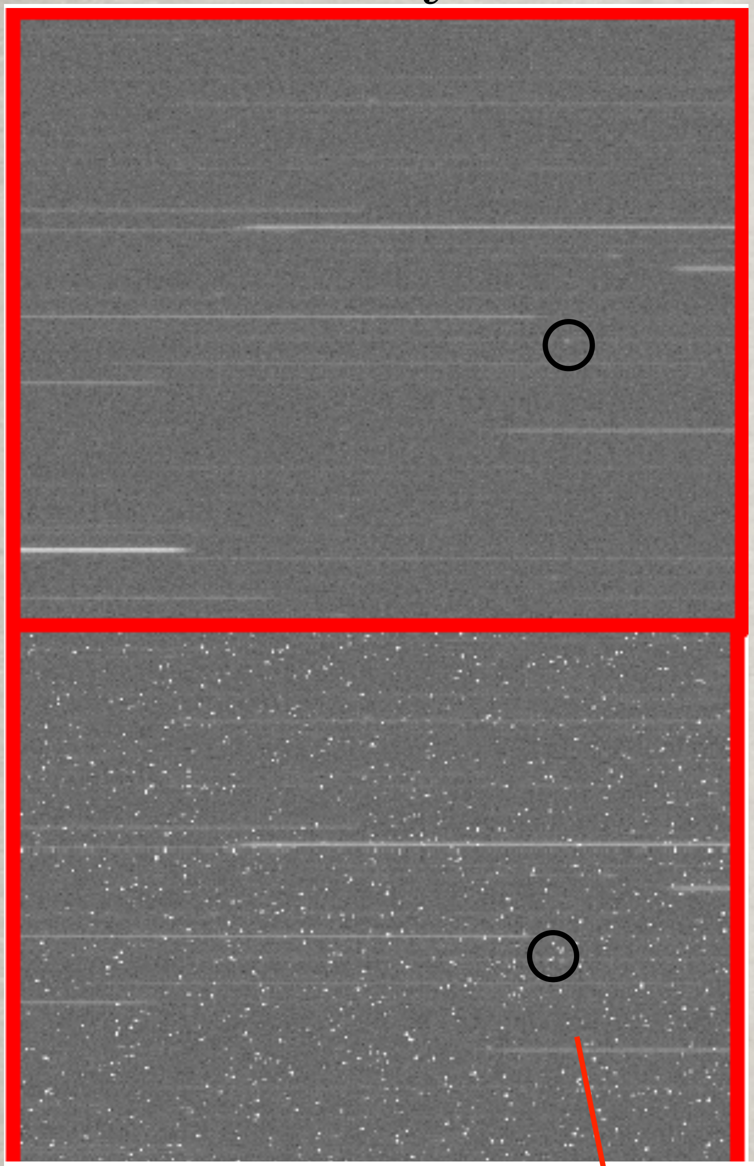

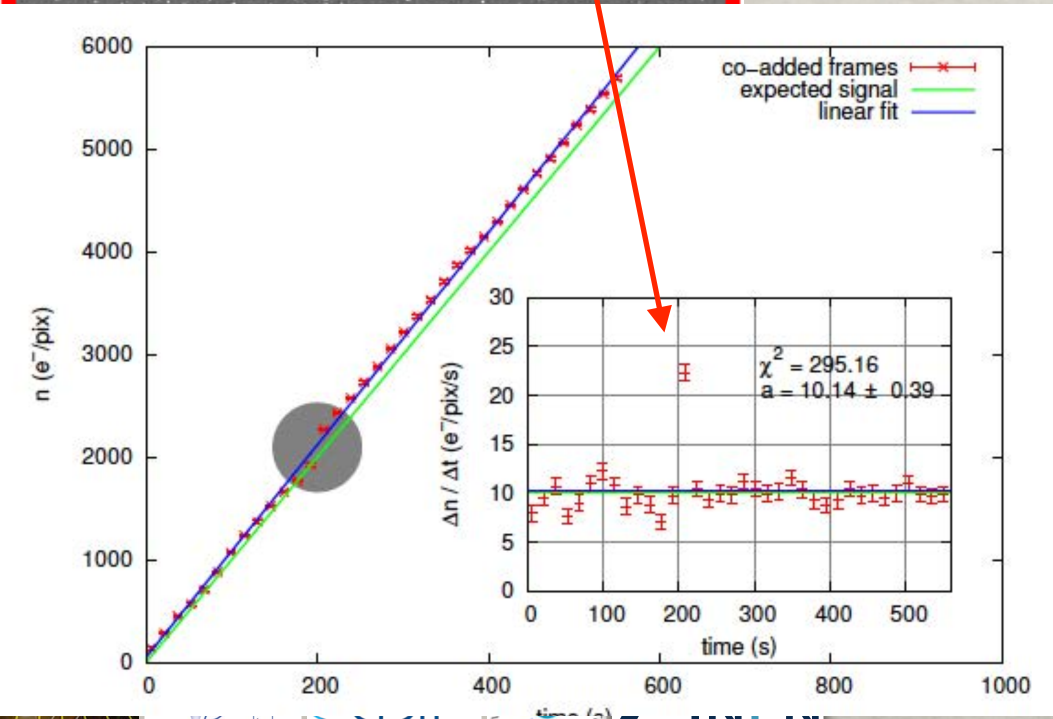

CCD

CCD woes

R. Massey & VIS team

Moreover: Charge Transfer Inefficiency modifies shapes! need to reconstruct

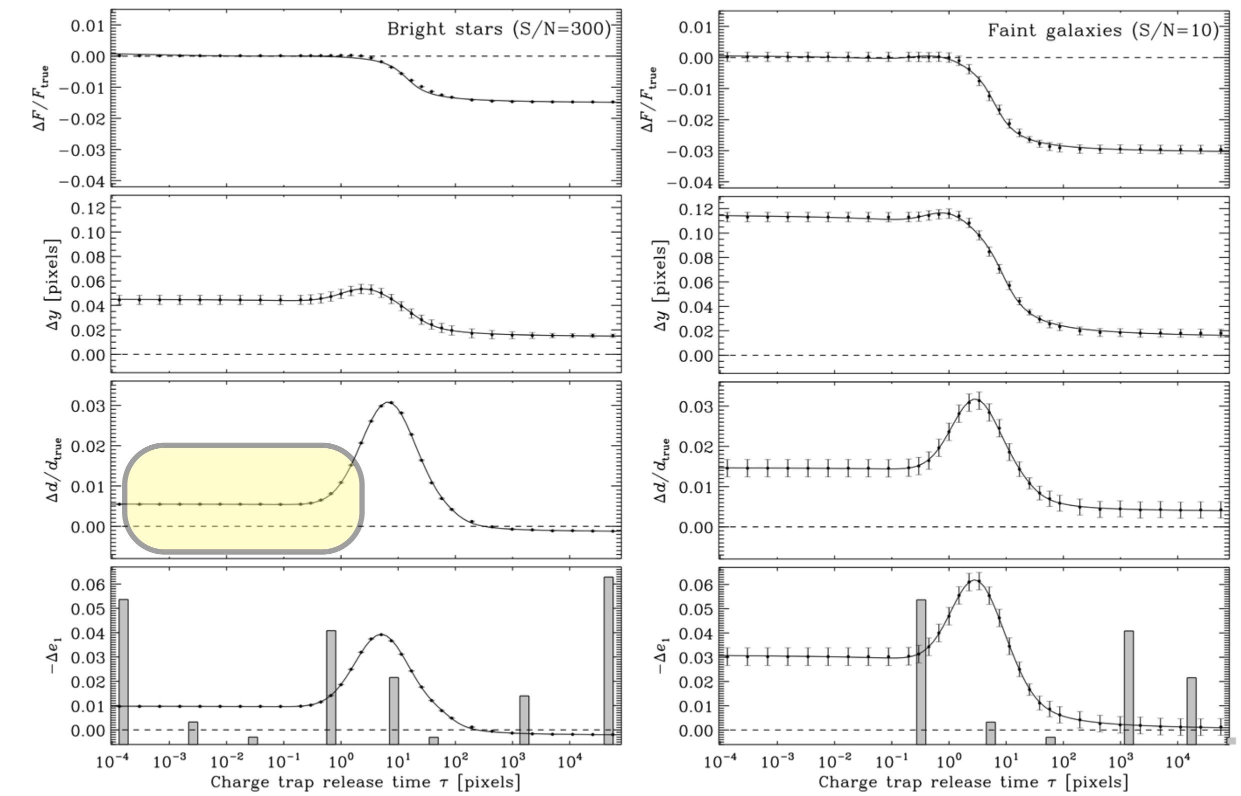

Figure 34 The degradation due to CTI on measurements of flux, astrometry, size and ellipticity. The curves show the response to different trap species of a bright star (left panel) or a faint galaxy (right panels), if there were an (arbitrarily chosen) trap density of 1 trap per pixel. The x axis is the release time of the charge trap species, in multiples of the CCD readout clock speed such that a temporal delay of one clock cycle is equivalent to a spatial displacement of 1 pixel. The histograms in the bottom panels show the population of trap species in CCD204 detectors as a function of their characteristic release time in the same units, for parallel readout (left panel) and serial readout (right panel).

Trails

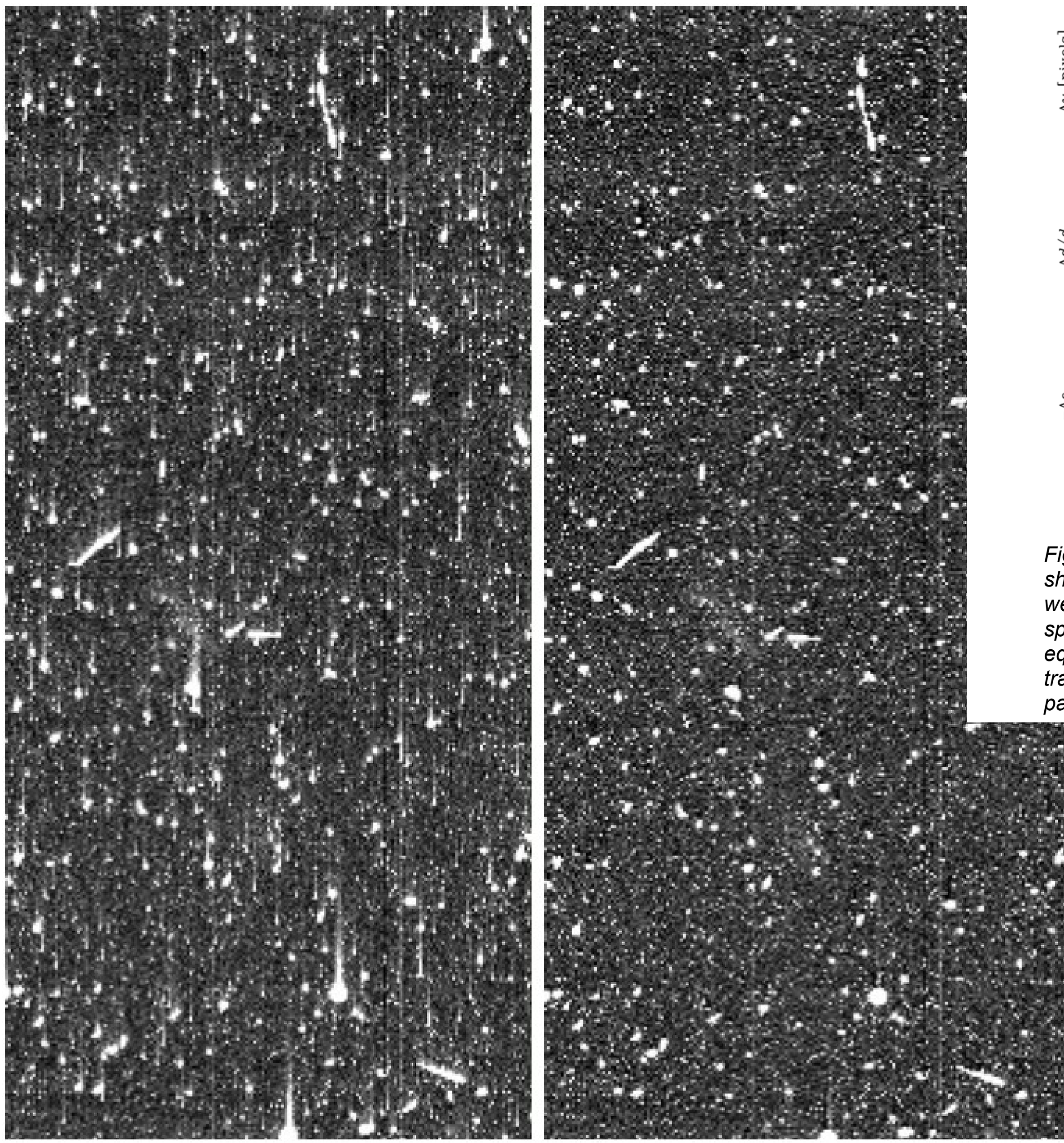

gure 35 Left: Real image from the Hubble Space Telescope, eight years after launch, showing charge iiling due to CTI. Right: The same image after correction using software like that planned for Euclid. The garithmic colour scale in the images has been chosen to enhance the visibility of the charge trailing. Note at the cosmic ray event trails correctly remain in the right hand image.

For gravitational lensing need to know very well the Point Spread Function (blurring of images):

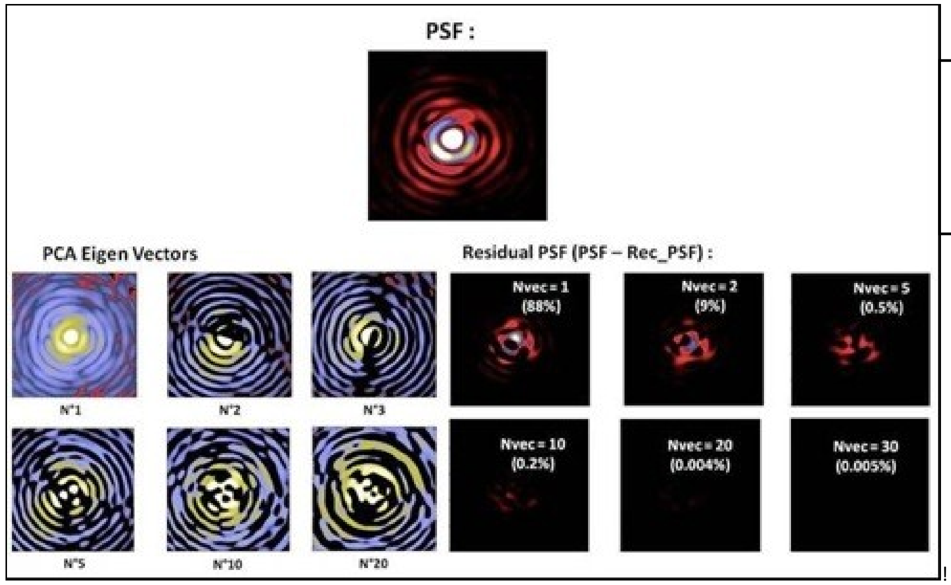

L. Miller & VIS team

Figure 39: VIS PSF eigenvectors and residuals as a function of number of eigenvectors used in the reconstruction of a given Euclid PSF

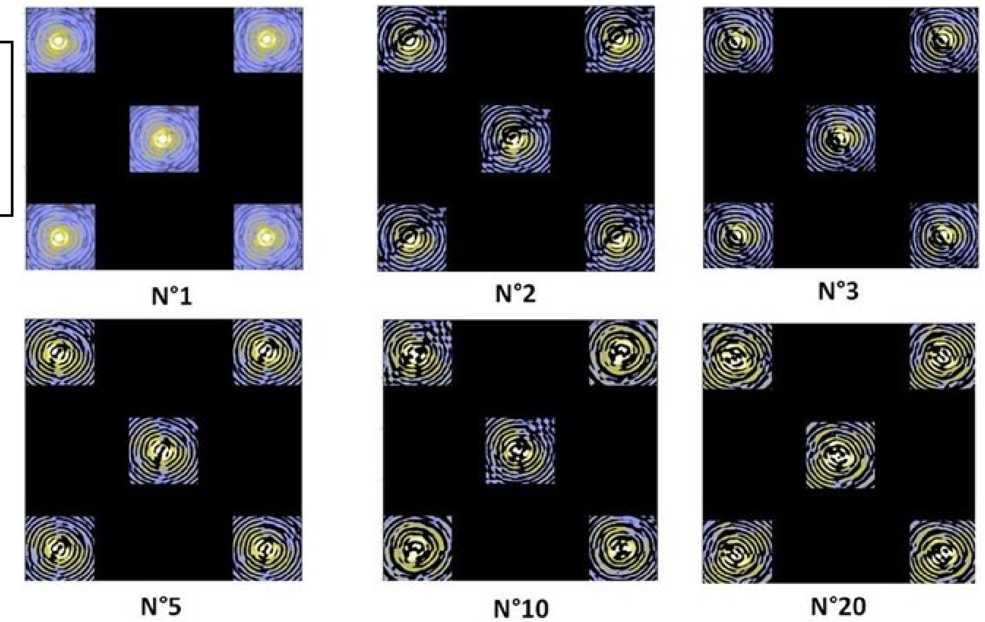

Figure 40: VIS PSF eigenvectors and as a function of number of eigenvectors used in the reconstruction over

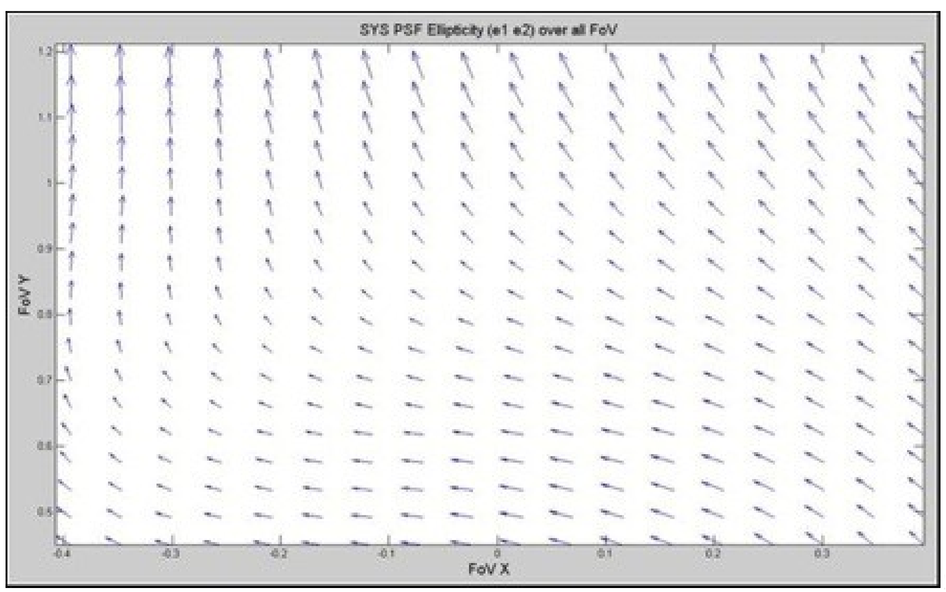

Figure 38: Euclid system VIS PSF ellipticity vector (e1, e2) map over the reference system full FoV

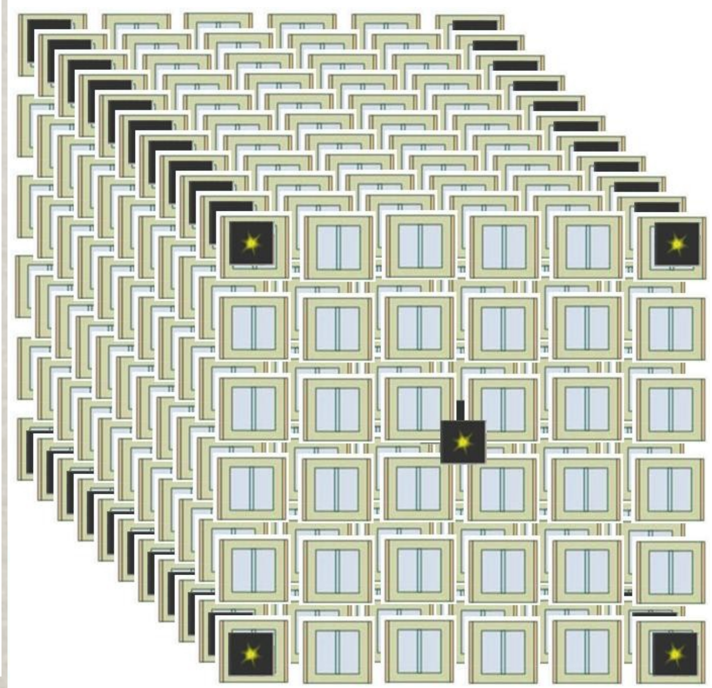

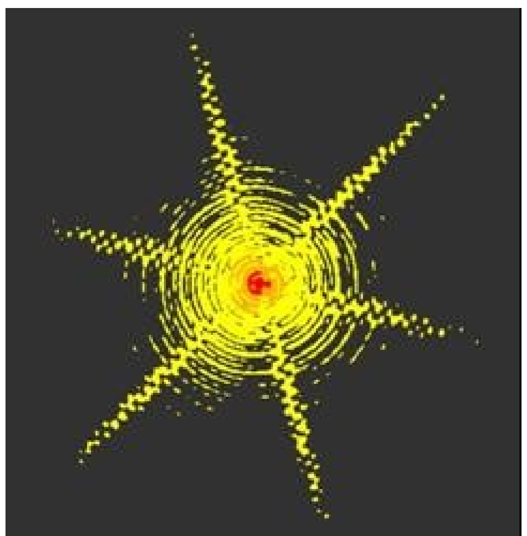

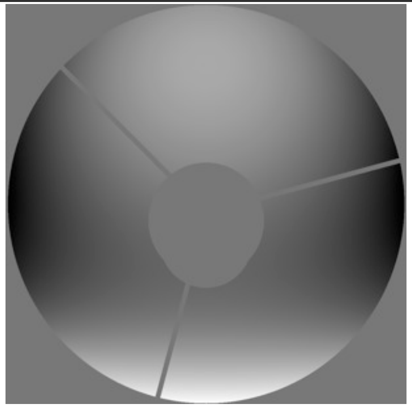

Exit pupil amplitude & phase:
low Zernike-order phase variations

PSF is wavelength (energy) dependent, so is different for blue or red galaxies!! Also polarisation effects

L. Miller

polarisation and object counts in deep fields

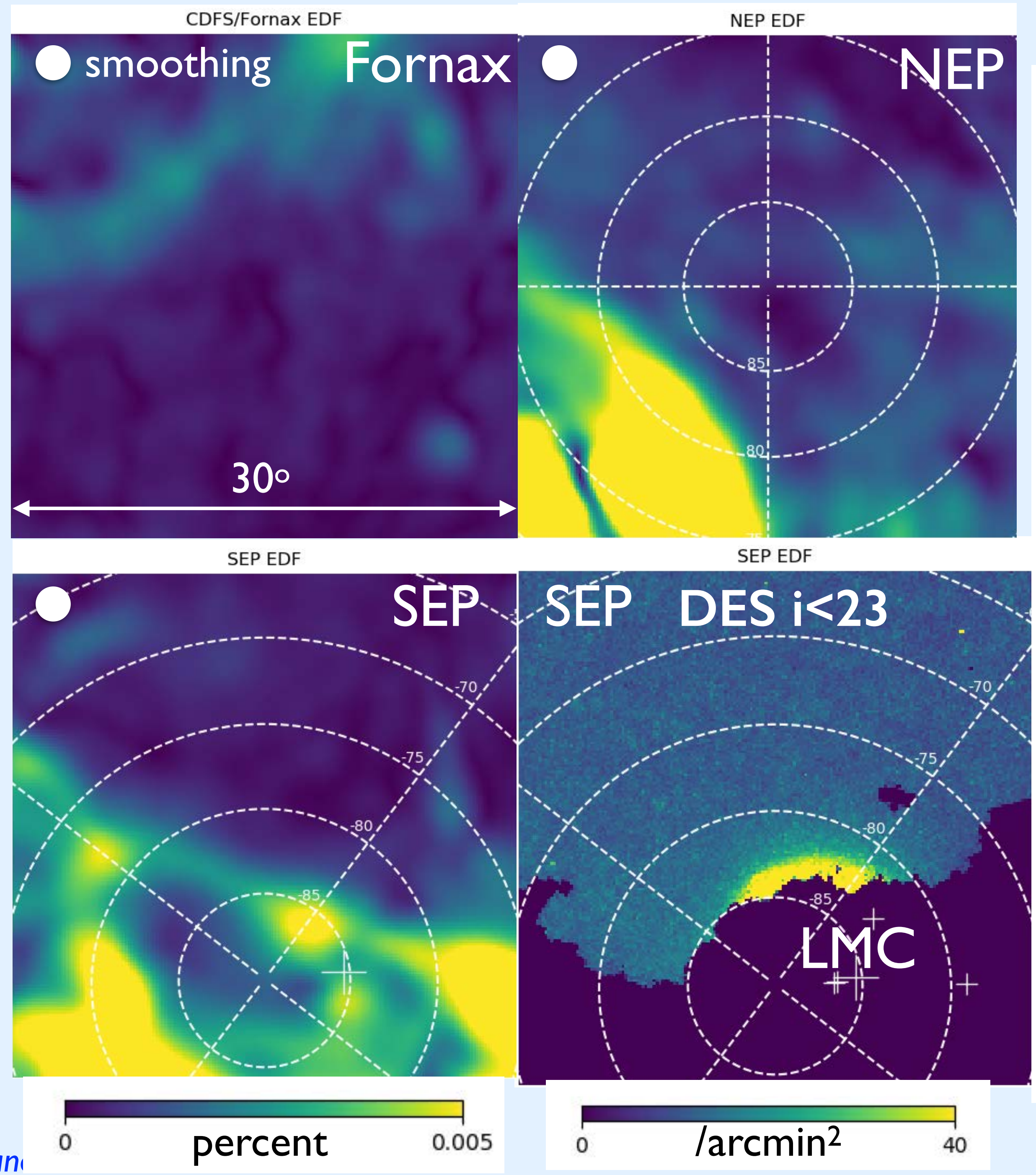

- Predicted polarisation for 3 deep fields smoothed with 2 degree FWHM, plus DES object counts near SEP/ LMC
- Polarisation noise <0.05 percent on these maps
- Need to avoid dust in all regions
- Need to avoid too high object counts (yellow/ green regions on DES plot) < 40/arcmin^2 (i<23)
- May need careful field selection and more accurate in-field stellar polarisation observations

Lan

Euclid calibration WG, Mar 2018

EDF-S “temp” & EDF-F & NEP seem OK (? TBD)

Photoz are crucial, need ground based photometry

Meneghetti

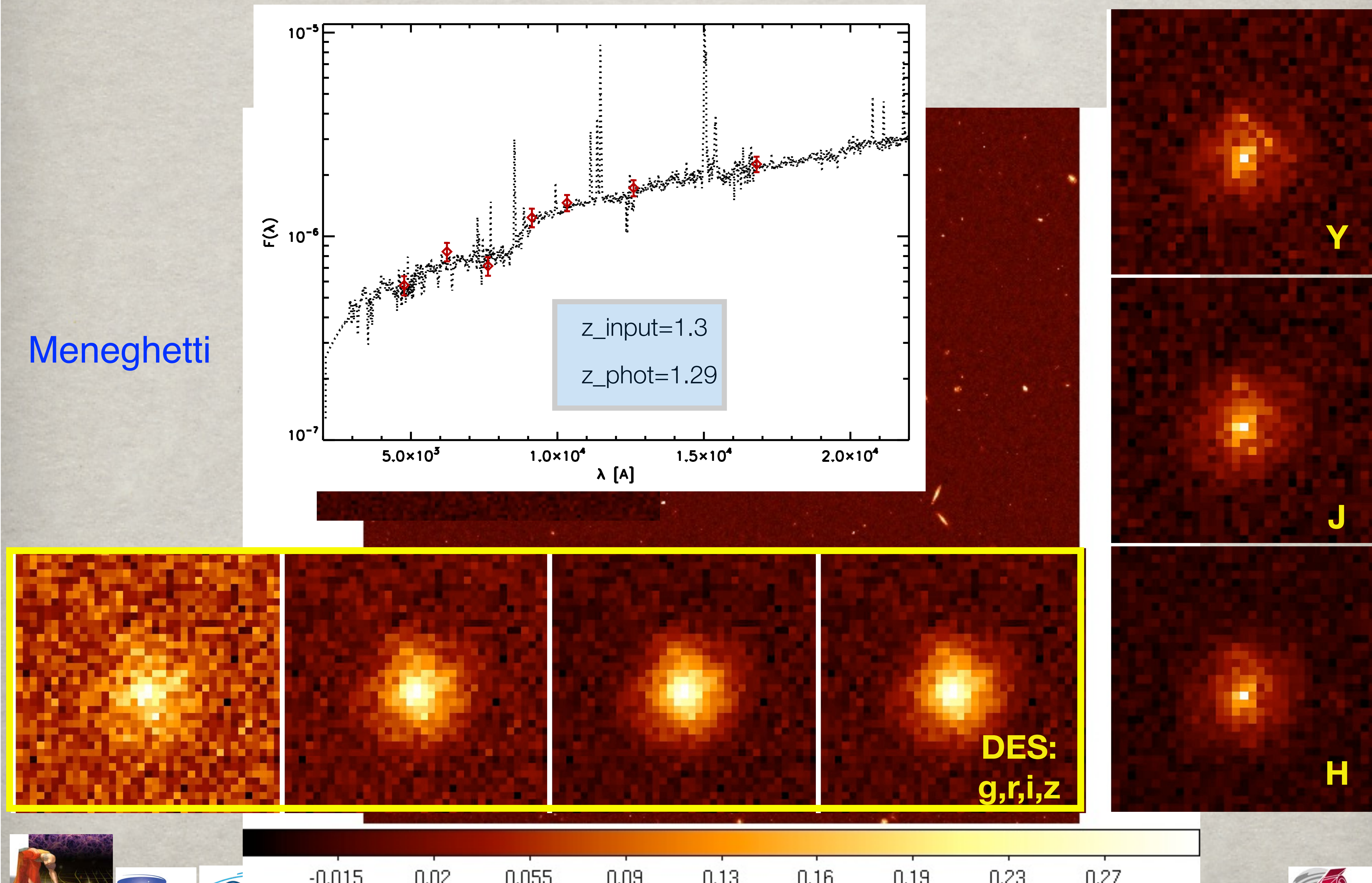

Model systematic effects (holes, boundaries, varying S/N etc)

Weak Lensing
(VIS, WLSWG, OU-SHE)

Shear field

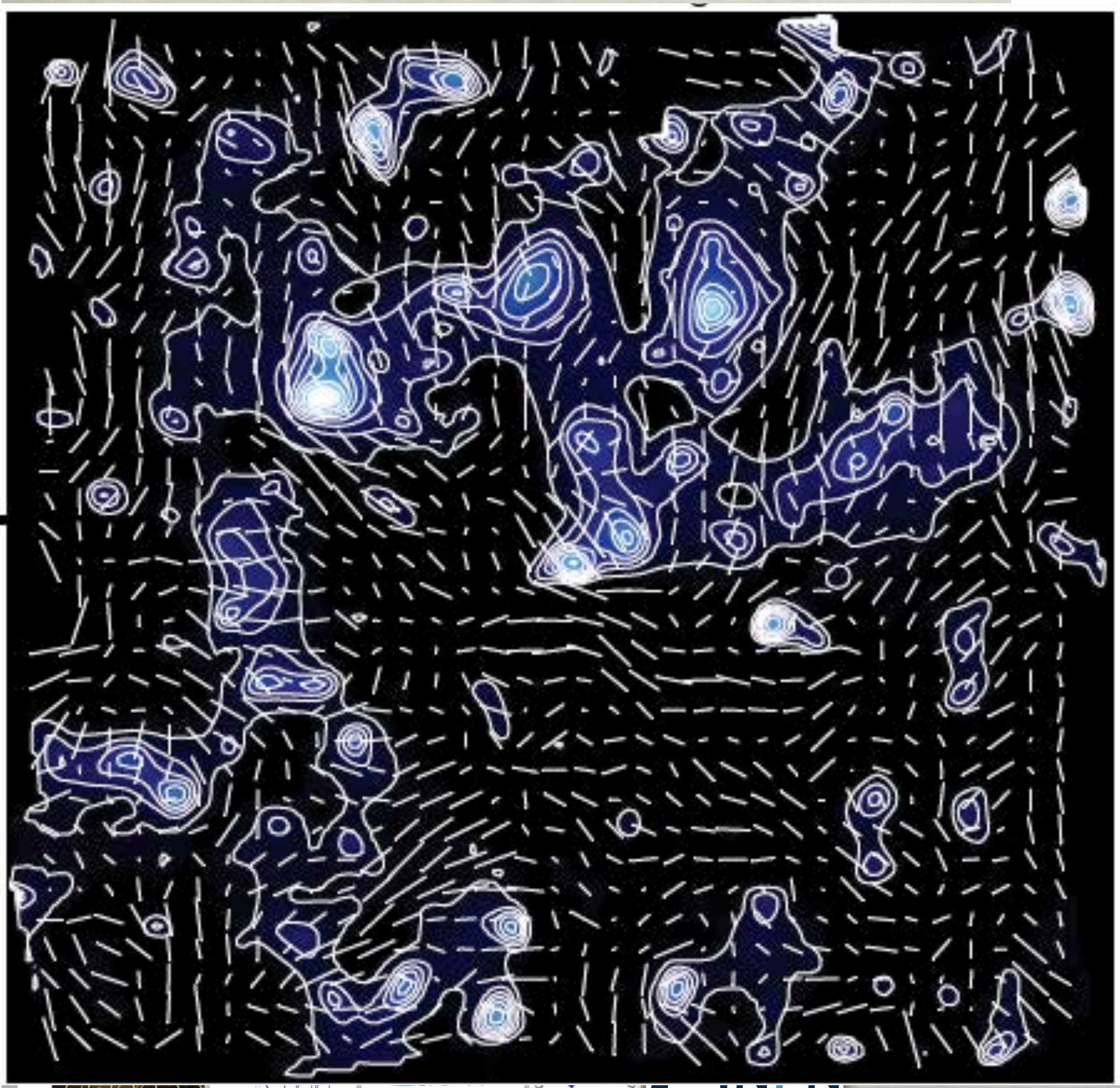

- True two-point correlation function C_{ij} will be affected by additive bias σ^2_{sys} and multiplicative bias M

$$\widehat{C_{ij}} = \left(1+\mathcal{M}^2\right) C_{ij} + \sigma^2_{\rm sys}$$

PSF sizes and ellipticities

$$\mathcal{M} = \sigma[R^2_{\rm PSF}]\left[\frac{1}{R^2_{\rm PSF}}(P^\gamma)^{-1}\left\langle\frac{R^2_{\rm PSF}}{R^2_{\rm gal}}\right\rangle\right] + \sigma[R_{\rm NC}]\left[\frac{1}{R_{\rm obs}-R_{\rm NC}}2(P^\gamma)^{-1}\left\langle\frac{R^2_{\rm PSF}}{R^2_{\rm gal}}\right\rangle\right]$$

$$\begin{aligned}\sigma^2_{\rm sys} \; &= \; \sigma^2[R^2_{\rm PSF}]\left[\frac{1}{R^4_{\rm PSF}}(P^\gamma)^{-2}\left\langle\frac{R^4_{\rm PSF}}{R^4_{\rm gal}}\right\rangle\langle\varepsilon^2_{\rm PSF}\rangle\right] + \sigma^2[R_{\rm NC}]\left[\frac{1}{(R_{\rm obs}-R_{\rm NC})^2}4(P^\gamma)^{-2}\left\langle\frac{R^4_{\rm PSF}}{R^4_{\rm gal}}\right\rangle\langle\varepsilon^2_{\rm PSF}\rangle\right]\\ &+ \; \sigma^2[\varepsilon_{\rm PSF}]\left[2(P^\gamma)^{-2}\left\langle\frac{R^4_{\rm PSF}}{R^4_{\rm gal}}\right\rangle\right] + \left(\sigma^2[\varepsilon_{\rm NC,1}]+\sigma^2[\varepsilon_{\rm NC,2}]\right)\left[(P^\gamma)^{-2}\left\langle\frac{R^4_{\rm PSF}}{R^4_{\rm gal}}\right\rangle\left\langle\frac{R^4_{\rm obs}}{R^4_{\rm PSF}}\right\rangle\right]\end{aligned}$$

errors in PSF sizes and ellipticities (knowledge)

universe

more simply:

$$\mathcal{M} = \sigma[R^2_{\rm PSF}]\,[m_1] + \sigma[R_{\rm NC}]\,[m_2]$$

$$\sigma^2_{\rm sys} = \sigma^2[R^2_{\rm PSF}]\,[a_1] + \sigma^2[R_{\rm NC}]\,[a_2] + \sigma^2[\varepsilon_{\rm PSF}]\,[a_3] + \left(\sigma^2[\varepsilon_{\rm NC,1}]+\sigma^2[\varepsilon_{\rm NC,2}]\right)[a_4]$$

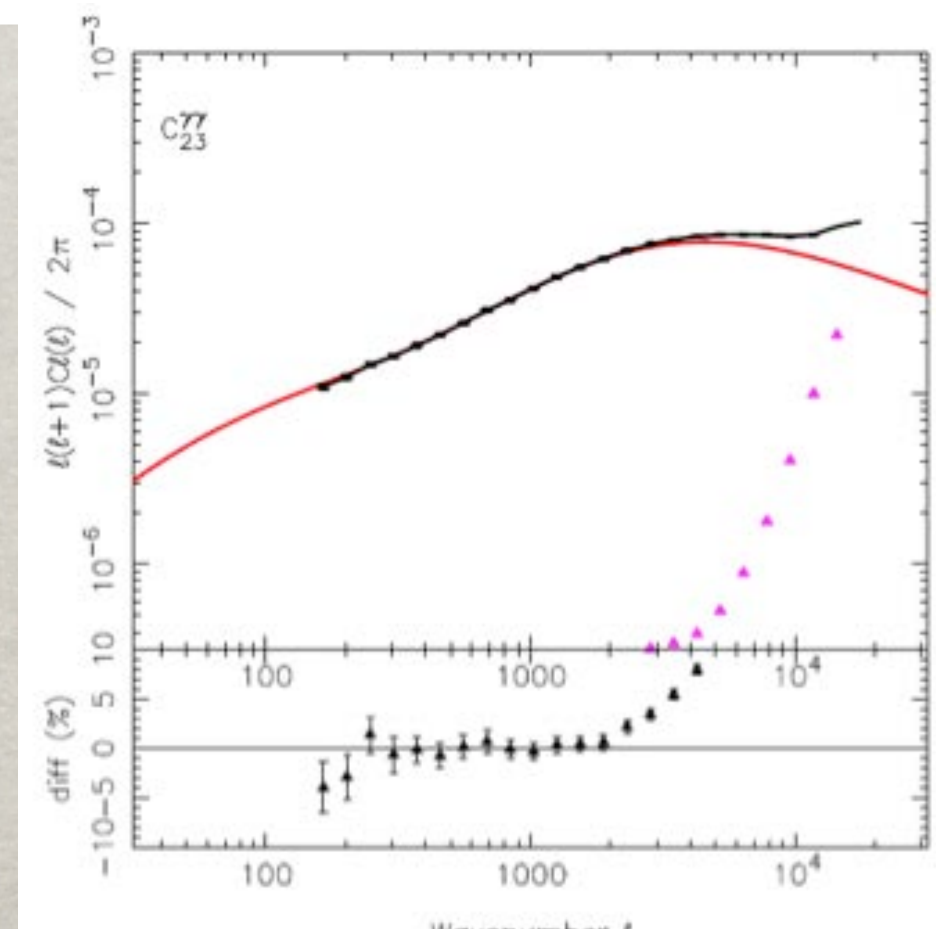

Effects on the angular power spectrum

EUCLID Survey(s)

Highly complex since start

3 kinds of data at once:
- VIS imaging
- Y, J, H photometry
- red grism slitless spectra

Lots of constraints (changed over time)

In 6 years need to do
- calibrations
- auxiliary fields
- deep fields
- wide survey

Need to fix priorities !!!

~2011

A scheme of the complex inter-relationships of the Euclid Survey produced at the start of the study. After a Commissioning phase lasting one month, the First Light phase is now called the Performance Verification phase, lasting two months. Both those phases take place before the start of the core mission, lasting six years. The examples shown for additional surveys are now likely to take place during a possible extension of the mission. However, over the years the main items have kept stable as shown, with an additional arrow connecting VIS to the Deep Survey

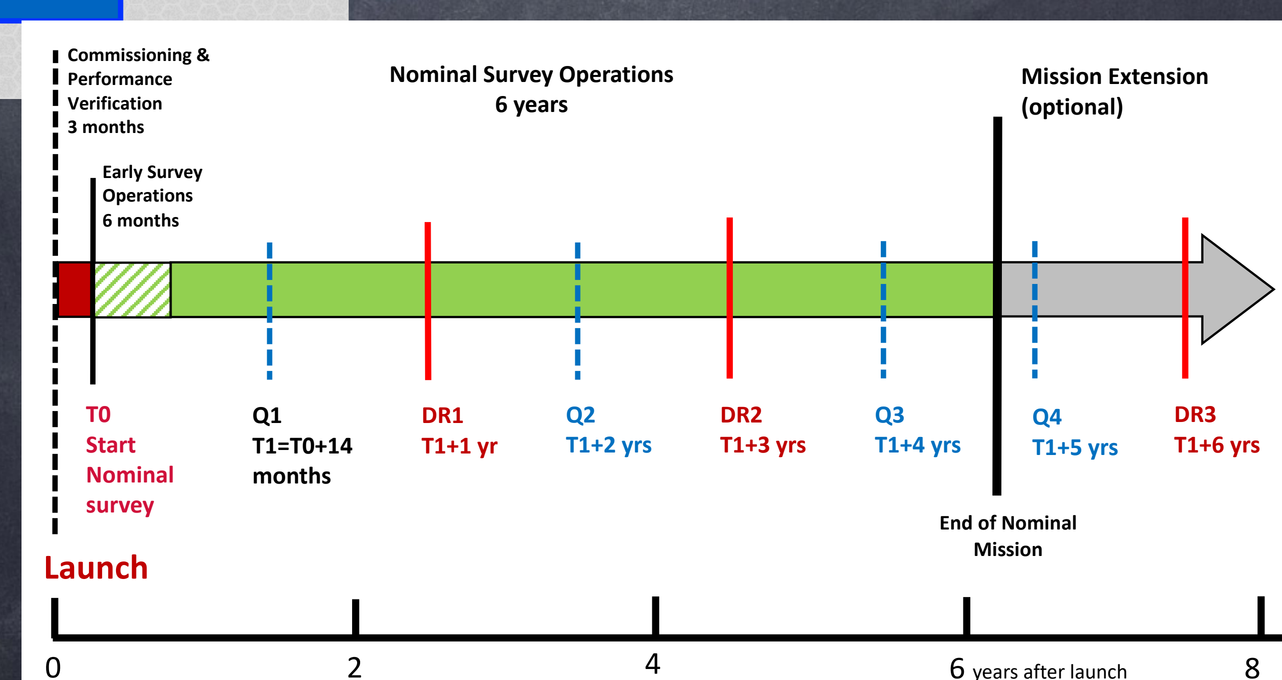

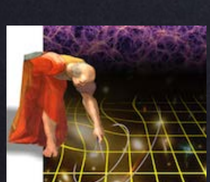

Zodiacal Light

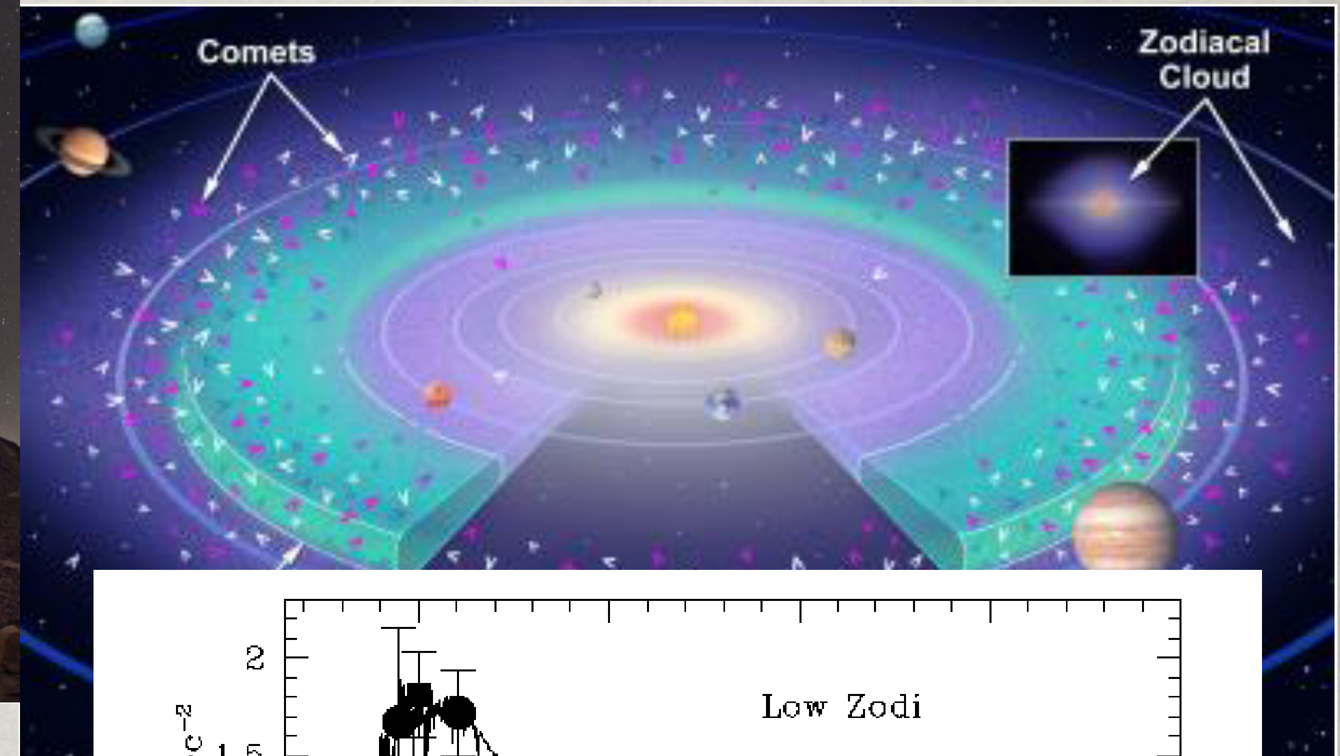

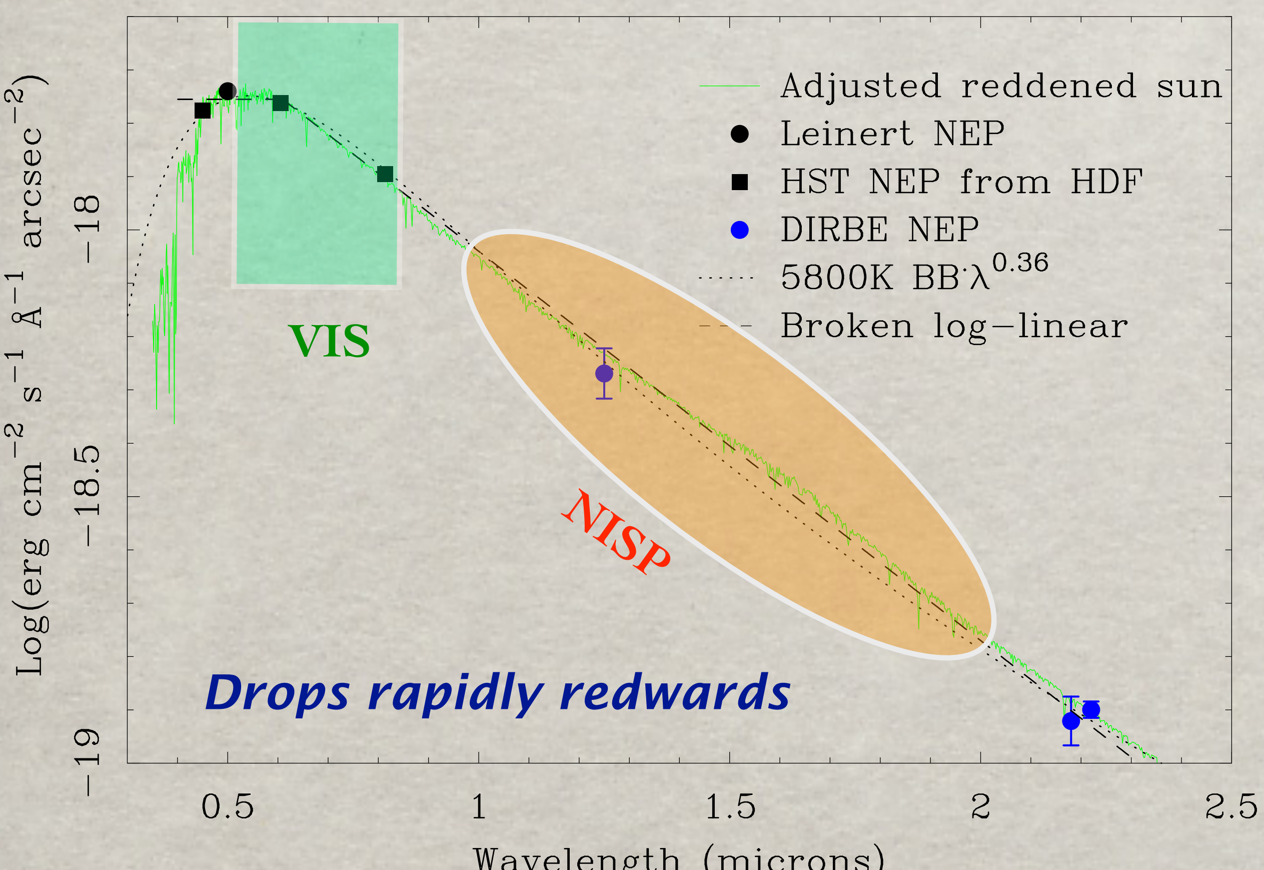

Figure 7: The solar spectrum, adjusted to match the observed zodiacal background (solid green). Simplified parameterization - a 5800° K blackbody scaled by $\lambda^{0.36}$ (dotted black). Broken power-law parameterization (dashed black).

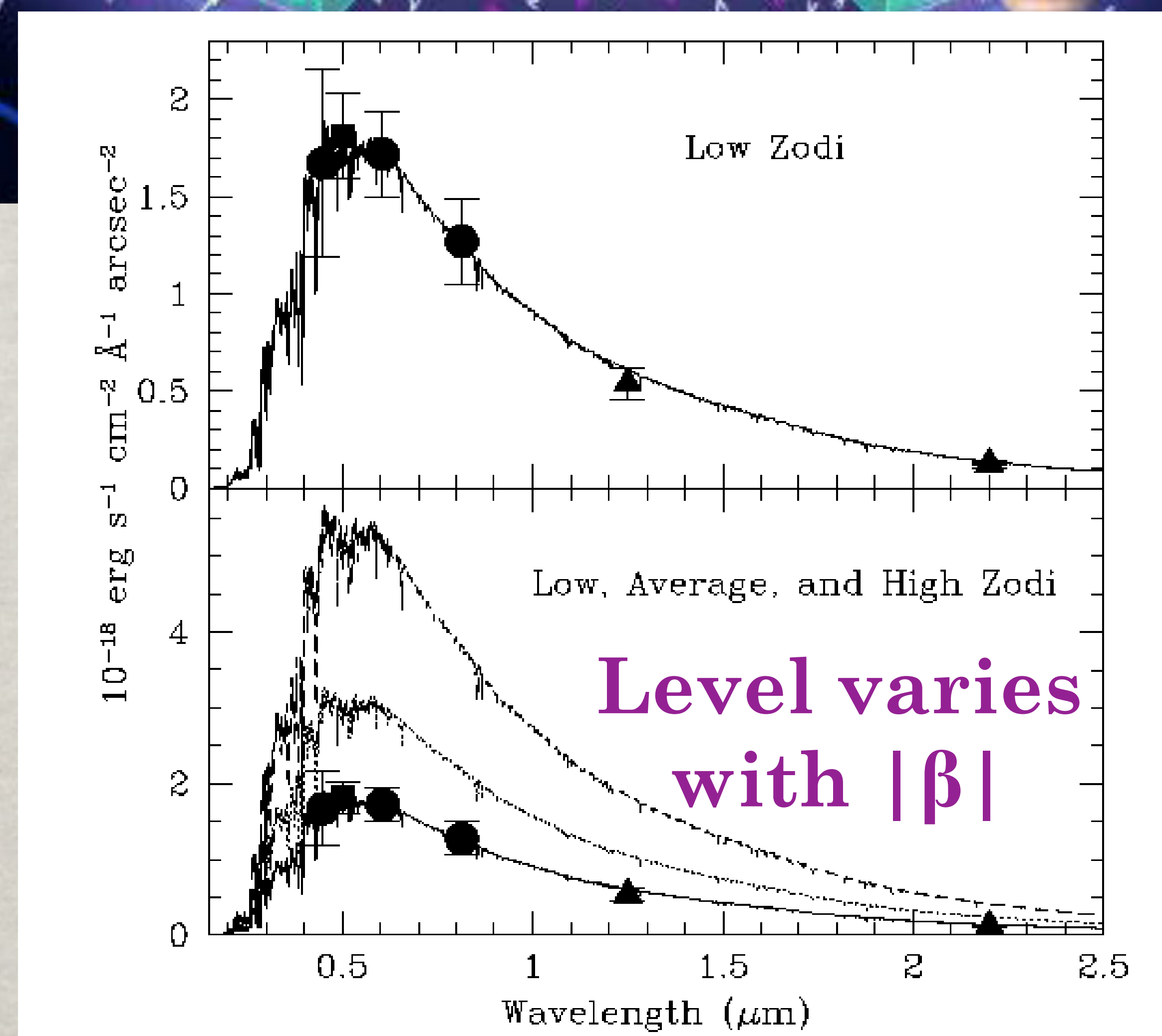

Figure 1. Upper panel. The spectrum of the zodiacal background light at the NEP compared to broad-band observations from the ground and HST observations. The circles are data at 0.450, 0.606 and 0.814 μm, respectively from the HDF; the square is Leinert et al. (1998) measure at 0.5 μm, and the triangles are measures from COBE/DIRBE at 1.25 and 2.2 μm. **Lower panel.** The comparison between the intensity of the three adopted normalizations of the zodiacal backgroud light. The lowest normalization is the one relative to the NEP, and it is shown together with the broad-band data points discussed above.

Zodiacal update

Tilted slab= sinusoid at NEP

B.Reach
(talk grabbed from the net)

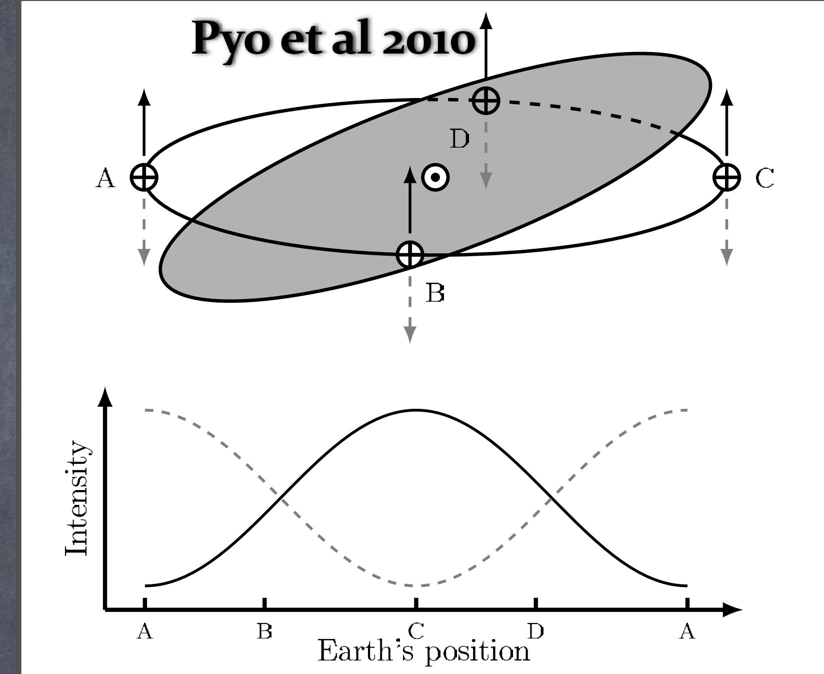

Fig. 5. Schematic diagram for the seasonal variation of NEP and SEP brightness due to tilt of the IPD cloud's symmetry plane. The Earth's positions marked by A, B, C, and D on the top frame correspond to the abscissas labeled by the same characters. In the top frame, the upward arrows point to the NEP while the downward ones point to the SEP. The NEP and SEP intensities are represented by a black, solid line and a gray, broken line, respectively, in the bottom frame.

Resonant structures in Zodiacal Cloud

- Smooth cloud traces mean orbital elements
  - Node randomized by Jupiter in 10^6 yr so only secular long-time-averaged perturbations survive
- Resonant effects in comoving frame with planet

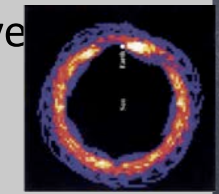

- *Spitzer Earth Ring experiment*
- Frame comoving with Earth
- Contours of the COBE/DIRBE zodiacal cloud model
- Trajectory of Spitzer (thick) with crosses every year
- Able to probe azimuthal structure of zoiacal cloud

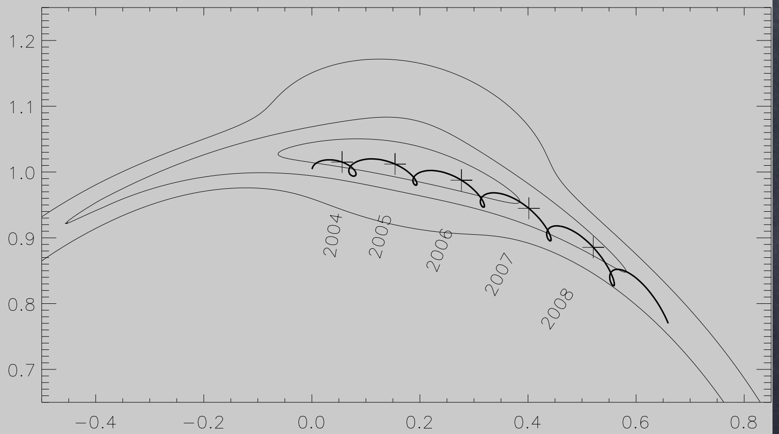

Observed brightness of North Pole

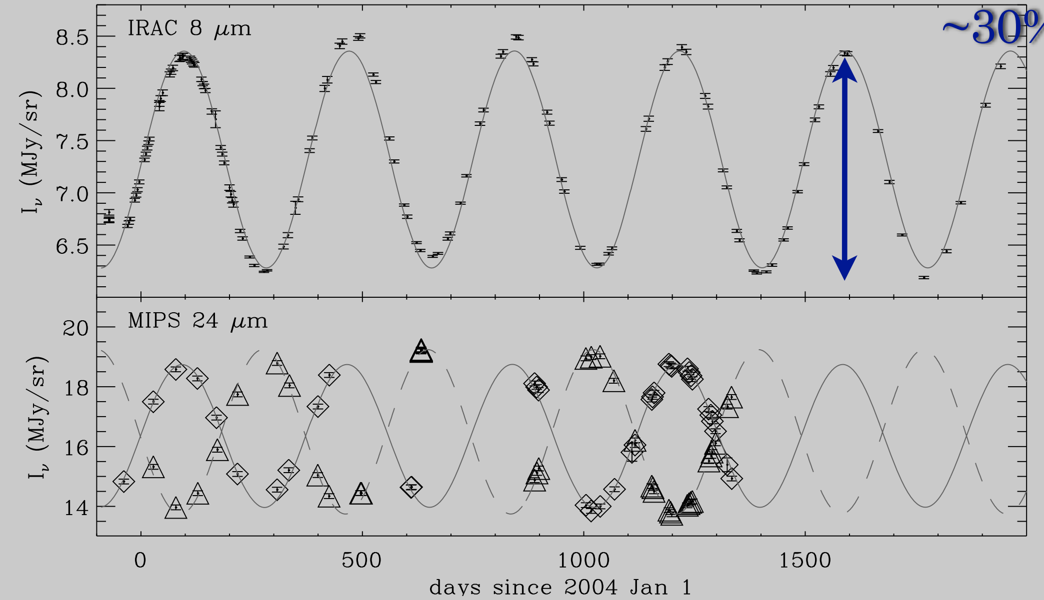

Sinusoidal variation due to inclination of zodiacal plane, and eccentricity of orbits

Infrared/Zodiacal Light

M. Maris: time dependence of zodiacal background

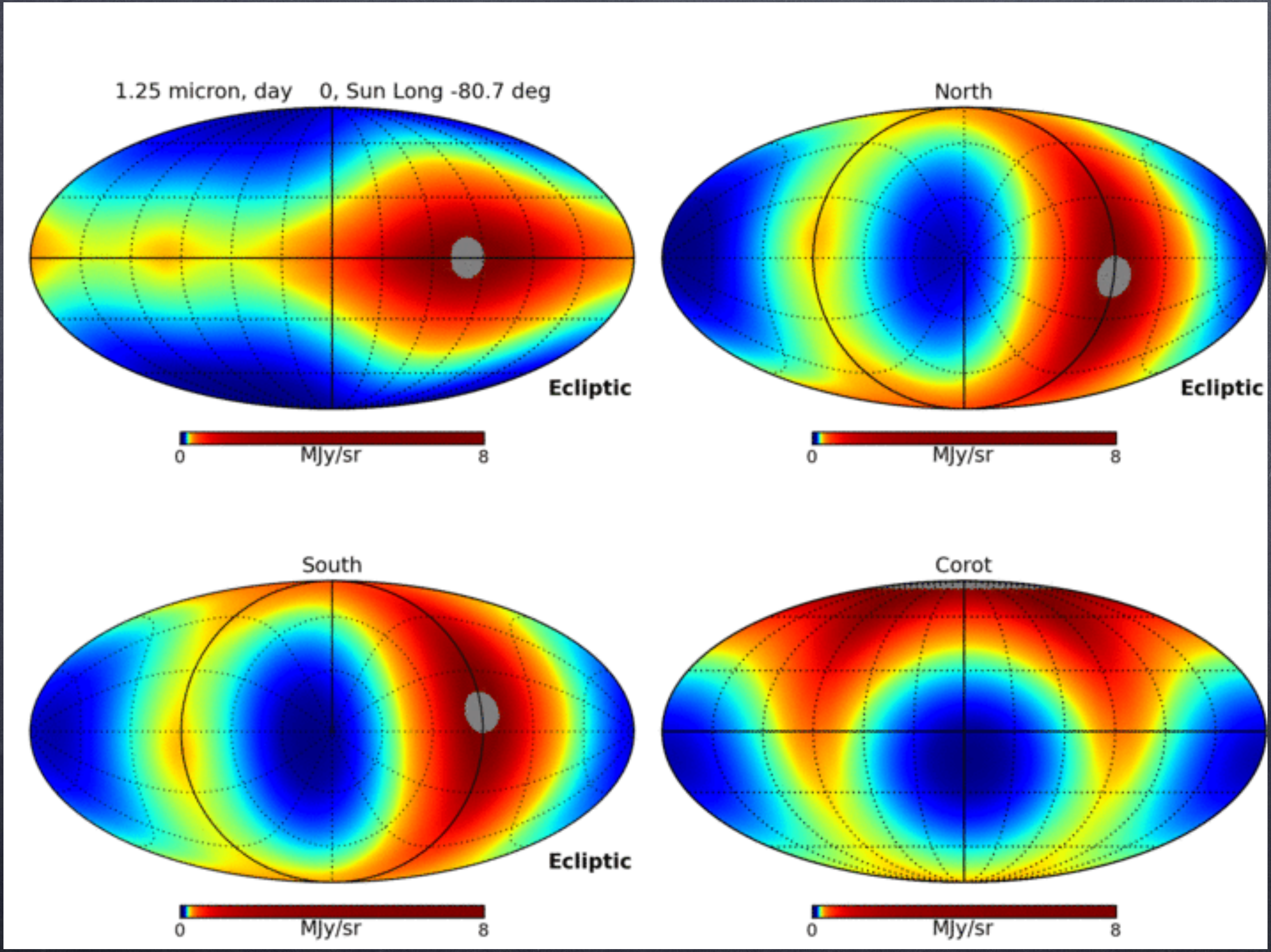

minimum not centered at Ecl poles